IDENTIFICATION AND CHARACTERIZATION OF BINDING TARGET PROTEINS OF CANCER STEM CELL INHIBITOR SALINOMYCIN IN HUMAN NEUROBLASTOMA

A Dissertation
Submitted to the Graduate Faculty
of the
North Dakota State University
of Agriculture and Applied Science

By

Shuang Zhou

In Partial Fulfillment of the Requirements
for the Degree of
DOCTOR OF PHILOSOPHY

Major Department:
Pharmaceutical Sciences

August 2015

Fargo, North Dakota

North Dakota State University
Graduate School

Title

IDENTIFICATION AND CHARACTERIZATION OF BINDING TARGET PROTEINS OF CANCER STEM CELL INHIBITOR SALINOMYCIN IN HUMAN NEUROBLASTOMA

By

Shuang Zhou

The Supervisory Committee certifies that this ***disquisition*** complies with North Dakota State University's regulations and meets the accepted standards for the degree of

DOCTOR OF PHILOSOPHY

SUPERVISORY COMMITTEE:

Dr. Erxi Wu
Chair

Dr. Larry Reynolds

Dr. Steven Qian

Dr. Bin Guo

Approved:

August 6, 2015
Date

Dr. Jagdish Singh
Department Chair

ABSTRACT

Salinomycin, a widely used anti-coccidial agent, was recently identified as a cancer stem cell (CSC) inhibitor from a library of 16,000 natural and commercial chemical compounds based on its highly selective inhibitory effect on breast CSCs, with more than 100-fold greater potency than paclitaxel. Salinomycin also exhibits cytotoxic effects on other types of cancer cells and CSCs and overcomes drug resistance. However, the exact mechanism of salinomycin, especially its direct binding target(s), and its effects on Neuroblastoma (NB) are yet not known.

NB is a common solid tumor and a leading cause of mortality in children. Currently, 35% of patients with NB remain incurable. In addition, the majority survivors of NB suffer from long-term side effects of current therapies and are at risk for disease relapse or getting a second, different cancer. More effective therapies are pressingly needed. Since the existence of CSCs in human NB cell lines and NB tumors has been well documented, and has been closely associated with chemoresistance or tumor relapse, therapeutic targeting of NB CSCs may be a critical novel approach for NB therapy.

Aiming to improve NB therapy, we examined the efficacy and mechanism of salinomycin in human NB cells. Our study showed that salinomycin markedly inhibits NB cell proliferation and tumorsphere formation. Treatment of salinomycin induced G2 cell cycle arrest with an up-regulation of Cyclin A and a down-regulation of p21 protein levels. We further identified Transcription intermediary factor 1-beta (TIF1β) and Nucleolin (NCL) as novel binding targets of salinomycin by using comprehensive methods, including chemical proteomics and functional genomics. We demonstrate that salinomycin induced phosphor-TIF1β mediated down-regulation of p53 and significantly suppressed the expression of CD34, a CSC marker, via disrupting the interaction of NCL with the CD34 promoter. Furthermore, by analyzing tumor

samples data from a cohort of 498 NB patients, we found that elevated levels of TIF1β and NCL in NB are associated with a poor outcome. These results provide a therapeutic rationale for evaluating of both salinomycin and its binding proteins, TIF1β and NCL, in NB.

ACKNOWLEDGEMENTS

It is a great pleasure to express my heartfelt gratitude to all whom in one way or another contributed in the completion of this thesis.

First and foremost, I offer my deepest gratitude to my advisor, Dr. Erxi Wu. I have been amazingly fortunate to have an advisor who always gave me both the academic and moral support I needed to move on. He encouraged me and directed me with his patience, motivation, enthusiasm, immense knowledge, and insightful advice. Dr. Wu is the mentor who truly made a difference in my life and helped me become fond of cancer research. I will never be able to convey my appreciation fully.

My thesis committee guided me through all these years. I am deeply thankful to my committee members: Dr. Larry Reynolds, Dr. Steven Qian, and Dr. Bin Guo, for their encouragement, insightful comments, and valuable suggestions. My sincere thanks also go to Dr. Jagdish Singh for giving me the opportunity to work in the Department of Pharmaceutical Sciences and use the core facilities in the department. I would also like to express my sincere appreciation to Janet Krom, Jean Trautmann and all the faculty and staff members in the Department of Pharmaceutical Sciences who have always been approachable and helpful to me.

I am so lucky to work with the intelligent, friendly, and cheerful people in the Wu Laboratory. My special thanks go to Dr. Fengfei Wang for her valuable advice and contribution to this thesis. I am also indebted to Dr. Xuejing Wang and Dr. Mingming Ma for their support and help on the experiments and their insightful suggestions. I would also like to thank other former and current lab members: Dr. Kruttika Bhat, Dr. Xuebing Ding, Zehui Li, and Ying Zhang, for providing such a stimulating and fun work environment.

I would also wish to take this opportunity to thank our collaborators, Dr. Wallace W Muhonen and Dr. John B Shabb for their help on the mass spectrometry experiments; Dr. Shi-Hua Xiang for in silicon models; and Dr. Min Wu for insightful discussions and funding support. I would also like to acknowledge the financial, academic and technical support of the North Dakota State University (NDSU), particularly in the award of NDSU Graduate School Doctoral Dissertation Fellowship that provided the necessary financial support for this research.

I have been blessed to have wonderful friends by my side all the time. I must acknowledge Hui Xu, Qunshu Zhang, Meiyan Sun, Yi Xu, Xiaoyu Yang, Xue Wang, Yue Li, Yan Gu, Mukta Sane, Varsha Meghnani, Amreen Mughal, Xiaoxi Wang, Jingyang Xiao, Yin Wu, Yun Zhou, Juechen Yang, Chao Pei, Lingchao Kong, and Zijian Wang, and many more friends. Thank you for being with me through thick and thin and adding tremendous happiness to my life.

Last but not the least, there aren't enough words in the world to express my appreciation to my beloved family. My parents and my sister are the most basic source of my life energy and a constant source of love, concern, support, happiness, and strength. I here dedicate this thesis to my family for their constant support and unconditional love.

TABLE OF CONTENTS

ABSTRACT iii

ACKNOWLEDGEMENTS v

LIST OF TABLES xi

LIST OF FIGURES xii

LIST OF ABBREVIATIONS xiv

CHAPTER 1. INTRODUCTION 1

1.1. Neuroblastoma (NB) 1

1.1.1. Signs and symptoms of NB 2

1.1.2. Etiology and risk factors of NB 2

1.1.3. Biological features of NB 3

1.1.4. NB staging and risk groups 4

1.1.5. Current therapies of NB and outcomes 6

1.2. CSC therapy 8

1.2.1. CSC theory: definition and experimental identification 8

1.2.2. Clinical implications of CSCs 9

1.2.3. CSCs in human NB 10

1.3. Salinomycin 11

1.3.1. Salinomycin as a coccidiostat 11

1.3.2. Pharmacokinetics and pharmacodynamics of salinomycin 12

1.3.3. Identification of salinomycin as CSC inhibitor 13

1.3.4. Anti-cancer effects of salinomycin 15

1.3.5. Possible molecular mechanisms of salinomycin 18

CHAPTER 2. MATERIALS AND METHODS 22

2.1. Cell culture 22
2.2. Drugs and chemicals 22
2.3. Transient transfections 22
2.4. Determination of cell proliferation 23
2.5. PI staining and flow cytometry analysis 24
2.6. Tumor-sphere formation assay 25
2.7. Binding protein identification 26
2.8. Mass spectrometry analysis 26
2.9. Peptide and protein identification 27
2.10. Western blotting analysis 28
2.10.1. Preparation of cell lysates 28
2.10.2. Protein concentration assay 28
2.10.3. Preparation of samples for loading into gels 29
2.10.4. Electrophoresis 30
2.10.5. Transfer 30
2.10.6. Blocking and detection 31
2.11. Analysis of cell surface markers by flow cytometry 32
2.12. Reverse transcription-quantitative PCR (RT-qPCR) 32
2.13. Immunoprecipitation assay 33
2.14. Immunofluorescence 34
2.15. Chromatin Immuno-Precipitation (ChIP)-qPCR assay 34
2.16. The expression levels of TIF1β and NCL in NB tumors and the correlation with NB patients' outcomes 39
2.17. Statistical analysis 39
CHAPTER 3. TO DETERMINE THE ANTI-CANCER EFFECTS OF SALINOMYCIN IN NB 40

3.1. Introduction 40

3.2. Results and Discussions 41

3.2.1. Determining the effects of Salinomycin on NB cell proliferation 41

3.2.2. Determining the role of salinomycin on NB cell cycle progression 42

3.2.3. Determining the role of salinomycin on cyclin A and p21 expression 44

3.2.4. Determining the role of salinomycin on NB tumorsphere formation 45

3.2.5. Determining the role of salinomycin on NB CSC like population 46

3.2.6. Determining the role of salinomycin on p53 48

CHAPTER 4. TO IDENTIFY THE FUNCTIONAL BINDING TARGET OF SALINOMYCIN IN NB 49

4.1. Introduction 49

4.2. Results and Discussions 50

4.2.1. Identification of potential binding targets of salinomycin by using DARTS analysis 50

4.2.2. Analysis of potential binding targets 51

4.2.3. Confirmation of the binding targets by western blotting analysis 53

4.2.4. Confirmation of the direct binding by IP assay 53

4.2.5. Baseline expression of TIF1β and NCL in NB cell lines 54

4.2.6. Knockdown of TIF1β and/or NCL in NB cell lines 55

4.2.7. Determining the effects of knockdown of TIF1β and/or NCL on NB cell proliferation and salinomycin's anti-proliferative effects 56

4.2.8. Determining the effects of knockdown of TIF1β and/or NCL on NB cell tumorsphere formation and salinomycin's anti-tumorigenic effects 57

CHAPTER 5. TO DETERMINE THE MECHNISM OF THE INTERACTION OF SALINOMYCIN WITH ITS BINDING TARGETS 59

5.1. Introduction 59

5.2. Results and Discussions 60

5.2.1. Effect of salinomycin on TIF1β expression in NB cells 60
5.2.2. Effect of salinomycin on the phosphorylation of TIF1β in NB cells 61
5.2.3. The role of TIF1β on salinomycin's regulation of p53 expression 61
5.2.4. Effects of salinomycin on the phosphorylation of NCL in NB cells 62
5.2.5. Effect of salinomycin on CD34 gene transcription 63
5.2.6. Effect of salinomycin on $CD34^+$ NB cells 64
5.2.7. The role of NCL on salinomycin's regulation of CD34 transcription 66
5.2.8. Subcellular localization and expression of NCL and CD34 upon salinomycin treatment 67
5.2.9. The role of NCL on salinomycin's regulation of CD34 protein expression 69
5.2.10. The role of NCL on salinomycin's regulation of $CD34^+$ cells 71
CHAPTER 6. SUMMARY, CLINICAL IMPLICATIONS, CONCLUSIONS, AND FUTURE DIRECTIONS 74
6.1. Summary and discussions 74
6.1.1. The effects of salinomycin in NB 74
6.1.2. Binding targets of salinomycin in NB 76
6.1.3. The mechanism of salinomycin in NB and the role of its binding targets 77
6.2. Clinical Implication 79
6.2.1. The correlation of TIF1β and NCL levels with NB patients' outcomes 79
6.2.2. The correlation of TIF1β and NCL levels with MYCN amplification 80
6.2.3. The correlation of the expression levels between TIF1β and NCL 82
6.3. Conclusions 82
6.4. Future directions 83
REFERENCES 87

LIST OF TABLES

Table Page

1. Symptoms of NB. 3
2. International Neuroblastoma Staging System 5
3. Biological factors and INRG risk groups. 6
4. Anti-cancer effects of salinomycin. 17
5. Sphere formation medium 25
6. Cell lysis buffer 28
7. Protein sample loading buffer (6 x) 29
8. Polyacrylamide gels for western blotting analysis 30
9. Primers and conditions used for the qRT-PCR 33
10. Buffer components for ChIP-qPCR. 36
11. Primers and conditions used for the ChIP-qPCR 38
12. Comparison of the anti-proliferative effects of salinomycin with other chemotherapeutic drugs in NB cells. 42

LIST OF FIGURES

Figure Page

1. Primary distribution of NB in children 1
2. Comparison between CSC therapy and conventional therapy 9
3. Structure of salinomycin 12
4. Research strategies for identification of salinomycin as a CSC inhibitor 14
5. Anticancer mechanisms of salinomycin 20
6. The effects of salinomycin on NB cell proliferation 41
7. The effect of salinomycin on NB cell cycle progression 43
8. Effects of salinomycin on cyclin A and p21 expression. 44
9. Salinomycin inhibits tumorsphere formation of NB cells 45
10. Salinomycin selectively inhibits CSC-like population ($CD133^+$ and c-kit^+ NB cells). 47
11. Salinomycin down-regulates p53 expression 48
12. Schematic presentation of the procedures of chemoproteomic strategy 50
13. Identification of salinomycin potential targets 51
14. Mass spectrometry analysis of potential salinomycin binding targets 52
15. Confirmation of NCL and TIF1β as salinomycin binding targets by Western blotting 53
16. Identification of salinomycin binding to NCL and TIF1β using anti-salinomycin affinity beads 54
17. Expression baseline levels of TIF1β and NCL in NB cells 55
18. Efficiency of siRNA knockdown of TIF1β and NCL in SH-SY5Y cells. 56
19. Salinomycin suppresses NB cell proliferation through NCL and TIF1β. 57
20. Tumorsphere formation assay of NB cells with NCL and TIF1β and salinomycin treatment.. 58
21. Effects of salinomycin on TIF1β expression levels in NB cells. 60

22. Salinomycin induces TIF1β serine 473/824 phosphorylation. 61

23. Salinomycin induces TIF1β serine 473/824 phosphorylation and associated down-regulation of p53. 62

24. Expression levels of NCL and phosphor-NCL in NB cells upon salinomycin treatment 63

25. Salinomycin inhibits CD34 gene transcription 64

26. Effect of salinomycin on CD34+ NB cells 65

27. A schematic diagram of the CD34 cDNA and the site for ChIP analysis 66

28. ChIP-qPCR analysis of NCL-CD34 promoter interaction 67

29. Decreased CD34 protein expression following exposure to salinomycin treatment 68

30. NCL sensitizes salinomycin's regulation on CD34 protein expression 70

31. Knockdown of NCL down-regulates CD34 protein expression and salinomycin's regulation on CD34 protein expression 71

32. Effect of salinomycin on $CD34^+$ NB cells in a NCL knockdown NB cells.. 72

33. Effect of salinomycin on $CD34^+$ NB cells in a NCL overexpression NB cells. 73

34. The expression of TIF1β and NCL in NB tumors and correlation of TIF1β and NCL levels with NB patients' outcomes.. 80

35. The correlation of TIF1β and NCL levels with poor prognostic markers 81

36. The correlation of TIF1β and NCL levels in NB patients. 82

37. Schematic representation of the interaction of salinomycin with its functional binding target proteins TIF1β and NCL in NB 83

LIST OF ABBREVIATIONS

ALDH	Aldehyde Dehydrogenase
ALK	Anaplastic Lymphoma Kinase
AML	Acute Myeloid Leukemia
BCRP	Breast Cancer Resistance Protein
CDDP	Cis-Diamminedichloroplatinum
CHCA	α-Cyano-4-Hydroxycinnamic Acid
ChIP	Chromatin Immunoprecipitation
CSCs	Cancer Stem cells
DARTS	Drug Affinity Responsive Target Stability
DMSO	Dimethylsulfoxide
DSS	Disuccinimidyl Suberate
EMT	Epithelial-Mesenchymal Transition
ES	Embryonic Stem
FBS	Fetal Bovine Serum
GIST	Gastrointestinal Stromal Tumors
GM-CSF	Granulocyte-Macrophage Colony-Stimulating Factor
HMLEs	Human Mammary Epithelial Cells
HNSCC	Head and Neck Squamous Cell Carcinoma
HSC	Hematopoietic Stem Cell
HSCT	Hematopoietic Stem Cell Rescue/Transplantation
INRG	International Neuroblastoma Risk Group
INRGSS	INRG Staging System
INSS	International Neuroblatoma Staging System

IP	Immuno-Precipitate
I-type	Intermediate-type
KIF1B	Kinesin-Like Protein 1B
LOH	Loss Of Heterozygosity
LRP6	Lipoprotein Receptor Related Protein 6
MDR	Multiple Drug Resistance
NEAA	Nonessential Amino Acids
MEM	Minimum Essential Medium
NB	Neuroblastoma
NB-CSCs	NB Cancer Stem Cells
NCL	Nucleolin
NF-κB	Nuclear Factor- κB
N-type	Neuroblastic-type
PES	Phenazine Ethosulfate
PHOX2B	Paired Mesoderm Homeobox Protein 2B
PI	Propidium Iodide
SCF	Stem Cell Factor
SD	Standard Deviation
S-type	Substrate-adherent-type
SPTA2	Spectrin Alpha II
TIF1β	Transcription Intermediary Factor 1-beta
TrkA	Tropomyosin receptor kinase A
TTL buffer	Tris-Triton Cell Lysis Buffer
uPA	urokinase-type Plasminogen Activator
5-Fu	5-Fluorouracil

CHAPTER 1. INTRODUCTION

1.1. Neuroblastoma (NB)

NB is a tumor derived from primitive neural crest cells of the sympathetic nervous system and is the most common extracranial solid tumor diagnosed in children as well as a predominant tumor in infants [1]. Each year, approximately 700 new cases are diagnosed in the United States [2]. This disease usually affects children under the age of five and can occur even before a child is born [2]. NB tumor most frequently originates in one of the adrenal glands, but can also develop in nerve tissues of other sides, such as neck, chest, abdomen, or pelvis (**Figure 1**). Unfortunately, at the time of diagnosis, in 50-70% of these cases, the disease has already metastasized [1].

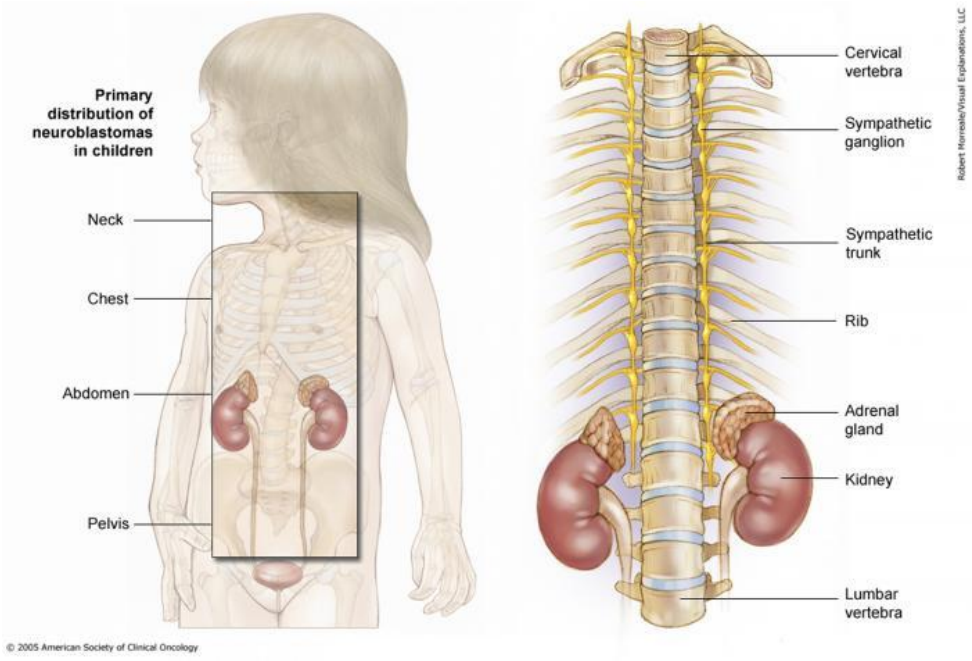

Figure 1. Primary distribution of NB in children (Illustration courtesy of the American Society of Clinical Oncology).

Recent advances in understanding the biology, pathology, and genetics of NB have allowed the classification of NB as low-, intermediate-, and high-risk groups. Although the outcomes for patients with low- or intermediate-NB are usually favorable, less than 40% of the children with high-risk NB respond to current available therapies [3, 4]. In addition, survivors of intermediate to high-risk NB often experience severe side effects caused by therapies currently in use, including hearing loss, alterations in growth and development, learning difficulties and greater risk of secondary cancers and disease relapse [1, 5, 6]. Thus, more effective and less harmful treatment strategies are pressingly needed.

1.1.1. Signs and symptoms of NB

Fatigue, loss of appetite, irritability, fever, and joint pain are common first symptoms of NB [1, 7, 8]. Since these symptoms can also be caused by medical conditions and diseases other than cancer, these vague signs make the early diagnosis of NB difficult. Along with the tumor growth, symptoms will be developed depend on the primary tumor locations and metastasis if present (**Table 1**).

1.1.2. Etiology and risk factors of NB

The etiology of NB is not well understood. The vast majority of NB cases are sporadic and non-familial. A small subset (~1-2%) of NB patients inherits a genetic predisposition to NB, such predisposition locus has been mapped at the short arm of chromosome 16 [9]. Rare germline mutations in the anaplastic lymphoma kinase (*ALK*) gene [10], paired mesoderm homeobox protein 2B (*PHOX2B*) gene [11], and kinesin-like protein 1B (*KIF1B*) gene have been implicated in familial NB [12].

Table 1. Symptoms of NB

Tumor location/ Tumor affecting organs	Major symptoms
Abdomen	Swollen belly; Constipation
Chest	Breathing problems
Spinal cord	Weakness; Inability to stand, crawl, or walk
Bone	Pain; Limping
Bone around the eyes or orbits	Distinct bruising and swelling
Bone marrow	Pallor from anemia; Bruising
Skin	Skin lesions or nodules under the skin with blue or purple patches
Eyes	Eyes bulge out; Dark circles under the eyes; Pupil constricted
Back	Weakness; Numbness; Paralysis of the legs
Hormone	Constant diarrhea; High blood pressure
Muscle	Sudden muscle jerks

The lifestyle-related risk factors playing major roles in many adult cancers, such as body weight, physical activity, diet, and tobacco use, were not found to play much of a role in NB as well as many other childhood cancers. In addition, no apparent environmental factor has been correlated with the incidence of NB. However, the incidence rates of NB are age dependent. The age of patients at diagnosis is mostly under 5 years old, and it is very rare in people over 10 years old [1, 13, 14].

1.1.3. Biological features of NB

Several molecular and cytogenetic features have been implicated in the pathogenesis and clinical prognosis of NB. For instance, near-triploidy DNA content has been associated with favorable outcome [15, 16], while *MYCN* oncogene amplification has been predominantly linked with more aggressive tumors [15, 17]. Besides the amplification of chromosome *2p24* locus where the *MYCN* gene located, trisomy for the long arm of chromosome *17* (17q) has been found

to occur in more than half of all NBs, and such gain of 17q is also associated with more aggressive NB [15, 18]. In addition, deletion of the short arm of chromosome *1* (1p) has been identified in 70-80% of the near-diploid tumors and is highly associated with *MYCN* amplification [15, 19]. The most common chromosome deletion detected so far is the allelic loss of chromosome *11q*, which was found in 43% of NB patients [20, 21]. Interestingly, this abnormality was implicated with lower event-free survival only in non-*MYCN* amplification patients with unknown reason [21]. Several abnormally expressed genes were also implicated in NB. For example, high levels of *Tropomyosin receptor kinase A* (TrkA) and TrkC gene expressions are highly correlated with favorable outcome, while its combination with MYCN amplification provides improved prognostic power [22]. Similarly, expression of the transmembrane receptor p75 has also been linked with favorable outcome [23]. In contrast, expression of full-length TrkB is strongly associated with *MYCN* amplification and is frequently observed in very aggressive NB tumors [24, 25], while truncated TrkB is usually found predominantly in more differentiated and lower-staged NB tumors [26].

1.1.4. NB staging and risk groups

On the basis of the anatomical presence of NB at diagnosis, the "International Neuroblastoma Staging System (INSS)" was established in 1986 and last revised on 1993 [27]. The criteria for different stages, from stage 1 to stage 4 special (4S), are shown in the following table (**Table 2**).

Table 2. International Neuroblastoma Staging System

Stages		Description
Stage 1 (21%)		Localized tumor confined to the area of origin. Tumor can be completely removed by surgery. Representative ipsilateral lymph nodes negative for tumor microscopically.
Stage 2 (15%)	**Stage 2A**	Localized tumor with incomplete gross resection. Representative ipsilateral non-adherent lymph nodes negative for tumor microscopically.
	Stage 2B	Localized tumor with/without complete gross resection. Representative ipsilateral lymph nodes positive for tumor microscopically. Identifiable contralateral lymph node negative for tumor microscopically.
Stage 3 (17%)		Un-resectable tumor infiltrating across midline with/without regional lymph node involvement; or localized tumor with contralateral region lymph node involvement; or midline tumor with bilateral lymph node involvement.
Stage 4 (41%)		Tumor disseminated to distant lymph nodes, bone, bone marrow, liver, or other organs except as defined by Stage 4S.
Stage 4S (6%)		Infant (Age <1 year old) with localized primary tumor with dissemination limited to skin, liver, or bone marrow.

Due to certain technical limitations of INSS criteria and the significantly advanced understanding of NB biology, especially the identification of the *MYCN* amplification and the application of recombinant DNA technology to screen chromosomal deletion, International Neuroblastoma Risk Group (INRG) project proposed a new pretreatment staging system uses established biological factors to predict how well treatment will work in the year 2009 [28]. Current risk stratification is designed on the basis of the new INRG Staging System (INRGSS), patient age, tumor grade, histopathology, DNA ploidy, as well as biochemical markers. The risk classification system of INRG and its associated molecular factors are shown in **Table 3** [29].

Table 3. Biological factors and INRG risk groups

Parameters	Low risk	Intermediate risk	High risk
MYCN	Normal	Normal	Amplified
Age	Usually < 1 year	Usually > 1 year	Usually >1 year
Stage	1, 2, 4S	2, 3, 4, 4S	2, 3, 4, 4S
DNA ploidy	Hyperdiploid, Near-triploid	Near-diploid, Near-tetraploid	Near-diploid, Near-tetraploid
17q gain	Rare	Common	Common
11q, 14q LOH	Rare	Common	Rare
1p LOH	Rare	Uncommon	Common
TrkA expression	High	Low or absent	Low or absent
TrkB expression	Truncated	Low or absent	High
TrkC expression	High	Low or absent	Low or absent
5-year survival rate	95%	90% to 95%	40% to 50%

Abbreviation: Loss of heterozygosity (LOH)

1.1.5. Current therapies of NB and outcomes

Risk based therapy is currently a hallmark of NB treatment. Patients with low risk NB may be cured by receiving surgery or chemotherapy alone, or even without any treatment [30]. Intermediate risk NB patients often receive chemotherapy before definitive resection. The amount and duration of chemotherapy is tailored based on the tumor biological risk factors and clinical parameters, as well as the patient's response to therapy [31]. Since some patients in recent studies have been observed successful resection without chemotherapy, to reduce the use of chemotherapy is a current trend to minimize side effects [32]. However, for patients with symptomatic life-threatening or organ-threatening tumor that does not respond to surgery and chemotherapy efficiently, radiation therapy will be applied [33].

Therapeutic strategies are much more complex for patients with high risk NB, which requires very intensive approaches and several types of treatments. Treatment is generally divided into three phases. During the "Introduction phase", dose-intensive cycles of chemotherapeutic drugs, such as cisplatin and etoposide alternating with vincristine, cyclophosphamide, and doxorubicin will be used, and the surgical resection of the primary tumor will be attempted after the response to chemotherapy [34]. The second phase is the "Consolidation phase", which involves myeloablative chemotherapy and hematopoietic stem cell rescue/transplantation (HSCT) and radiation therapy to the site of the primary tumor [34, 35]. However, the optimal dose of radiation therapy has not been determined. The "Maintenance phase" is the final phase to treat the potential minimal residual disease after the first two phases. Patients are usually treated with differentiating agent isotretinoin post HSCT for 6 months along with immunotherapy, such as using chimeric anti-GD2 antibody ch14.18 combined with Granulocyte-macrophage colony-stimulating factor (GM-CSF) and interleukin-2 [34-36]. Unfortunately, even with these intensive therapeutic approaches, the outcome for high risk NB is still unsatisfactory and the survivors of intermediate to high-risk NB often have to experience severe side effects.

The unsatisfactory clinical outcomes of NB underscore the need for the development of new treatments with novel action mechanisms. Recently, a stem cell like population in NB, namely NB cancer stem cells (NB-CSCs), has been linked with higher potential for treatment resistance and disease relapse [37-39]. CSCs in NB thus appear as attractive targets for novel therapeutics.

1.2. CSC therapy

CSCs are distinct rare cell populations identified in many cancers with the unique features including self-renewal and immortal [40]. Aberrant regulation of gene expression and some signaling pathways has been observed in CSCs [41]. Due to the close relationship of CSCs with cancer initiation, progression, metastasis, drug resistance, as well as cancer recurrence [41, 42], CSC-targeted therapeutic strategies are considered as a new promising direction for eradicating malignancies.

1.2.1. CSC theory: definition and experimental identification

CSCs are defined as cells within the tumor that capable of self-renewal and generating the heterogeneous lineages of cancer cells that comprise the tumor. One of the important early observations led to the CSC theory was that despite most tumors arise from a single cell; cells within a tumor are not identical. This phenomenon is also known as tumor heterogeneity, which supports the hypothesis that a small fraction of cells- the pluripotent CSCs- can generate bulk tumor cells with different phenotypes, which leads to the emergence and growth of tumor. The first conclusive experimental evidence was reported by Bonnet and Dick at 1997 on *Nature Medicin*e showing that a subpopulation of $CD34^+$ $CD38^-$ acute myeloid leukemia (AML) cells possess the capacities of self-renewal, differentiation, and proliferation and are able to reconstitute a heterogeneous tumor in NOD/SCID immune-deficient mice [43]. The first discovery of CSCs in solid tumor was followed in 2003 in human brain gliomas by isolating the clonogenic and sphere-forming CSCs [44]. With the advances in CSC biology and animal models, as well as the improvement on detecting technologies, currently, the CSC theory has

gained validation in many kinds of cancers, such as cancers in the breast, pancreas, prostate, head and neck, colon, liver, bladder and lung [41].

1.2.2. Clinical implications of CSCs

Current clinical treatment regimens shrink the bulk tumor cells but often fail to eradicate the CSCs, which might result in drug resistance and tumor recurrence. Thus, CSC theory provides a potential for the discovery and development of CSC-oriented therapies which may conquer the chemo- or radio-therapy resistant or refractory tumor (**Figure 2**).

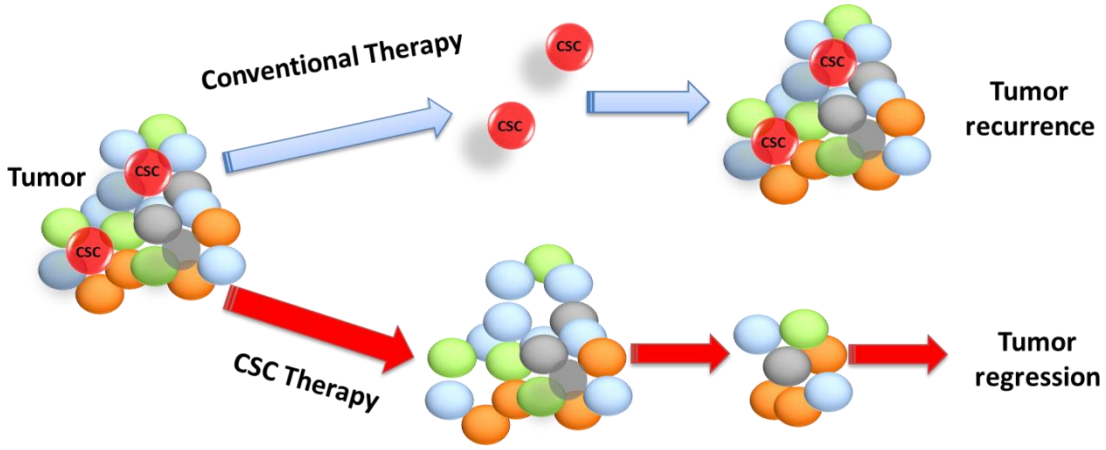

Figure 2. Comparison between CSC therapy and conventional therapy.

Over the past several years, a tremendous amount of efforts has been invested on developing CSC targeting therapy. To achieve more accurate CSC targeting and less side effect, one of the hot directions is to selectively target the CSC surface markers, such as CD44 [45], CD90 [46], CD133 [44] and CD33 [47]. For example, humanized anti-CD33 mouse monoclonal antibody conjugated with cytotoxic agent has been developed to be widely used in AML treatment [48, 49]. Critical signaling elements and pathways specifically involved in CSCs are also common targets for CSC therapy research, with the Notch, Wnt, Hedgehog, and NFκB

pathways most heavily studies and the inhibitions of these pathways have shown alluring potential to inhibit systemic metastases *in vitro* and *in vivo* [50]. ATP-driven efflux transporters are commonly up-regulated in CSCs [42]. Several molecular drugs inhibiting ABC cassette are currently under clinical trials and showed promising results. For instance, MS-209 have been found to overcome drug resistance in breast cancer and other cancers (*ClinicalTrials.gov Identifier: NCT00004886*) and the combination of the ABC inhibitor tariquidar with docetaxel, etoposide, mitotane, and vincristine plus surgery in treating patients with primary, recurrent, and metastatic adrenocortical cancer is now under phase II clinical trial investigation (*Clinical-Trials.gov identifier: NCT00073996*). Increasing evidence has suggested that therapeutic targeting CSCs may lead to improvement and even evolution of cancer treatment.

1.2.3. CSCs in human NB

During normal development, neural crest stem cells undergo differentiation in the process of embryogenesis to form the adrenal medulla and sympathetic ganglia. The failure of such proper differentiation leads to NB, which may develop in adrenal medulla and anywhere in the sympathetic nervous system [51]. Analyzing NB cells for lineage markers revealed that NB cells are of an immature neuroblastic phenotype which are characterized by weak expression of neuronal markers such as GAP-43, HNK-1, NPY, and chromogranin A & B [52, 53]. In addition, many NB cell lines contain a subset of cells harboring stem cell markers such as CD133, CD34, c-kit and nestin [37, 38, 54, 55]. Based on the phenotypes, NB cells are of heterogeneity origin [38, 52, 54, 55]. Recent study indicates that the major cause of therapy resistance or relapse is due to the existence of CSCs [39]. Indeed, it has been further demonstrated that a subset of NB cells expressing the stem cell marker proteins, such as CD133 and c-Kit, are highly tumorigenic and have more potential to develop therapy resistance [37, 38, 56]. Current conventional

therapies including chemotherapy, radiotherapy and immunotherapy may kill the large population of tumor cells but potentially leave behind the CSCs. Since the existence of CSCs in human NB cell lines and NB tumors from patients has been well documented by previous studies [1, 37, 39], therapeutic targeting of NB CSCs may be a critical novel approach to conquer the challenges in the treatment of NB. To this end, understanding the mechanism of the CSC targeting drugs and identifying their molecular targets may improve the understanding and treatment of NB.

1.3. Salinomycin

Salinomycin, traditionally used as an anticoccidial drug, has recently been shown to possess anti-cancer and anti-CSC activities and also to overcome multi-drug resistance in numerous studies using human cancer cell lines and xenograft mice as well as in clinical pilot studies in cancer patients. Therefore, salinomycin may be considered as a promising novel anti-cancer agent despite its largely unknown mechanism of action.

1.3.1. Salinomycin as a coccidiostat

Salinomycin (molecular formulae, $C_{42}H_{70}O_{11}$) is a monocarboxylic polyether antibiotic isolated from *Streptomyces albus* strain (Stain No. 80614) (**Figure 3**). The usage of salinomycin in veterinary medicine can be traced back to 1980s [57] as a broad spectrum antimicrobial agent with activity against gram-positive bacteria, fungi, and parasites [57-59]. Today, salinomycin is one of the most widely used coccidiostats in poultry in the United States [59-63].

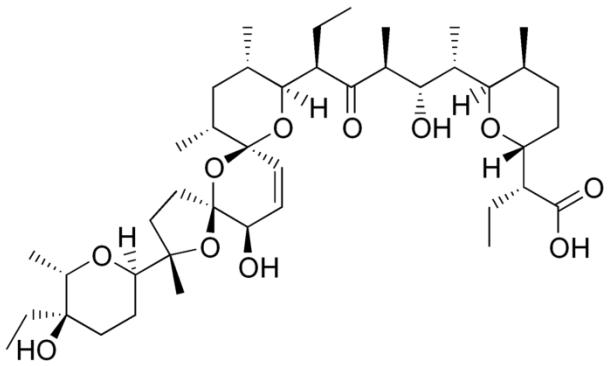

Figure 3. Structure of salinomycin.

As an antimicrobial drug, salinomycin primarily functions as an ionophore that facilitate the transport of cations (K^+, Na^+, Ca^+ or Mg^{2+}) through cell membranes of the target organisms including protozoa and gram-positive bacteria. Most notably, such facilitated transport increases intracellular calcium to levels toxic to coccidians, by inducing the selective disposition of osmoregulatory organelles in the cell thereby disrupting the osmotic balance and resulting in eventual demise of the responsive organisms [64, 65]. However, such ionophoric properties and mechanisms are unlikely to suffice or even applicable for explaining the observed specificity of salinomycin on CSCs and multidrug resistant cancer cells. Indeed, several studies have shown that salinomycin activates unconventional pathways of cell death, increases DNA damage, and inhibits Wnt signaling pathway, all of which purportedly have been linked to anti-cancer activities of salinomycin in various types of cancers [66-72].

1.3.2. Pharmacokinetics and pharmacodynamics of salinomycin

The pharmacokinetic parameters of salinomycin as an antimicrobial and anticoccidial antibiotic have been extensively studied in many animal species. By virtue of its lipid solubility, it is readily and rapidly absorbed in the gastro-intestinal tract and distribute throughout the serum

and tissues. In respect to tissue distribution, fat tissues showed the highest affinity for salinomycin followed by liver and muscle tissues in chicken [73]. Salinomycin is able to penetrate blood brain barrier, though the existence of P-glycoprotein could limit its oral availability and brain penetration [74]. Liver is the primary metabolism site for salinomycin and its rapid metabolism of salinomycin yields a spectrum of numerous metabolites [75]. The elimination of salinomycin is moderately fast. It has been suggested that 24 hours should be an adequate withdrawal period for salinomycin in chickens [73]. The oral LD50 values of salinomycin in broiler chickens and laying hens were 108 and 104 mg/kg body weight respectively [76], while the reported LD50 value of salinomycin in horse is only 0.6 μg/kg [77, 78].

In a recent reported case study, a patient with advanced and metastatic squamous cell carcinoma of the vulva received intravenous administration of 200-250 μg/kg salinomycin every second day combined with other chemotherapeutic drugs such as erlotinib showed favorable clinical effects [79]. Though the pharmacokinetic parameters of salinomycin as an anticoccoidal agent have been established and may provide insights on pharmacokinetic/pharmacodynamic studies of salinomycin in CSCs and human cancer cells, the pharmacokinetic/pharmacodynamic studies of salinomycin in CSCs and human cancer cells are still not clear and deserve further investigation.

1.3.3. Identification of salinomycin as CSC inhibitor

Accumulating evidence shows that the presence of CSC is the major cause of cancer recurrence after therapy, attributable to CSCs' self-renewal and tumor initiating capability which can repopulate the tumor mass and consequently resist to therapy [40, 41, 80, 81]. Moreover, in clinical studies, CSCs also present significant challenge owing to their unique endowment with

an enhanced DNA repair system, up-regulation of drug efflux pumps and robust expression of anti-apoptotic proteins [39, 42, 82, 83]. Therefore, eradication of CSCs may be considered as a key to the circumvention of cancer relapse and chemo-resistance, the major obstacles in current cancer therapy. Whereas the epithelial-mesenchymal transition (EMT) has long been recognized as a key feature of cancer invasion and metastasis [84-86], Mani et al. (2008) showed that the induction of EMT in both human mammary epithelial cells (HMLEs) and mammary carcinomas is accompanied by the enrichment of cells with epithelial stem cell properties [87]. Subsequently, Gupta et al. showed that EMT transformation of HMLER breast cancer cells (human mammary epithelial cells overexpressing hTERT, SV40 T/t and H-RasV12) resulted in the appearance of tumorigenic and chemo-resistant CSC like cells (HMLER^{shEcad}) (**Figure 4**). Using these CSC like cells as an *in vitro* model system, Gupta et al. (2009) screened over 16,000 compounds using a high-throughput strategy and identified that salinomycin was the only one showing both high selectivity and strong efficacy in depleting breast CSCs *in vitro* (**Figure 4**).

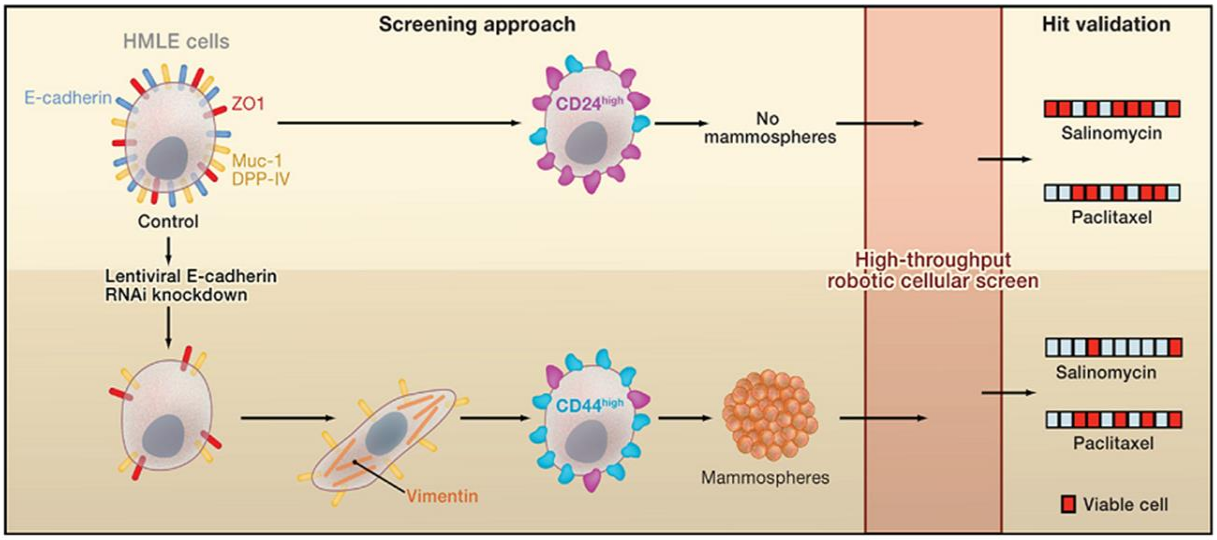

Figure 4. Research strategies for identification of salinomycin as a CSC inhibitor [88].

Indeed, the pharmacological efficacy of salinomycin is more than 100-fold potency than paclitaxel, a commonly used anti-breast cancer drug [89], and displayed profound inhibitory activity on tumor seeding, growth and metastasis in NOD/SCID mice *in vivo* [89]. The extraordinary properties and presumed clinical implications of salinomycin discovered by this seminal research laid the foundation for a flurry of studies conducted thereafter examining salinomycin's anti-cancer effects in various cancer types and model systems. **Table 4** summarizes the effects of salinomycin on various types of cancer and cancer stem cells, providing cumulative compelling evidence for its consideration as a promising anti-cancer drug for cancer therapy [66, 67].

1.3.4. Anti-cancer effects of salinomycin

Following the discovery of salinomycin as a CSC killer, the pharmacological effects of salinomycin have been tested *in vitro* and *in vivo* (**Table 4**). For instance, $CD133^+$ as a marker of cancer stem cell in many cancer types was utilized by Dong et al. to demonstrate that $CD133^+$ colorectal cancer stem cell like cells were sensitive to salinomycin treatment, but not to conventional treatment oxaliplatin, in respect to cell proliferation, colony formation, cell migration and invasion. The observed effects were accompanied by an up-regulation of the epithelial cell marker E-cadherin expression and a suppression of the mesenchymal cell marker Vimentin, thereby further implicating the inhibitory effect on the EMT process by salinomycin [90]. Consistent with this finding, Basu et al. observed that the mesenchymal-like subpopulations within squamous cell carcinomas show resistance to conventional cytotoxic therapy but not to salinomycin *in vitro* and *in vivo* [91]. $Kit^{low}CD44^+CD34^-$ cells in gastrointestinal stromal tumors (GIST) are clonogenic cells with the capability of self-renew and differentiation. Bardsley et al.

shows that salinomycin blocked the proliferation of $Kit^{low}CD44^{+}CD34^{-}$ cells and increased their sensitivity to imatinib in mice [92]. Human leukemia stem cell-like KG-1a cells are known to exhibit resistance to chemotherapeutic drugs via the expression of functional ABC transporters such as P-glycoprotein, breast cancer resistance protein (BCRP), and MRP8 which are capable of increasing efflux of drugs. Fuchs et al. observed severe cytotoxic effects of salinomycin on KG-1a cells. Unlike the conventional chemotherapeutic drugs, such as etoposide and doxorubincin, salinomycin is able to overcome ABC transporter-mediated multidrug and apoptosis resistance [93]. Riccioni and colleagues further reported salinomycin as a P-glycoprotein inhibitor by showing its inhibition of the cell growth of P-glycoprotein overexpression multiple drug resistance (MDR) cancer cell lines and the P-glycoprotein mediated drug efflux [94]. Moreover, the selective cytotoxic effect of salinomycin on tumor stem cells was also detected in osteosarcoma *in vitro* and *in vivo*. Salinomycin also sensitizes these CSCs to conventional chemotherapy drugs including methotrexate, adriamycin, and cisplatin [95]. Very recently, salinomycin shows profound cytotoxicity on aldehyde dehydrogenase (ALDH) high stem like gastric cancer cell lines surpassing 5-fluorouracil (5-Fu) and cis-diamminedichloroplatinum (CDDP) [96]. The combinatorial treatment with trastuzumab and salinomycin by targeting HER2-positive cancer cells and CSCs together has led to enhanced cell death in mammospheres [97]. Due to its promising anticancer activity, a few clinical case studies of salinomycin have been conducted in therapy-resistant cancer patients, e.g. a patient with metastatic invasive ductal breast cancer, and revealed potential strong efficacy of salinomycin on eliminating CSCs and inducing clinical tumor regression [79]. All the aforementioned studies strongly suggest that salinomycin is a new promising agent for cancer therapy.

Table 4. Anti-cancer effects of salinomycin

Cancer Type	Cancer Cell	CSC or Cancer Stem Like Cell	Chemo- or Radio-resistant Cancer Cell	Reference
Breast Cancer	√	√	√	[67, 69, 89, 97-102]
T cell Leukemia	√		√	[68]
Human Acute Lymphoblastic Leukemia	√		√	[68]
Human Uterus Sarcoma	√		√	[68, 69]
Burkitt's Lymphoma	√		√	[68]
Human Promyeloblastic Leukaemia	√	√	√	[93]
Murine Gastrointestinal Stromal Tumors		√		[92]
Human Liver Hepatocellular Carcinoma	√			[69]
Human Lung Adenocarcinoma	√	√		[103]
Human Colorectal Cancer	√	√		[90, 98]
Squamous Cell Carcinomas	√		√	[91, 104]
Chronic Lymphocytic Leukemia	√			[71]
Osteosarcoma		√	√	[95]
Prostate Cancer	√			[105-107]
Gastric Cancer		√		[92, 96]
Pancreatic Cancer	√			[108]
Human Ovarian Epithelial Cancer	√			[94]
Human Ovarian Cancer	√			[109]
Human Cholangiocarcinoma	√			[110]
Human Glioblastoma	√	√		[111, 112]
Human Medulloblastoma	√			[113]

Table 4. Anti-cancer effects of salinomycin (continued)

Cancer Type	Cancer Cell	CSC or Cancer Stem Like Cell	Chemo- or Radio-resistant Cancer Cell	Reference
Human Uterine Leiomyoma	√			[114]
Human Nasopharyngeal Carcinoma	√			[115]

1.3.5. Possible molecular mechanisms of salinomycin

As mentioned previously, the ionophoric attributes of salinomycin underlying its efficacy in protozoa and gram-positive bacteria may not be applicable for explaining its ability to eradicate CSCs or circumvent multidrug resistance in responsive cancer cells. Instead, activation of unconventional pathways of cell death, enhanced DNA damage, and inhibition of Wnt signaling pathway, appear to be more germane to the multi-dimensional anti-CSC and anti-tumorigenic activities of salinomycin [66-71]. Fuchs and colleagues showed that salinomycin induces apoptosis in human cancer cells and overcome apoptosis resistance through a pathway independent of activation of p53, caspase, CD95/CD95L system and the proteasome [68]. Kim et al. observed that salinomycin induces massive cell apoptosis accompanied with caspase-3 activation and cleavage of PARP-1 in human prostate cancer cells which is attributed to accumulated ROS and mitochondrial membrane depolarization [105]. Ketola and colleagues showed that increased levels of oxidative stress play important roles in salinomycin induced prostate cancer cell growth inhibition [106].

Kim et al. demonstrated that combined administration of salinomycin with doxorubicin or etoposide led to increased DNA damage and resulted in massive apoptosis in drug resistant cancer cells [69]. Mechanistic studies revealed that by increasing DNA damage through

enhancing the expression levels of p53 and H2AX and reducing the expression of anti-apoptotic p21, salinomycin sensitizes cancer cells to DNA damaging agents, doxorubicin and etoposide [69]. In a separate study, salinomycin treatment increased DNA damage and induced G2 arrest, thereby, sensitizing cancer cells to radiation treatment. Similarly, salinomycin could suppress the elevated p21 level resulted from radiation treatment and promote the expression and activation of H2AX and p53 [70]. These studies suggested that patients may benefit from the combined use of salinomycin with other chemotherapeutic drugs and radiation therapy.

A recent report from Verdoodt and colleagues raised, for the first time, that the autophagic cell death is another mechanism of induced cell death elicited by salinomycin in colon and breast cancer cells [31]. This conclusion was based on the phenomenon that cell death induced by salinomycin accompanied with common features of autophagy such as formation of the multiple vacuoles and increased uptake of autophagy markers. Most recently, the induction of ROS and its consequently activation of JNK pathway have also been observed and linked to salinomycin induced autophagic cell death [98]. In addition to the inhibition of cell viability and induction of cell death, Kuo et al. observed that salinomycin induces differentiation of head and neck squamous cell carcinoma (HNSCC) stem cells associated with the activation of EMT and the phosphorylation of Akt [104].

Wnt signaling is critical for mammalian development, stem cell renewal, and cancer progression [116, 117]. Lu et al. have discovered that nanomolar concentrations of salinomycin exhibit profound inhibition on Wnt signaling which is otherwise constitutively activated in chronic lymphocytic leukemia cells and the expression of Wnt target genes were subsequently down-regulated [71]. This study further showed that salinomycin interrupts Wnt signaling by impeding the phosphorylation of lipoprotein receptor related protein 6 (LRP6), a Wnt co-

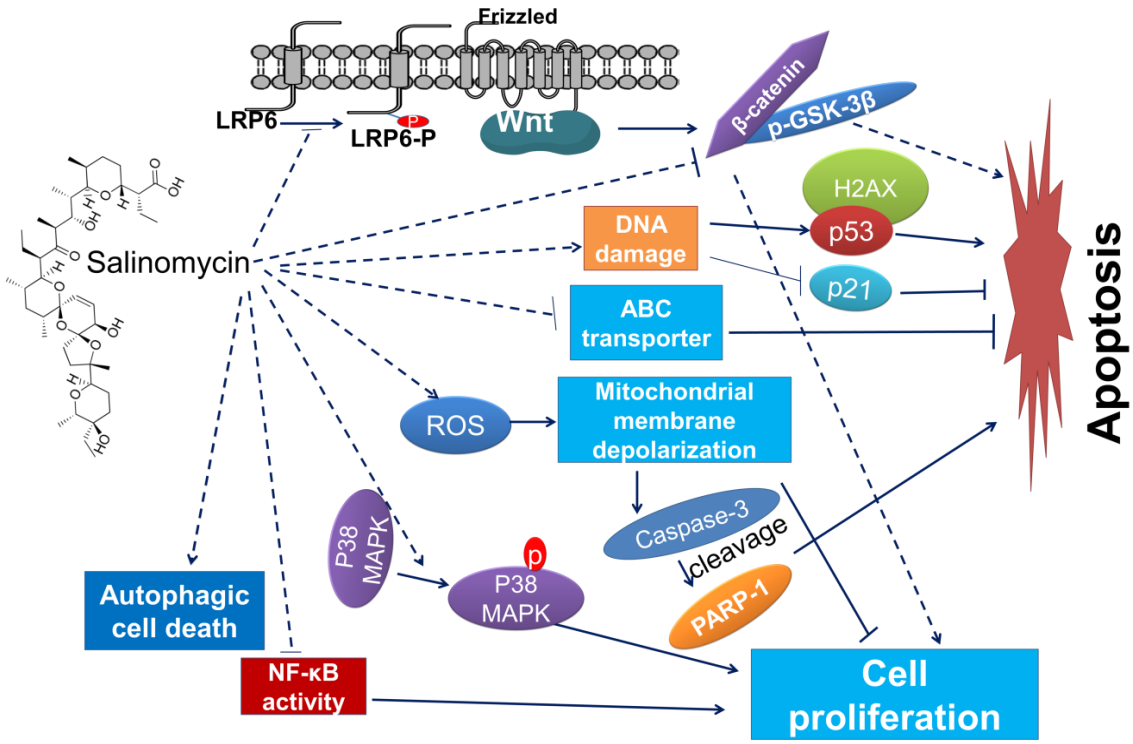

Figure 5. Anticancer mechanisms of salinomycin [72]. Salinomycin exerts its inhibition on Wnt signaling pathway through its suppression on the phosphorylation of LRP6 and the expression of β-catenin and p-GSK-3β. It also induces the production of ROS and mitochondrial membrane depolarization, which consequently results in the activation of caspase-3, the induction of PARP-1cleavage, and the elicitation of DNA damage. These events subsequently induce tumor cell death and inhibit cancer cell growth. Moreover salinomycin is able to induce autophagic cell death and inhibiting NF-κB pathway and activating p38 MAPK pathway through so far unclear mechanisms [69-71, 98, 105-107, 109, 121].

receptor, and consequently resulting in its degradation [71]. Nuclear factor- κB (NF-κB) is critical for multiple cellular functions, such as cell proliferation and defense of oxidant induced cellular damage, which are key elements for tumorigenesis and metastasis [118, 119]. Notably, NF-κB pathway is activated in prostate stem-like tumor-initiating cells and suppression of NF-κB results in prostate CSC apoptosis [107]. By using a luciferase reporter assay, Ketola et al. have shown that growth inhibition and induction of oxidative stress in prostate cancer cells is mediated by salinomycin via the suppression of NF-κB pathway activity [106]. More recently, Zhang and colleagues discovered that salinomycin-induced apoptosis in OV2008 ovarian cancer

cells is associated with activating p38 MAPK signaling, a critical pathway in cancer development [109, 120]. We have also observed the inhibitory effects of salinomycin on Notch and PDGFR signaling pathways [113]. The major pathways affected by salinomycin are summarized in **Figure 5**.

However, the exact mechanism of how salinomycin regulates the complex cell signaling in cancer and CSCs remains largely unclear, especially the cellular targets of salinomycin are not known, underscoring the requirement for further studies and elucidation of its mechanism of action.

CHAPTER 2. MATERIALS AND METHODS

2.1. Cell culture

NB cell lines, SH-SY5Y, IMR32, and SK-N-AS, were obtained from ATCC. Cells were maintained in Minimum Essential Medium (MEM) (Cellgro, Catalog # 15-010) supplemented with 4 mM L-glutamine (ATCC, Catalog # 30-2214), 100 units/ml penicillin (Gibco, Catalog # 15140-122), 100 µg/ml streptomycin (Gibco, Catalog # 15140-122), 1% sodium pyruvate (Cellgro, Catalog # 25-000-CI), 1% nonessential amino acids (NEAA, Gibco, Catalog # 11140), and 10% fetal bovine serum (FBS, ATCC, Catalog # 30-2020) at 37°C with 5% CO_2.

2.2. Drugs and chemicals

Salinomycin (Catalog # S4526) and propidium iodide (PI, Catalog # 81845) were purchased from Sigma. Formaldehyde was purchased from Alfa Aesar (Ward Hill, MA). Dimethyl sulfoxide (Catalog # 472301), ethanol (absolute, 200 proof, for molecular biology, Catalog # E7023), sodium phosphate (Catalog # S3264), sodium bicarbonate (Catalog # S6014), sodium chloride (Catalog # S5886), caps (Catalog # C2632), glycine (Catalog # G8898), Trizma base (Catalog # T1503), and Triton X-100 (Catalog # T9284) were obtained from Sigma. Glycerol (Catalog # IC800688) was purchased from VWR. Ammonium persulfate (Catalog # AC201531000) was purchased from ACROS Organics.

2.3. Transient transfections

For transient transfection, NB cells were seeded (1 x10^6 /well) in 6-well plates a day before transfection, and TIF1β (Life Technology, Catalog # AM16708), NCL (Qiagen, Catalog # GS4691) siRNA, GFP plasmids (Addgene, [Plasmid # 11153]) [122], or GFP-NCL plasmids

(Addgene [Plasmid # 28176]) [123] was transfected transiently with Lipofectamine 2000 (Invitrogen, Catalog # 11668027) in opti-MEM (Life Technology, Catalog # 51985091) reduced serum medium for 4 h following the manufacturer's instruction. Briefly, for each well to be transfected, siRNA stock solution (100 µM, in RNase free water) was diluted in 250 µL Opti-MEM reduced serum medium to final concentrations of 100 or 150 nM and mixed with 15 µL of transfection reagent pre-diluted in 250 µL Opti-MEM. For each well to be transfected, plasmids DNAs were diluted in 250 µL Opti-MEM reduced serum medium to final amount of 2500 ng. After 5 min incubation at room temperature, the transfection mixes were added to the cells in a final volume of 2 mL medium. The serum starved cells were then replaced with equal volume of MEM medium and kept in culture for 24 h or 48 h at 37°C in a CO2 incubator. Cells were then harvested for total RNA for PCR and protein for Western blotting analysis.

2.4. Determination of cell proliferation

The CellTiter 96® AQueous One Solution Cell Proliferation Assay is a colorimetric method to determine the number of viable cells in proliferation or cytotoxicity assays. The CellTiter 96® AQueous One Solution Reagent contains a novel tetrazolium compound [3-(4,5-dimethylthiazol-2-yl)-5-(3-carboxymethoxyphenyl)-2-(4-sulfophenyl)-2H-tetrazolium, inner salt; MTS] and an electron coupling reagent (phenazine ethosulfate; PES). PES has enhanced chemical stability that allows it to be combined with MTS to form a stable solution. The MTS tetrazolium compound is bioreduced by cells into a colored formazan product that is soluble in tissue culture medium. This conversion is presumably accomplished by NADPH or NADH produced by dehydrogenase enzymes in metabolically active cells. The quantity of formazan

product as measured by the absorbance at 490nm is directly proportional to the number of living cells in culture.

To analyze the cell proliferation, NB cells (1 x10^5 /well) maintained in complete medium were placed in 96-well plates overnight. Salinomycin at various concentrations or identical volume of control (DMSO) was added to the appropriate wells. The cells were treated for 48 hr before adding 20 µl of MTS solution (Promega, Catalog # G3580). After 4 hr incubation, the number of cells in each well was determined by measuring the optical densities at 490 nm. The results were expressed as the percentages of the control cultures. Experiments were performed in triplicate. The results are presented as percentage normalized to the value in the control group.

2.5. PI staining and flow cytometry analysis

Cells (1 x10^6 /well) maintained in complete medium were placed in 6-well plates overnight. Salinomycin or identical volume of control (DMSO) was added to the appropriate wells. The control and treated cells were cultured for additional 24 hr, and the cells were then treated with 10 µL ribonuclease A (Catalog # R6513) (10 mg/mL) and 400 µL PI (50 µg/mL) for 30 min at room temperature in the dark. PI is a fluorescent dye that binds specifically to DNA. This property has led to its common use in evaluation of cell cycle, aneuploidy and apoptosis by flow cytometry. When excited by a laser light at 488 nm, PI emits a signal that can be monitored by the red wavelength detector. Cell cycle data were acquired on the Cell Lab Quanta^{TM} SC system (Beckman Coulter) and red fluorescence (PI=DNA content) was collected in FL3 detector. The percentage of cells in different phases of the cell cycle was computed using Flow Jo (TreeStar, OR). At least 10,000 cells were analyzed.

2.6. Tumor-sphere formation assay

Tumorsphere formation assay was performed using a previous reported method [38]. Tumorsphere-media consisted of a 50:50 mix of F12 and DMEM (Invitrogen, Catalog # 11320-033), supplemented with 20 ng/ml EGF (R&D systems, Catalog # 236-EG-01M), 40 ng/ml bFGF (R&D systems, Catalog # 233-FB-01M), 1% B27 (Life technology, Catalog # 17504-044) and N2 supplements (Life technology, Catalog # 17502-048), 2 µg/ml heparin (Sigma, Catalog # H3393), 0.1 mM β-mercaptoethanol (Sigma, Catalog # M6250) and 1× antibiotic/antimycotic (Mediatech, Catalog # 30-004-CI).

Table 5. Sphere formation medium

	Stock	Volume
DMEM:F12	1 x	48.089 mL
EGF	10 µg/µL	1 µL
bFGF	5 µg/ml	400 µL
N2	100 x	500 µL
Heparin	10 µg/µL	10 µL
Antibiotics	100 x	500 µL
B27 (before use)	100 x	500 µL

200 cells were seeded in 200 µl medium into each well in Ultra-low attachment 96 well plate (Corning, Catalog #3474). The numbers of tumorsphere formed in each condition were counted at day 7 under phase-contrast microscope using the 10x magnification lens.

2.7. Binding protein identification

Binding protein identification was performed by a modified method as previously described [124]. Briefly, SH-SY5Y cells ($2x10^6$) were treated with salinomycin or DMSO as control and 40 min later, cells were lysed with TTL buffer. After centrifugation (32,869 g) using Thermo Scientific Microfuge 11R with F14 rotor, 10 min, lysates were diluted to the same final volume and protein concentration with cell lysis buffer. All steps were performed on ice or at 4 °C to prevent premature protein degradation. 50 µg of lysate was then quickly warmed to room temperature and proteolysed with 100 ng of thermolysin for 10 min. To stop proteolysis, 0.5 M EDTA (pH 8.0) was added to each sample at a 1:10 ratio, mixed well, and placed on ice. Samples were then boiled in SDS-PAGE sample buffer and subjected to 12% Tris-HCl SDS-PAGE and EZBlue^{TM} Gel Staining (Sigma).

2.8. Mass spectrometry analysis

In-gel trypsin digestion was performed using a similar method to the published procedures [125]. Gel bands were excised and destained. Proteins were reduced in-gel with 4 mM dithiothreitol in 50 mM ammonium bicarbonate for 15 min at 60^{o}C. Iodoacetamide was added to make 16 mM and alkylation was allowed to proceed for 30 min at room temperature in the dark. The reaction was quenched with an additional 3 mM dithiothreitol. The gel slice was then equilibrated with ammonium bicarbonate, dehydrated with 100% acetonitrile (ACN), and rehydrated in 0.02 µg Trypsin Gold (Promega) in 40 mM ammonium bicarbonate. Digestion was allowed to proceed overnight at 37 ^{o}C. Approximately 50 µl of peptides were extracted. The samples were acidified with formic acid to make 0.1% final concentration. Samples were analyzed by rpHPLC and spotted onto a MALDI target plate using a TEMPO-LC integrated

nanoflow HPLC/spotter. A total of 8.8 µl sample was injected onto a Protecol C18 0.3 x 10 mm trap (3 µm 300A pore size). The samples were desalted with 2% ACN/0.1% formic acid v/v (Buffer A) for 10 min at a flow rate of 10 µl/min. Peptides were eluted in-line through a 0.1 x 100 mm Magic AQ C18 (5 µm) column using a 30 min gradient from 100 % Buffer A to 60% Buffer A, /60% Buffer B (98% ACN/0.1% formic acid) at a flow rate of 1 µl/min. Eluate was mixed post-column with an equal volume of 10 mg/ml α-cyano-4-hydroxycinnamic acid (CHCA) in 75% ACN/0.1% formic acid. The matrix/eluant mix was spotted at 18 sec/spot. Column was regenerated at 70% ACN/0.1% formic acid. Spot sets were analyzed on an AB4800 MALDI TOF/TOF mass analyzer. The m/z range was 800-4000. Top 10 precursors per spot were selected for MS/MS with the weakest precursor first.

2.9. Peptide and protein identification

Raw spectra were converted to T2D files using 4000 series Explorer version 3.5.28193. These files were submitted to Mascot Distiller v.2.3.2. (Matrix Science) to generate uncentroided peak lists. Processed spectra were searched against Swissprot database (v. 57.15) using Mascot v. 2.3.02 (Matrix Science). The search parameters were trypsin with up to one missed cleavage, carbamidomethyl (C) as fixed modification. Variable modifications were Acetyl (Protein-N-term), ammonia loss (N-term C), Gln>pyro-Glu (N-term Q), Oxidation (M). Mass values were monoisotopic. Peptide mass tolerance was 100 ppm and fragment ion tolerance was 0.25 Da. Mascot searches were combined and analyzed in Scaffold v. 3.00.08 (Proteome Software, Inc.) to validate peptide and protein identifications. Peptide identifications with >95% probability and protein identifications with > 99% probability and at least two identified peptides were accepted.

2.10. Western blotting analysis

2.10.1. Preparation of cell lysates

Whole cell lysates were prepared by using Tris-Triton cell lysis buffer (TTL buffer, 1% Triton X-100, 50 mM Tris-HCl pH 7.4, 5% glycerol, 100 mM NaCl) supplemented with protease inhibitor cocktail (Roche Applied Science) and phosphatase inhibitor cocktail 100x (Cell Signaling). 150 µL of cell lysis buffer was added to each well of the 6 well plate and incubated for 10 min on ice. Cells in the 6 well plate were then scraped with a plastic scraper. The lysate was collected in 1.5 mL centrifuge tubes and then centrifuged at 24149 g for 10 min at 4 °C. The supernatant was collected and stored at -80 °C for further analysis.

Table 6. Cell lysis buffer

	Volume (3 mL)
1 M Tris, pH7.4	1.5 mL
5 M Nacl	60 µL
Glycerol	150 µL
Triton X-100 (100%)	30 µL
Protease inhibitor	600 µL
dH2O	660 µL

Proteinase inhibitor stock solution: one tablet in 10 ml water

2.10.2. Protein concentration assay

The protein concentration in the cell lysates was measured using a Bio-Rad Protein Assay Dye Reagent Concentrate (Bio-Rad, Catalog # 500-0006) according to the manufacturer's instructions. The basic principle for the protein concentration assay is based on that the

absorbance maximum for an acidic solution of Coomassie Brilliant Blue G-250 dye shifts from 465 nm to 595 nm when binding to protein occurs.

For each 10 μL of protein standard or diluted cell lysate, 200 μL of the diluted Bio-Rad Protein Assay Dye Reagent Concentrate were added in each well of a 96-well plate. Solutions were incubated at room temperature for 5-20 min and analyzed using a Microplate reader (SpectraMax M5, Molecular Devices) at 595 nm. Comparison to a standard curve using bovine serum albumin (BSA) standard solutions provides a relative measurement of protein concentration.

2.10.3. Preparation of samples for loading into gels

Sufficiently denature sample protein can ensure target protein fall into the expected molecule weight range, because it can reduce the influence from higher structures which may lead to variance in electrophoretic velocity. After equilibrated to the same concentration, samples were denatured at 95 °C for 5 min in SDS-PAGE sample loading buffer. The samples can be stored at -80 °C for further analysis.

Table 7. Protein sample loading buffer (6 x)

	Volume (10 mL)
500 mM Tris-HCL, pH 6.8	7 mL
Glycerol	3 mL
SDS	1 g
DTT	0.93 g
Bromphenol blue	1.2 mg

2.10.4. Electrophoresis

The protein samples were separated using polyacrylamide gel electrophoresis based on the premise that the negatively charged (by SDS) protein samples will move to the positively charged electrode through the acrylamide mesh of the gel. Smaller proteins migrate faster and the proteins are thus separated according to size. The concentration of acrylamide determines the resolution of the gel.

Table 8. Polyacrylamide gels for western blotting analysis

	Resolving Gel (10%)	**Stacking Gel (4%)**
1.5 M Tris buffer (pH 8.8)	1.9 mL	
1.0 M Tris buffer (pH 6.8)		1 mL
H_2O	2.95 mL	2.25 mL
Acrylamide/bis-acrylamide (30 % solution)	2.5 mL	625 µL
10% SDS	75 µL	40 µL
10 % APS	75 µL	40 µL
TEMED	3 µL	4 µL

2.10.5. Transfer

In order to make the proteins accessible to antibody detection, they were transferred by electric current from the gel to nitrocellulose membrane. Sponges, filter paper and nitrocellulose membrane were soaked in transfer buffer (10 mM CAPS pH 10.5, 20% (v:v) methanol) for 15 min. The gel was then placed in the "transfer sandwich" composed of sponge-filter paper-gel-nitrocellulose membrane-filter paper-sponge, and pressed together by a support grid. This supported gel sandwich was then placed in the tank filled with transfer buffer. The proteins were then electro-transferred to the membrane at constant current (200 mA) for 2 h on ice.

2.10.6. Blocking and detection

Blocking the membrane prevents non-specific background binding of the primary and/or secondary antibodies to the membrane. The membrane was soaked in TBST 5% milk solution (TBST= 2L 1*TBS +2ml 1*Tween; 10x TBS: 176g NaCl, 24.22g Tris base, 2L water, pH 7.4) with shaking at room temperature.

Western blot relies on the primary antibody to detect the protein of interest from the thousands of proteins on the membrane. Using an antibody recognizes the primary antibody (a secondary antibody), a protein-primary antibody-secondary antibody sandwich will be established. The secondary antibodies are usually labeled with horse radish peroxidase enzyme, which, in the presence of its substrates, will emit light during the enzyme catalyzed reaction.

Immunoblots were probed with antibodies specific for TIF1β (Abcam, Catalog # ab10483), NCL (Abcam, Catalog # ab22758), anti-TIF1β-phosphorylated (Ser473) (Biolegend, Catalog # 644602), anti-TIF1β-phosphorylated (S824) (Abcam, Catalog # ab10483 ab70369), purified anti-Nucleolin-phosphorylated (Thr76/Thr84) (Biolegend, Catalog # 609403), p53 (Santa Cruz, Catalog # sc-1311-R), Bcl-2 (Santa Cruz, Catalog # sc-492), cyclin A (Santa Cruz, Catalog # sc-751), p21 (Santa Cruz, Catalog # sc-397), or CD34 (Santa Cruz, Catalog # sc-9095) and reprobed with anti-β-actin antibody (Sigma, Catalog # A2228) to serve as a loading control. Signals of targeted proteins were detected by the Immun-Star HRP peroxide Luminol/ Enhancer (Bio–Rad, Catalog # 170-5040) and recorded on BioBlue-XR Autoradiography Film (Alkali Scientific).

2.11. Analysis of cell surface markers by flow cytometry

Flow cytometry is a technique for counting particles using electronic detection apparatus, which involves labeling cells with a fluorescent marker, and suspending cells in a stream of fluid which passes through, and is measured by a fluorescence measuring station. NB cells (1 $x10^6$ /well) maintained in complete medium were placed in 6-well plates overnight. Salinomycin or identical volume of control (DMSO) was added to the appropriate wells at 1µM. After 24 hr of treatment, the cells were stained with anti-CD133 (Biobyt), or anti-CD34 (Biolegend, Catalog # 343602), or anti-CD117(c-kit) (Biolegend, Catalog # 313201), and Anti-Mouse IgG FITC (Sigma, Catalog #F0257). Mouse IgG (Santa Cruz, Catalog # sc-2025) was used as isotype control. Cells were analyzed on BD Accuri^{TM} C6 (BD Biosciences). The percentage of cells with different markers was computed using Flow Jo (TreeStar, OR). At least 10,000 cells were analyzed.

2.12. Reverse transcription-quantitative PCR (RT-qPCR)

RNA was isolated from NB cells using the RNeasy Plus Mini Kit (Qiagen, Catalog # 74136) by following the manufacturer's protocol. The quantity and purity of RNA were determined using a NanoDrop 1000 spectrophotometer (Thermo Scientific). 1 µg of total RNA was used to prepare cDNA using SuperScript first-strand synthesis system (Invitrogen) by following the instructions provided by the manufacturer. Primers used in this study are listed in **Table 9** and synthesized by Integrated DNA Technology. The original cDNA reaction mixture was diluted to one-tenth of the reaction volume. 2 µl of the diluted cDNA was used as the template in the quantitative PCR reaction. PCR amplification was performed using SYBR

GreenER qPCR SuperMix (Invitrogen) and 7500 Fast & 7500 Real-Time PCR System (Life technology).

Table 9. Primers and conditions used for the qRT-PCR

Gene	Primer Sequences (5'-3')	Sizes of PCR Products (bp)	Annealing Temperature (°C)	Cycle of Amplification
CD133	Forward: AGAAATGCACCAGCGACAGA Reverse: CGCCTTGTCCTTGGTAGTGT	256	60	45
CD34	Forward: CCCAGCCAACGTTTCAACTC Reverse: CGCACAGCTGGAGGTCTTAT	232	60	45
c-Kit	Forward: TGACTTACGACAGGCTCGTG Reverse: CAGAAGTCTTGCCCACATCG	258	60	45
GAPDH	Forward: GAGTCAACGGATTTGGTCGT Reverse:TTGATTTTGGAGGGATCTCG	234	57	45

2.13. Immunoprecipitation assay

Immunoprecipitation (IP) was conducted using the Pierce crosslink magnetic IP/Co-IP kit (Thermo Scientific, Catalog # 88805) according to the manufacturer's instructions. Briefly, whole cell lysates were prepared by using Tris-Triton cell lysis buffer (1% Triton X-100, 50 mM Tris-HCl pH 7.4, 5% glycerol, 100 mM NaCl) supplemented with protease inhibitor cocktail (Roche Applied Science). Cell lysates were then incubated with 10 μM salinomycin for 1 hr at 4°C. 5μg of antibody was used for each IP reaction and cross-linked to Protein A/G magnetic beads using disuccinimidyl suberate (DSS). For each IP reaction, 2 mg of protein lysates were reacted with specific antibody cross-linked beads overnight at 4 °C. The beads were then collected with a magnet stand and washed three times with washing buffer (0.2% Tween PBS). Bound proteins were eluted by heating at 95°C in 6 x SDS-PAGE sample buffer and subjected to

Western blotting analysis. Immunoblots were probed with antibodies specific for TIF1β (Abcam, Catalog # ab10483) and NCL (Abcam, Catalog # ab22758). Anti-salinomycin antibody was purchased from Abcam (Catalog # ab123955). Normal sheep IgG (Santa Cruz, Catalog # sc-2717) and rabbit IgG (Santa Cruz, Catalog # 2027) were served as control.

2.14. Immunofluorescence

SH-SY5Y cells were fixed using 4% formaldehyde for 15 min at room temperature and treated with 0.1% Triton X-100 for 15 min and blocked by 5% BSA for 20 min, then incubated overnight at 4°C with the anti-NCL (Abcam, Catalog # ab22758) and anti-CD34 (R&D Systems, Catalog # MAB72271) primary antibodies. Cells were then incubated with goat anti-mouse IgG-R-Phycoerythrin (Sigma, Catalog # P9287) and goat anti-rabbit IgG-FITC (Santa cruz, Catalog # sc-2012) secondary antibodies for 2 hr at room temperature. Nuclei were stained with 0.5 µg/ml Hoechst 33258 dye (Invitrogen, Catalog # H3569) for 5 min. The cells were visualized and photographed using Leica DMi 8 fluorescence microscope.

2.15. Chromatin Immuno-Precipitation (ChIP)-qPCR assay

Cells (5 x10^6 /well) maintained in complete medium were placed in 10 cm cell culture plate overnight. The next day cells were treated with salinomycin for 4 hr and later cross-linked with 10 ml of 1% formaldehyde for 30 min at room temperature. The reaction was ceased by adding 1 ml of 1.37 M glycine and mixed immediately. The plates were then placed on ice and washed thrice with Buffer A (PBS supplemented with protease inhibitor cocktail). Cells were then trypsinized and the detached cells were harvested by centrifugation at 168 g for 5 min at 4°C. The pellet was re-suspended in 500 µl of Buffer B (0.625 mM Hepes, pH7.8, 1.5mM

MgCl2, 0.03M KCl, 0.01% Igepal CA-630, 1mM DTT) and kept on ice for 10 min. The cells were dounced 10-15 times to release the nuclei. The released nuclei were then harvested by centrifuging at 336 g for 5 min. The cells were re-suspended in 500 µl of Buffer C (50mM Hepes, pH7.9, 4mM NaCl, 1mM EDTA, 1% Triton X-100, 0.1% sodium deoxycholate, 0.1% SDS) supplemented with protease inhibitor cocktail. Sonication was performed (using Branson Digital sonifier ®) at 30% amplitude for 10 sec each three times. The samples were then centrifuged at 32869 g for 15 min at 4°C. The supernatant was collected and pre-cleaned with 50 µl of the Protein-A sepharose^{TM} CL–4B (GE Healthcare) slurry (80 mg in Buffer C per 500 µl of the lysate) with constant rotation for 1 h in a cold room. The samples were centrifuged at 336 g for 5 min and the supernatant containing the pre-cleaned chromatin was collected. 50 µl aliquot of each sample was saved to serve as the Input DNA. 5 µl of primary antibody (Anti-NCL (abcam) or control Rabbit IgG (Santa Cruz) were added to the rest of the sample and incubated in a cold room with constant rotation for overnight. Next day, 50 µl of Protein-A sepharose slurry was added to each sample and incubated for 2 h with constant rotation in the cold room. Then, centrifugation was performed at 1677 g for 3 min. The beads were then washed twice each time with Buffer C, Buffer D (2.5 mM Hepes, pH7.9, 0.5 M NaCl, 1mM EDTA, 1% Triton X-100, 0.1% sodium deoxycholate, 0.1% SDS, protease inhibitor cocktail), Buffer E (2.5 mM Hepes, pH7.9, 12.5 mM NaCl, 1mM EDTA, 1% Triton X-100, 0.1% sodium deoxycholate, 0.1% SDS) and TE buffer (10 mM Tris, 1 mM EDTA, pH 8.0). 200 µl of Elution buffer (0.05 M Tris, pH 8.0, 1mM EDTA, 0.05% SDS, 0.05M sodium bicarbonate) was then added to the beads and incubated at 65°C for 10 min. Centrifugation was performed at 32869 g for 1 min and the supernatant was collected. Beads were eluted again to obtain a total 400 µl of elute. In parallel, the saved input DNA was thawed and 350 µl of elution buffer was added to bring the total

volume up to 400 µl. 16.5 µl of 5M NaCl was added to each tube and incubated at 65°C overnight for reverse-cross-linking. 2 µl of RNAse (Sigma) was added the next day and incubated at 37°C for 1 h. 4 µl of EDTA (0.5 M) and 2 µl of Proteinase K (Qiagen) was added and incubated at 42°C for 2 h. DNA were then extracted with chloroform/isoamyalcoholonce by centrifuging at 32869 g for 10 min. The aqueous phase was collected to which 40 µl of sodium-acetate (3M) and 1 ml of ethanol was added and was incubated at -20°C overnight for precipitation. The samples were centrifuged at 32869 g for 30 min the next day and the pellets were washed once with 80% EtOH. The immuno-precipitate (IP) and the Input sample pellets were re-suspended in 50 µl of Tris, pH 8.5. The chromatin precipitates were then taken for qPCR. The buffers used for the ChIP assay are listed in **Table 10**.

Table 10. Buffer components for ChIP-qPCR

Buffer A	**Volume in 50 ml stock (ml)**
1X PBS	50
Protein cocktail inhibitor	1 tablet
Buffer B	**Volume in 50 ml stock (ml)**
25 mM Hepes, pH7.8	1.25
50 mM $MgCl_2$	1.5
1 M KCl	0.5
0.1% Igepal CA-630	0.05
50 mM DTT	1
Distilled water	45.7
Protein cocktail inhibitor	1 tablet

Table 10. Buffer components for ChIP-qPCR (continued)

Buffer C	**Volume in 50 ml stock (ml)**
1 M Hepes, pH7.9	2.5
140 mM NaCl	1.4
50 mM EDTA	1
20% Triton X-100	2.5
10% sodium deoxycholate	0.5
20% SDS	0.25
Distilled water	41.85
Protein cocktail inhibitor	1 tablet
Buffer D	**Volume in 50 ml stock (ml)**
50 mM Hepes, pH7.9	2.5
5 M NaCl	5
50 mM EDTA	1
20% Triton X-100	2.5
10% sodium deoxycholate	0.5
20% SDS	0.25
Distilled water	38.25
Protein cocktail inhibitor	1 tablet

Table 10. Buffer components for ChIP-qPCR (continued)

Buffer E	Volume in 50 ml stock (ml)
50 mM Hepes, pH7.9	2.5
250 mM NaCl	2.5
50 mM EDTA	1
10% sodium deoxycholate	0.5
20% SDS	0.25
20% Triton X-100	2.5
Distilled water	40.75
Protein cocktail inhibitor	1 tablet
Elution buffer	**Volume in 50 ml stock (ml)**
1 M Tris, pH 8.0	2.5
50 mM EDTA	1
1% SDS	2.5
1 M sodium bicarbonate	2.5
Distilled water	41.5

The following primers were used for quantitative analysis (**Table 11**).

Table 11. Primers and conditions used for the ChIP-qPCR

Gene	Primer Sequences (5'-3')	Sizes of PCR Products (bp)	Annealing Temperature (°C)	Cycles
CD34 promoter	Forward: GATGGTGATGGGGAACTAAATGG Reverse: GCCAGTAACAATCTTGCAAAAGG	338	60	45
GAPDH	Forward: GAGTCAACGGATTTGGTCGT Reverse: TTGATTTTGGAGGGATCTCG	234	57	45

2.16. The expression levels of TIF1β and NCL in NB tumors and the correlation with NB patients' outcomes

A set of 498 NB samples previously detected by microarray in the database was used for TIF1β and NCL expression [126]. Using the R2 software (http://r2.amc.nl), we analyzed the expression levels of TIF1β and NCL in NBs and determined the correlation of TIF1β and NCL levels in NBs with their clinical outcomes. The expression levels of TIF1β and NCL were also analyzed in different subgroups based on MYCN amplification, risk group and INSS stage. The statistical analysis of each gene in different groups of NBs was evaluated by one-way ANOVA. The correlations between the expression levels of TIF1β and NCL with patients' survival were analyzed using chi-squared test and Kaplan-Meier curves. Survival was measured from the time of initial diagnosis until the date of death or the date of last follow up owing to progressive nature of the disease. The survival distribution was estimated using Kaplan-Meier curves, and optimal cut-off selection (chi-squared test p-value). P-values < 0.05 were considered to be statistically significant.

2.17. Statistical analysis

All quantitative data from *in vitro* assays are represented as mean ± standard deviation (SD). Statistical tests were performed with the Minitab 16.1.1 software package. Comparisons between two groups were carried out using paired student's t test. $p < 0.05$ was used as the criterion for statistical significance.

CHAPTER 3. TO DETERMINE THE ANTI-CANCER EFFECTS OF SALINOMYCIN IN NB

3.1. Introduction

Neuroblastoma (NB) is the most frequently diagnosed solid extracranial malignancy in the pediatric population. More than 30-50% of high-risk cases remain incurable due to the emergence of therapy-resistance [1, 127]. The failure to respond to chemotherapeutic regimens and fear of disease relapse and distant organ dissemination are underpinned by the presence of CSCs, which are not effectively eliminated by conventional chemotherapies [37, 38, 56]. The unsatisfactory clinical outcomes of NB underscore the need for the development of novel treatment.

Recently, a stem cell like population in NB, namely NB-CSCs, has been observed with higher potential for treatment resistance [37-39]. Studies also indicate that most of NB cell lines contain a subpopulation expressing stem cell surface markers, e.g., CD133, c-kit, and nestin [37, 38]. Based on the expression levels of stem cell markers, differentiation potential and the capacity for tumorigenisis, NB cells may be classified as neuroblastic (N), substrate-adherent (S), and intermediate (I) phenotypes [37, 128]. Of note, N- and I-NB cell types are less differentiated with higher potential to form tumors *in vivo* compared to S-type that is considered to be non-tumorigenic [37, 128].

In this study, we used three NB cell lines, SH-SY5Y, IMR32, and SK-N-AS, respectively, as a preclinical model to determine the unexplored efficacy of salinomycin on NB and the targets of salinomycin. SH-SY5Y and IMR32 containing N-type cells are considered as CSC rich cell lines, while SK-N-AS is a typical S-type cell line [37, 128].

3.2. Results and Discussions

3.2.1. Determining the effects of Salinomycin on NB cell proliferation

To determine the efficacy of salinomycin on NB cells, we first analyzed the effects of salinomycin on NB cell proliferation in three NB cell lines. Cells were treated with various concentrations (0.25 – 4 μM) of salinomycin and analyzed for cell proliferation by using MTS assay. Our data showed that salinomycin exhibited marked inhibition of cell proliferation in a dosage dependent manner, and the IC50 values for the inhibitory effects of salinomycin on cell proliferation at 48 h were at 1μM for the N-type tumorigenic SH-SY5Y and IMR32 cells, and > 4 μM for the S-type non-tumorigenic SK-N-AS cells [37, 128], indicating salinomycin is more effective in tumorigenic cells (**Figure 6**) .

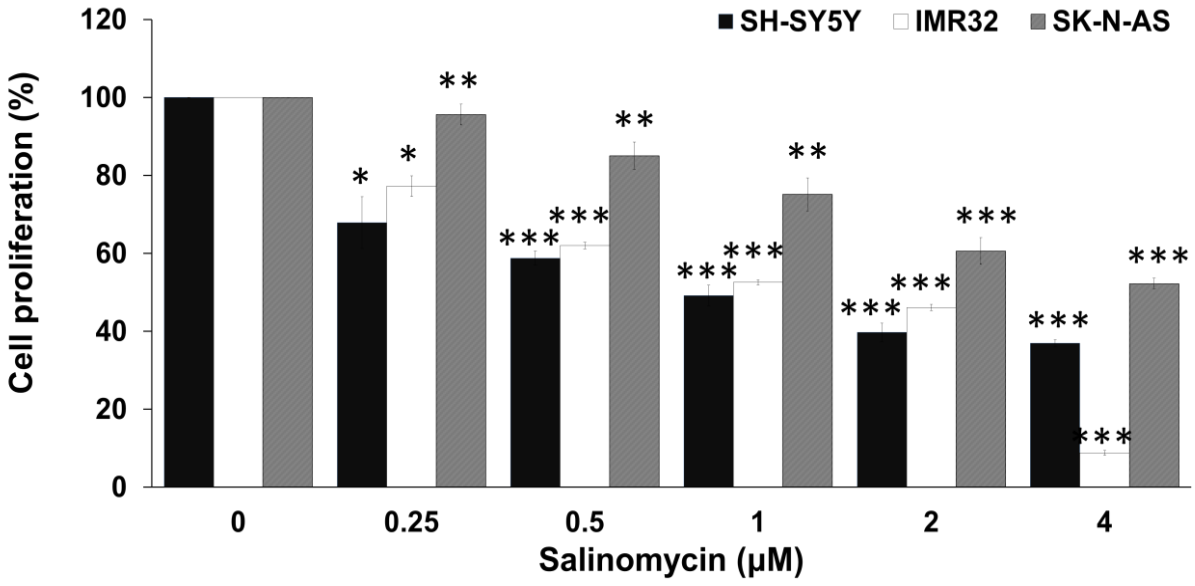

Figure 6. The effects of salinomycin on NB cell proliferation. Salinomycin suppresses NB cell proliferation. Cell viability was assessed using MTS assay 48 hr after salinomycin treatment. *p<0.05, **p<0.01, and ***p<0.001.

In addition, the IC50 value of salinomycin in N-type NB cells is much lower than some currently being used chemotherapeutic drugs for NB, e.g. carboplatin, in the same *in vitro* cell line systems with reduced possibility of side effects (**Table 12**) [19].

Table 12. Comparison of the anti-proliferative effects of salinomycin with other chemotherapeutic drugs in NB cells

Chemotherapeutic Drug	**IC 50 (μM) (72hr)**		**Major Side effects**
	SH-SY5Y	**IMR32**	
Etoposide	0.3	3	Bone marrow suppression
Cyclophosphamide	1	3	Damage to bladder (carcinogenic); Bone marrow suppression
Carboplatin	12	70	Damage to Kidney; Bone marrow suppression
Doxorubincin	0.1	8	Damage to heart
Vincristin	0.01	0.1	Damage to nerves and kidney
Melphalan	3	30	Bone marrow suppression
	IC 50 (μM) (48hr)		
Salinomycin	1	1	Few side effects on normal cells; requires further investigation

3.2.2. Determining the role of salinomycin on NB cell cycle progression

We then determined the effects of salinomycin on cell cycle progression using PI staining analysis. We observed that salinomycin induces cell death as indicated by an increased sub-G0 population. In addition, in all the three cell lines, a significant number of cells ($P<0.05$) were found to be arrested at G2 phases of the cell cycle in salinomycin treated cells (**Figure 7**).

The percentage of cells in the G2 phase were elevated from 16.5%, 19.9%, and 9.5% to 30.3%, 44.3%, and 27.5% for SH-SY5Y, IMR32, and SK-N-AS cells respectively in salinomycin treated cells as shown in **Figure 7**. The G2/M checkpoint is an important cell cycle checkpoint that insures that cells do not enter mitosis before they have a chance to repair damaged DNA [129]. The cell cycle arrest on G2 phases may contribute to the inhibitory effects of salinomycin on NB cells.

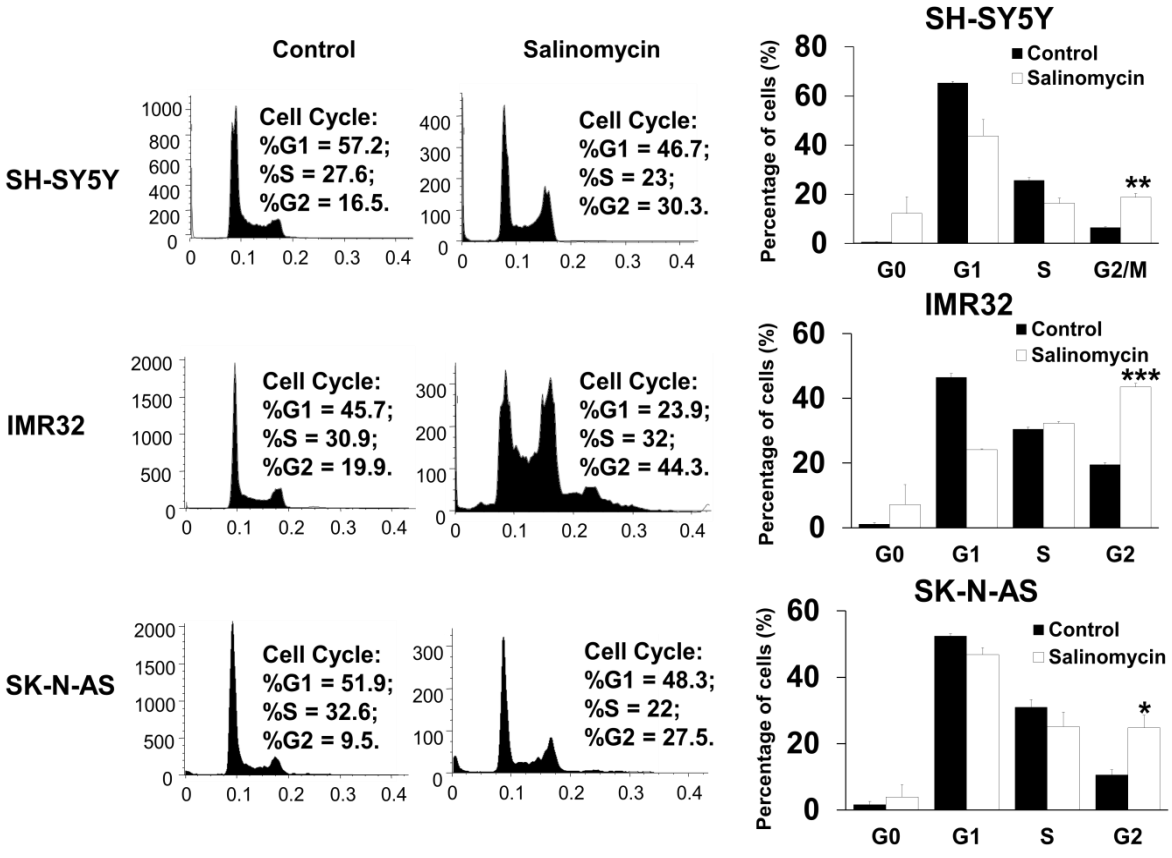

Figure 7. The effect of salinomycin on NB cell cycle progression. Quantification of cell population in each cell phase by PI staining. Cells treated with salinomycin or control vehicle for 24 hr, and the cells were stained with PI and analyzed by flow cytometry. *p<0.05, **p<0.01, and ***p<0.001.

3.2.3. Determining the role of salinomycin on cyclin A and p21 expression

Cyclin A is known to regulate the G2/M transition in a p53 dependent manner [130, 131]. We then analyzed the expression of cyclin A and the anti-apoptotic protein p21[132] in response to salinomycin treatment.

In our study, we treated NB cells with 1 μM, 4 μM salinomycin or vehicle control for 24 hr and analyzed the protein expression of cyclin A and p21. Our data show that the levels of cyclin A were significantly up-regulated while the anti-apoptotic protein p21 was down-regulated in NB cells in a dose dependent manner (**Figure 8**). These results are consistent with salinomycin's inhibitory effect on cell cycle progression and promoting effect on cell death.

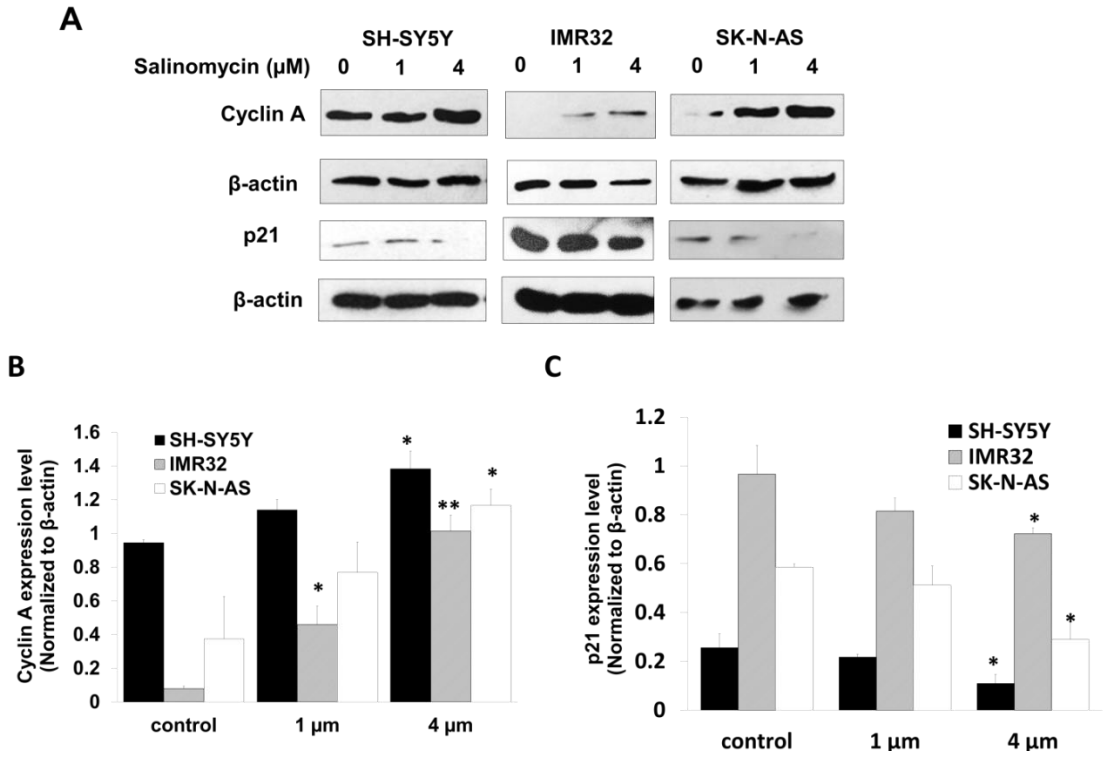

Figure 8. Effects of salinomycin on cyclin A and p21 expression. (A) Cells were treated with salinomycin at indicated concentrations for 24 hr and whole cell lysates were extracted for western blotting. Immunoblots were probed with antibodies specific for cyclin A or p21, and reprobed with anti-β-actin antibody to serve as a loading control. (B) Quantification of salinomycin's effects on cyclin A expression. (C) Quantification of salinomycin's effects on p21 expression. *$p<0.05$ and **$p<0.01$.

3.2.4. Determining the role of salinomycin on NB tumorsphere formation

As introduced earlier, CSCs have been defined functionally by two major criteria: their ability to undergo self-renewal and their ability to produce differentiated progeny. A sphere formation assay is used to identify the stem cell characteristic of self-renewal *in vitro* since only self-renewal cells are able to form the 3D sphere-shaped structure (tumorsphere, in the case of cancer cells) in suspension [133].

To determine the efficacy of salinomycin on NB cells and CSCs, we then analyzed the effects of salinomycin on NB cell tumorsphere formation in three NB cell lines. In response to salinomycin treatments, we observed significant suppressive effects on tumorsphere formation in SH-SY5Y and IMR32 cells. As expected, the s-type non-tumorigenic SK-N-AS cells did not form tumorsphere in culture. These results indicate that salinomycin suppresses the activities of NB CSCs (**Figure 9**).

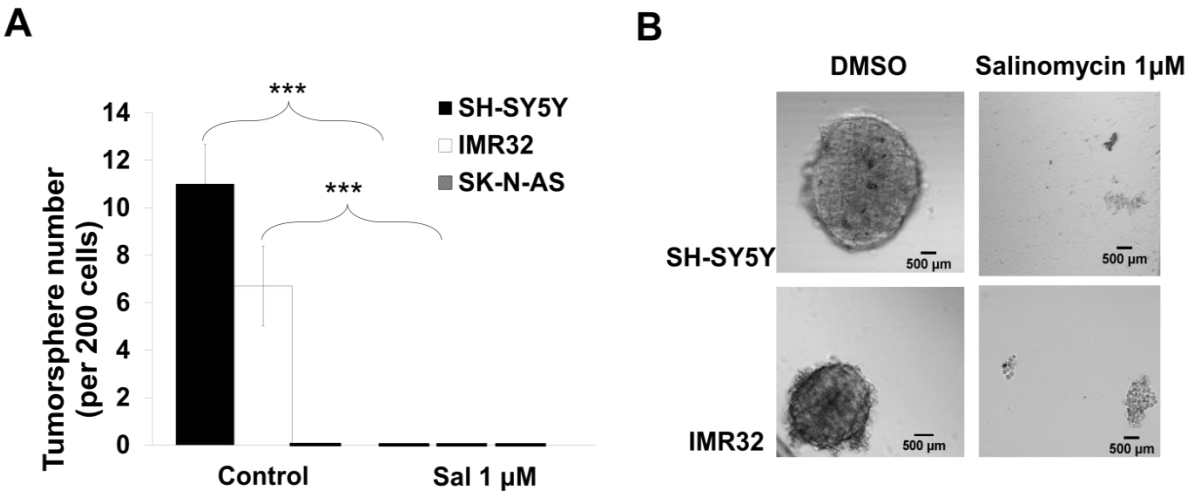

Figure 9. Salinomycin inhibits tumorsphere formation of NB cells. (A) All tested NB cell lines except non-tumorigenic SK-N-AS form tumorsphere and salinomycin suppresses NB cell tumorsphere formation. Cells treated with salinomycin or DMSO control were grown in tumorsphere-media, and the number of tumorspheres was counted at day 7, ***$p<0.001$. (B) Salinomycin suppresses NB cell tumorsphere formation. Cells treated with salinomycin or DMSO control were grown in tumorsphere-media. Images were captured at day 7.

3.2.5. Determining the role of salinomycin on NB CSC like population

CD133 and c-kit are CSC related surface markers and the existence of NB cells expressing these molecules is implicated in NB treatment failure [37, 38]. The effect of salinomycin on the suppression of NB cell tumorsphere formation suggests that salinomycin suppresses the NB-CSCs since a tumorsphere is a spherical formation developed from the proliferation of CSCs. To verify the possible roles of its inhibitory effects on NB CSCs, NB cells were treated with salinomycin or vehicle control for 24 hr and the amount of CSC-like ($CD133^+$ and $c\text{-}kit^+$) NB cells were detected by Flow Cytometry.

As expected, the S-type SK-N-AS cells showed significantly lower levels or no expression of the three markers compared with the other two N-type tumorigenic NB cells (**Figure 10**). Salinomycin showed significant inhibitory effects on $CD133^+$ and $c\text{-}kit^+$ NB cells as shown in **Figure 10**. A previous report suggested that c-kit and its ligand stem cell factor (SCF) are preferentially expressed in NB tumors with MYCN amplification [134]. Consistent with this finding, our data showed that the IMR32 cell line with MYCN amplification contains significantly higher ($P<0.001$) amount of $c\text{-}kit^+$ cells in comparison with the other two MYCN non-amplified cell lines; treatment with salinomycin resulted in approximately 50% reduction of the $c\text{-}kit^+$ cells in SH-SY5Y and SK-N-AS cells, and more than 70% decrease of the $c\text{-}kit^+$ population in IMR32 cells (**Figure 10**).

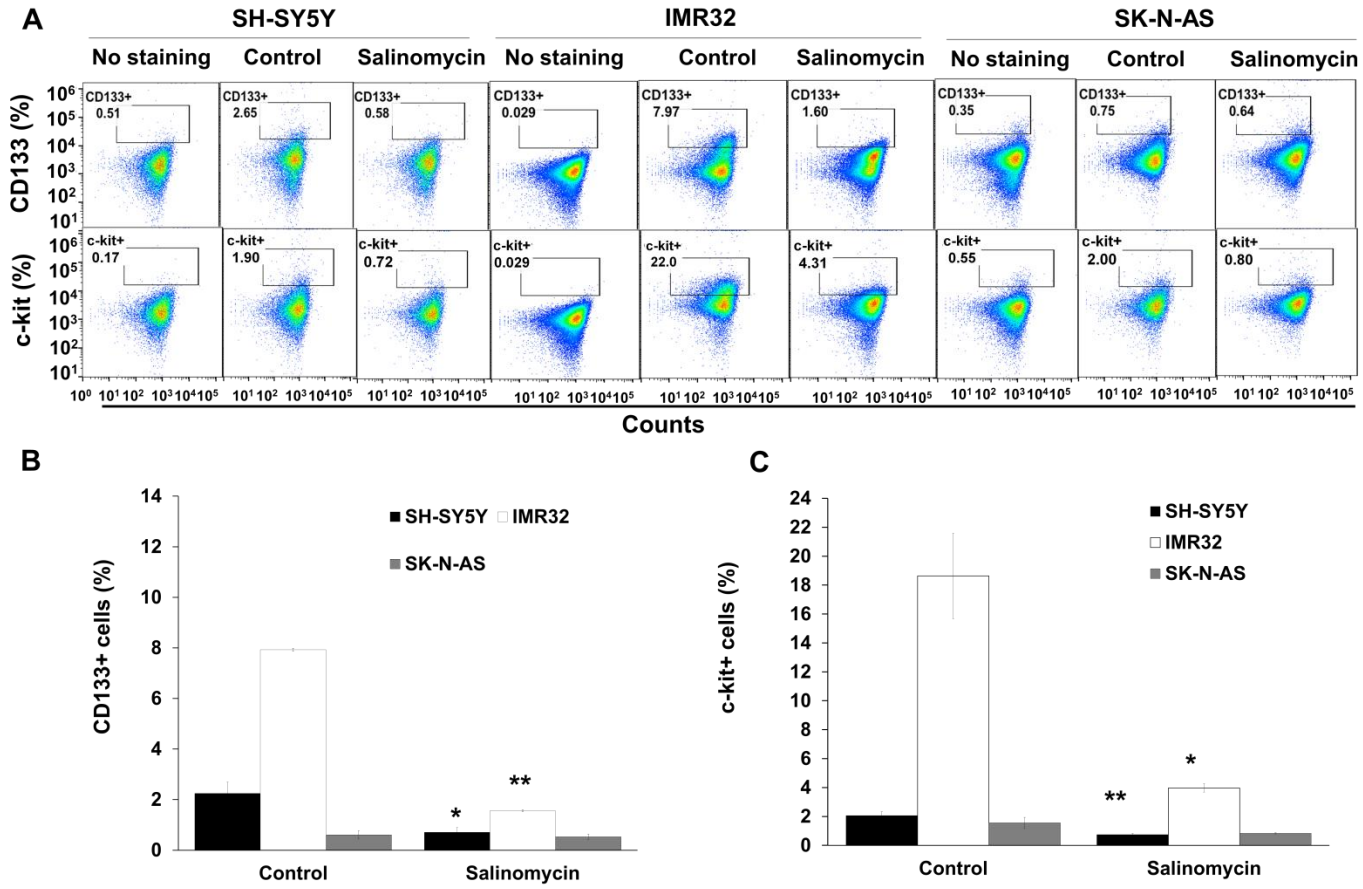

Figure. 10. Salinomycin selectively inhibits CSC-like population (CD133$^+$ and c-kit$^+$ NB cells). (A) After treated with salinomycin or vehicle control for 24 hr, NB cells were stained with anti-CD133, anti-c-kit or IgG control and anti-Mouse IgG- FITC and analyzed using a flow cytometry. Representative results for each marker are shown. (B) Salinomycin inhibits CD133$^+$ NB cells. (C) Salinomycin inhibits c-kit+ NB cells. Data represent the mean ± SD of triplicate experiments. *p<0.05, **p<0.01.

3.2.6. Determining the role of salinomycin on p53

It has been reported that p53 is required for the maintenance of the neuroblastic tumorigenic phenotype of NB and the down-regulation of p53 results in the conversion of N-type tumorigenic NB cells to the substrate-adherent fibroblast-like non-tumorigenic S-type NB cells [135].

To test the effect of salinomycin on p53, we analyzed the expression levels of p53 in NB cells upon salinomycin treatment. Our data show that salinomycin treatment markedly reduced the expression level of p53 in all the three cell lines (**Figure 11**).

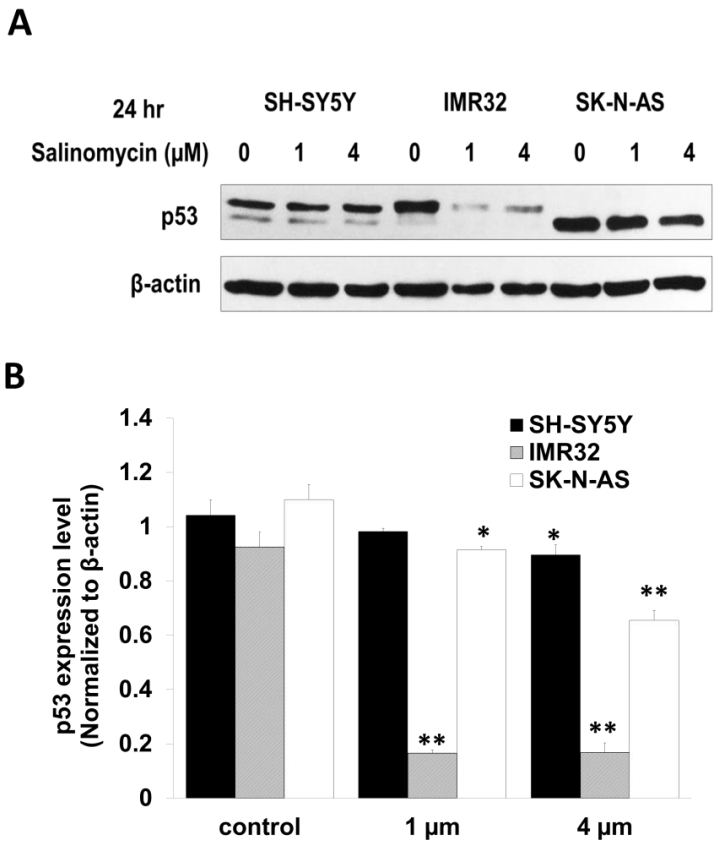

Figure 11. Salinomycin down-regulates p53 expression. (A) Cells were treated with salinomycin at indicated concentrations for 24 hr and whole cell lysates were extracted for western blotting. Immunoblots were probed with antibodies specific for p53, and reprobed with anti-β-actin antibody to serve as a loading control. (B) Quantification of salinomycin's effects on p53 expression. *$p<0.05$ and **$p<0.01$.

CHAPTER 4. TO IDENTIFY THE FUNCTIONAL BINDING TARGET OF SALINOMYCIN IN NB

4.1. Introduction

To explore approaches that selectively eradicate the CSC population is a novel and potentially promising direction of improving anti-cancer therapy. The anti-cancer and anti-CSC effects of salinomycin have been observed in many types of cancers *in vitro* and *in vivo* [66]. We have observed profound cytotoxicity of salinomycin against NB cells *in vitro* in our preliminary study. The expanding evidence for salinomycin's remarkable efficacy and anti-CSC capability provides strong impetus for the need for continued study to elucidate its action mechanisms. To this end, identification of its binding proteins is pivotal.

Many therapeutic drugs and preventive agents initiate their biological effects by binding directly to the proteins in human cells. To discover and identify the target molecules for various clinical therapeutic modalities has many benefits: (1) to provide researchers and medical experts understanding of the mechanisms and to reduce the side effects, (2) to lay a foundation for personalized medicine by identifying patients with a deficiency in drug targets, for treatment using alternative therapies, (3) facilitate new drug discoveries by using the targets to search for more effective drugs or new agents, (4) identify drugs and chemopreventive agents that have more than one target and can be used for different therapeutic and preventive purposes. Thus, in this study, we used comprehensive approaches to identify functional binding targets of salinomycin in NB.

4.2. Results and Discussions

4.2.1. Identification of potential binding targets of salinomycin by using DARTS analysis

To understand the underlying mechanism of salinomycin on NB and NB CSC-like population, we postulate the existence of cellular protein targets that bind and interact with salinomycin. To test and evaluate this hypothesis, we first applied a modified "drug affinity responsive target stability" (DARTS) method to identify salinomycin's binding proteins in SH-SY5Y cells [124]. This approach is based on the premise that, when proteins interact with molecules such as a drug, to form a drug-protein complex, such interactions may result in conformational changes, which consequently reduces the sensitivity to proteolytic enzymes (**Figure 12**).

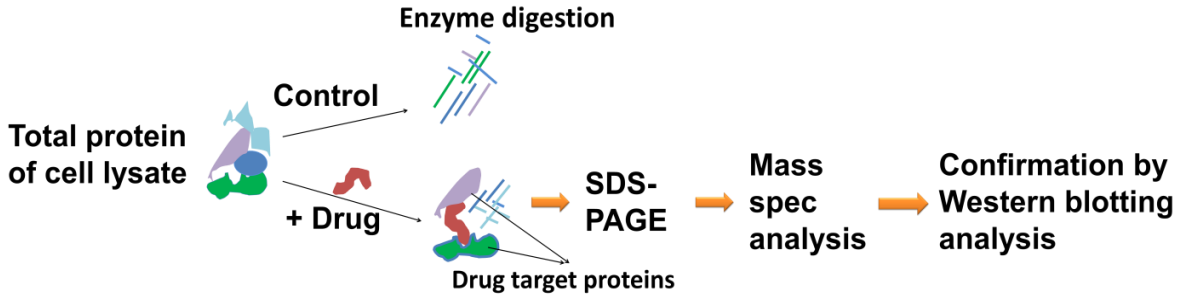

Figure 12. Schematic presentation of the procedures of chemoproteomic strategy.

In this study, we performed the above mentioned DARTS method using biochemical affinity beads coupled with chemoproteomics to identify salinomycin binding proteins and to explore the interaction of salinomycin with its binding proteins in NB cells that harbor cancer stem cell characters [37, 38, 56]. As shown in **Figure 13**, the bands on the gel with increased densities upon the salinomycin treatment compared to the control were considered drug binding target protein containing lysates and were selected for mass spectrometry analysis.

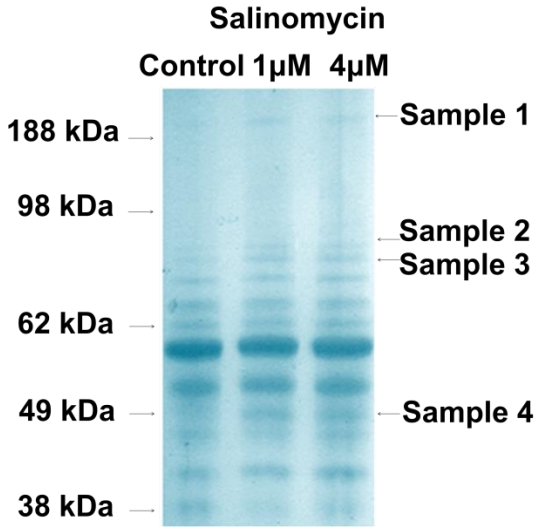

Figure 13. Identification of salinomycin potential targets. Intact SH-SY5Y cells were treated with salinomycin and whole cell lysates were subjected to thermolysin digestion and EZBlue^{TM} Gel Staining. A comparison of the gel separation patterns of the mock cell lysate with salinomycin-treated cell lysate after thermolysin digestion reveals existence of several unique salinomysin-protected bands.

4.2.2. Analysis of potential binding targets

The mass spectrometry analysis provided us a list of binding target protein candidates for salinomycin (**Figure 14**). We then analyzed the candidate proteins at size, probability of hits, and biological functions of putative targets. By excluding proteins exist in all types of cells and functionally irrelevant with CSCs, e.g. Spectrin alpha II (SPTA2), and proteins with relatively low hits, e.g., Calreticulin, and proteins less likely to be involved in CSC and NB development, e.g., transitional endoplasmic reticulum ATPase. Transcription intermediary factor 1-beta (TIF1β) and Nucleolin (NCL), which are actively associated with stem cell functions and cancer progression [136, 137], were selected for further investigation.

(A) The number of unique spectra for each protein hit is listed here:

Probability Legend:	Accession Number	Molecular Weight	Protein Grouping Ambiguity	Sample 1	Sample 2	Sample 3	Sample 4
over 95%							
80% to 94%							
50% to 79%							
20% to 49%							
0% to 19%							
Bio View: Identified Proteins (15)							
RecName: Full=Spectrin alpha chain, brain; AltName: Full=Alpha-II	SPTA2_HUMAN	285 kDa	★	3			
RecName: Full=Spectrin beta chain, brain 1; AltName: Full=Beta-II	SPTB2_HUMAN	275 kDa		6			
RecName: Full=Alpha-actinin-1; AltName: Full=Alpha-actinin	ACTN1_HUMAN (+11)	103 kDa			5		
RecName: Full=Elongation factor 2; Short=EF-2.	EF2_HUMAN (+7)	95 kDa				3	
RecName: Full=Endoplasmin; AltName: Full=94 kDa glucose-regulated	ENPL_HUMAN (+2)	92 kDa	★			16	
RecName: Full=Transitional endoplasmic reticulum ATPase; Short=TER	TERA_HUMAN (+4)	89 kDa				2	
RecName: Full=Transcription intermediary factor 1-beta;	TIF1B_HUMAN (+2)	89 kDa			2		
RecName: Full=Heat shock protein HSP 90-beta; Short=HSP 90;	HS90B_HUMAN (+5)	83 kDa	★	0	1	3	
RecName: Full=Nucleolin; AltName: Full=Protein C23.	NUCL_HUMAN (+2)	77 kDa			7		
RecName: Full=Splicing factor, proline- and glutamine-rich;	SFPQ_HUMAN (+1)	76 kDa				6	
RecName: Full=Tubulin alpha-1A chain; AltName: Full=Alpha-tubulin	TBA1A_HUMAN (+18)	50 kDa	★				8
RecName: Full=Heterogeneous nuclear ribonucleoprotein H;	HNRH1_HUMAN (+6)	49 kDa					2
RecName: Full=Calreticulin; AltName: Full=CRP55; AltName:	CALR_HUMAN (+4)	48 kDa					2
RecName: Full=Protein S100-A9; AltName: Full=Calgranulin-B;	S10A9_HUMAN	13 kDa			2		
Tubulin beta-2C chain OS=Homo sapiens GN=TUBB2C PE=1 SV=1	TBB2C_HUMAN (+3)	?	★				3

(B) Below is the summary of protein hits:

Probability Legend:	Accession Number	Molecular Weight	Protein Grouping Ambiguity	Sample 1	Sample 2	Sample 3	Sample 4
over 95%							
80% to 94%							
50% to 79%							
20% to 49%							
0% to 19%							
Bio View: Identified Proteins (15)							
RecName: Full=Spectrin alpha chain, brain; AltName: Full=Alpha-II	SPTA2_HUMAN	285 kDa	★	100%			
RecName: Full=Spectrin beta chain, brain 1; AltName: Full=Beta-II	SPTB2_HUMAN	275 kDa		100%			
RecName: Full=Alpha-actinin-1; AltName: Full=Alpha-actinin	ACTN1_HUMAN (+11)	103 kDa			100%		
RecName: Full=Elongation factor 2; Short=EF-2.	EF2_HUMAN (+7)	95 kDa				100%	
RecName: Full=Endoplasmin; AltName: Full=94 kDa glucose-regulated	ENPL_HUMAN (+2)	92 kDa	★			100%	
RecName: Full=Transitional endoplasmic reticulum ATPase; Short=TER	TERA_HUMAN (+4)	89 kDa				100%	
RecName: Full=Transcription intermediary factor 1-beta;	TIF1B_HUMAN (+2)	89 kDa			100%		
RecName: Full=Heat shock protein HSP 90-beta; Short=HSP 90;	HS90B_HUMAN (+5)	83 kDa	★	62%	50%	100%	
RecName: Full=Nucleolin; AltName: Full=Protein C23.	NUCL_HUMAN (+2)	77 kDa			100%		
RecName: Full=Splicing factor, proline- and glutamine-rich;	SFPQ_HUMAN (+1)	76 kDa				100%	
RecName: Full=Tubulin alpha-1A chain; AltName: Full=Alpha-tubulin	TBA1A_HUMAN (+18)	50 kDa	★				100%
RecName: Full=Heterogeneous nuclear ribonucleoprotein H;	HNRH1_HUMAN (+6)	49 kDa					100%
RecName: Full=Calreticulin; AltName: Full=CRP55; AltName:	CALR_HUMAN (+4)	48 kDa					100%
RecName: Full=Protein S100-A9; AltName: Full=Calgranulin-B;	S10A9_HUMAN	13 kDa			100%		
Tubulin beta-2C chain OS=Homo sapiens GN=TUBB2C PE=1 SV=1	TBB2C_HUMAN (+3)	?	★				100%

Figure 14. Mass spectrometry analysis of potential salinomycin binding targets. (A) The number of hits of unique spectra for each protein hit. (B) The summary of protein hits. Different colors represent different probability for the peptide matching as displayed in the table. To identify the peptides and proteins, raw spectra were converted to T2D files using 4000 series Explorer version 3.5.28193. These files were submitted to Mascot Distiller v.2.3.2. (Matrix Science) to generate uncentroided peak lists. Processed spectra were searched against Swissprot database (v. 57.15) using Mascot v. 2.3.02 (Matrix Science). Mascot searches were combined and analyzed in Scaffold v. 3.00.08 (Proteome Software, Inc.) to validate peptide and protein identifications. Peptide identifications with >95% probability and protein identifications with > 99% probability and at least two identified peptides were accepted.

4.2.3. Confirmation of the binding targets by western blotting analysis

To evaluate these two potential targets, we applied the NB cell lysate to the DARTS method in both SH-SY5Y and IMR32 cell lines followed by western blotting analysis with antibodies specific to NCL and TIF1β (**Figure 15**). As shown by **Figure 15**, protein bands with increased densities upon the salinomycin treatment compared to the control for NCL and TIF1β were both observed, revealed that NCL and TIF1β are potential binding proteins of salinomycin.

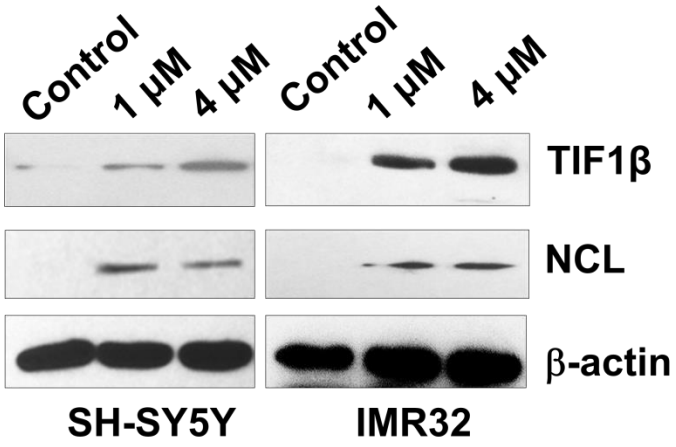

Figure 15. Confirmation of NCL and TIF1β as salinomycin binding targets by Western blotting. Intact SH-SY5Y cells were treated with salinomycin at indicated concentration for 24 hr and whole cell lysates were subjected to DARTS and western blotting analysis with antibodies against NCL and TIF1β. β-actin served as a loading control.

4.2.4. Confirmation of the direct binding by IP assay

To further confirm that salinomycin interacts with NCL and TIF1β, an IP assay using affinity beads was performed. As shown in **Figure 16**, when applied anti-salinomycin conjugated beads to the total protein lysate for the immunoprecipitation assay, both NCL and TIF1β are detected. We thus concluded that NCL and TIF1β are binding protein targets of salinomycin.

In addition, by using anti-NCL conjugated beads for IP, we show that NCL binds to TIF1β (**Figure 16B**). This is in line with previous report showing the co-IP of NCL and TIF1β and their possible role in enhancing tumor cell growth.[138]

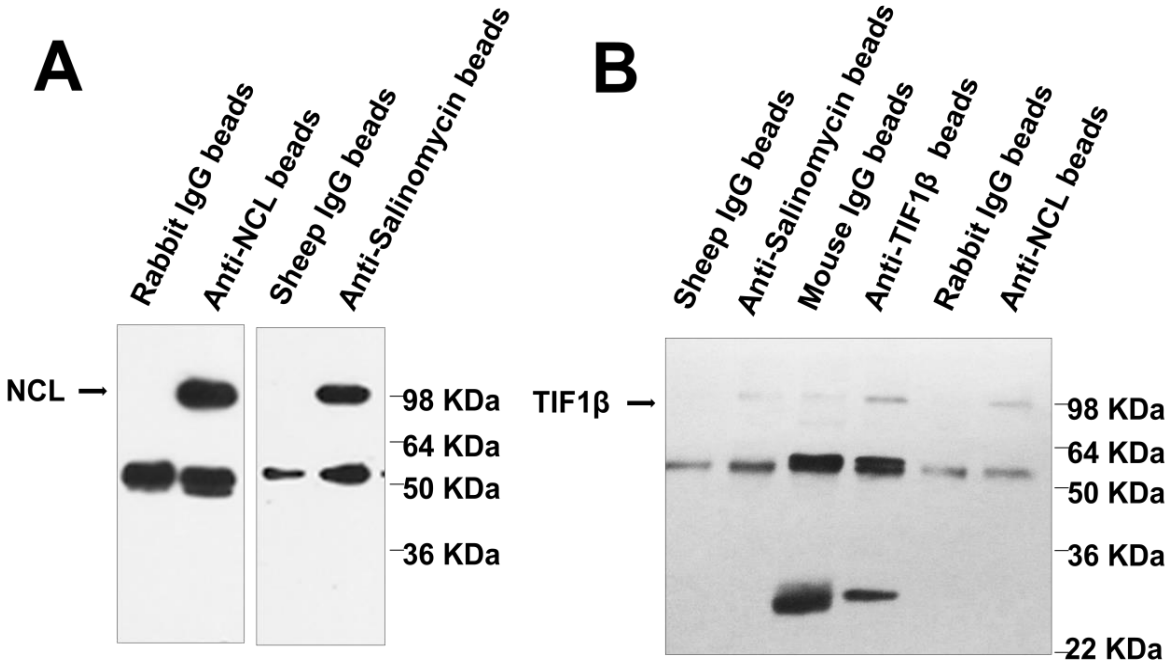

Figure 16. Identification of salinomycin binding to NCL and TIF1β using anti-salinomycin affinity beads. (A) Binding of salinomycin to NCL by IP assay using anti-salinomycin conjugated affinity beads. (B) Binding of salinomycin to TIF1β by IP assay using anti-salinomycin conjugated affinity beads and the binding of NCL to TIF1β by IP assay using anti-NCL conjugated affinity beads followed by immunobloting analysis using anti-TIF1β antibody. The specific target proteins are indicated by arrows.

4.2.5. Baseline expression of TIF1β and NCL in NB cell lines

TIF1β and NCL are multifunctional proteins involved in numerous cellular processes, including cell growth, differentiation, proliferation, apoptosis, cell cycle progression, and are critical for stem cell maintenance and differentiation [136, 137]. To explore the possible roles of TIF1β and NCL in NB cells, we first analyzed the baseline expression of TIF1β and NCL in NB cell lines (**Figure 17**).

Both TIF1β and NCL are expressed in a relatively high level in NB cell lines. The expression level was highest in the MYCN amplified cell line IMR32 and was lowest in the S-type non-tumorigenic cell line SK-N-AS for both TIF1β and NCL in the tested three NB cell lines.

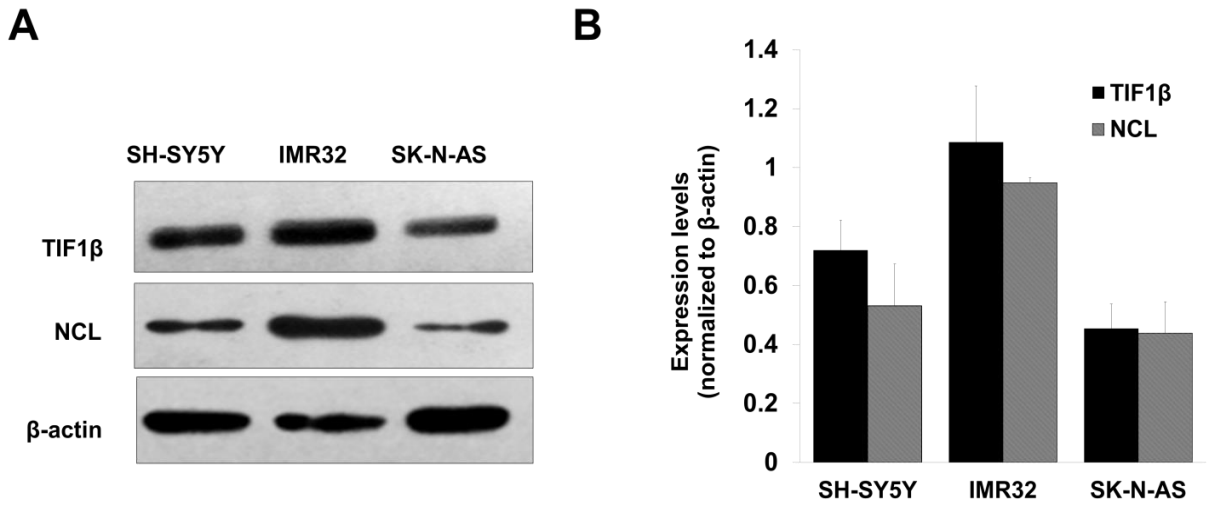

Figure 17. Expression baseline levels of TIF1β and NCL in NB cells. (A) Whole cell lysates were analyzed by Western blotting. β-actin served as a loading control. (B) Quantification of basal levels of TIF1β and NCL in three NB cell lines from Western blotting analysis.

4.2.6. Knockdown of TIF1β and/or NCL in NB cell lines

To explore the possible roles of TIF1β and NCL in NB cells, we performed the siRNA knockdown experiment using siRNAs against TIF1β or NCL, as well as the combination. The knockdown efficiency are shown in **Figure 18**.

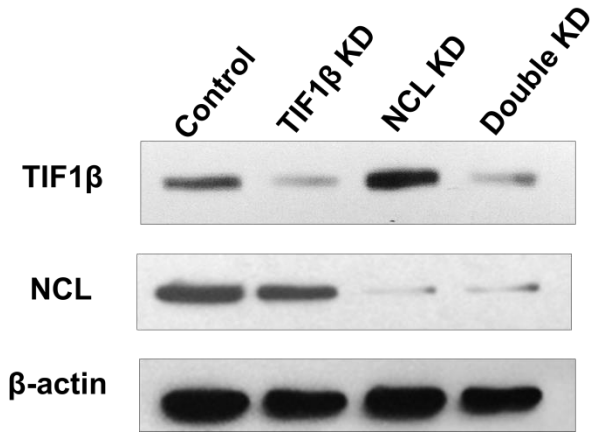

Figure 18. Efficiency of siRNA knockdown of TIF1β and NCL in SH-SY5Y cells. Cells were treated with siRNAs specific to TIF1β and NCL respectively for 48 hr, and the knockdown efficiency was confirmed by Western blotting analysis.

4.2.7. Determining the effects of knockdown of TIF1β and/or NCL on NB cell proliferation and salinomycin's anti-proliferative effects

TIF1β and NCL were both shown to be implicated with cancer cell proliferation [139, 140]. To explore the possible roles of TIF1β and NCL in NB cells, we analyzed the effects of siRNAs against TIF1β and/or NCL and the combination of TIF1β and NCL siRNAs with salinomycin on NB cell proliferation. As shown in **Figure 19**, knockdown of TIF1β or NCL reduced the cell proliferation by 10% and 30%. Double knockdown of TIF1β and NCL reduced the cell proliferation by about 55%, indicating the important roles of these two molecules in NB cell proliferation. Moreover, notably, the combination of salinomycin with knockdown TIF1β and NCL had no additional effects on cell proliferation, suggesting that TIF1β and NCL are functional targets of salinomycin.

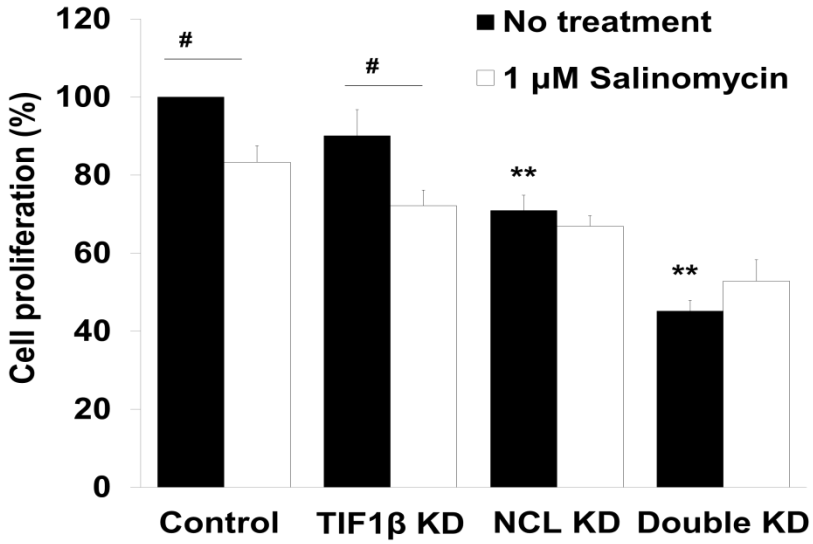

Figure 19. Salinomycin suppresses NB cell proliferation through NCL and TIF1β. Cells incubated with NCL and TIF1β siRNAs overnight were treated with DMSO control or 1 μM salinomycin. After 24 hr, the number of viable cells in each well was determined using MTS assay. */#p<0.05, **/##p<0.01, and ***/###p<0.001.

4.2.8. Determining the effects of knockdown of TIF1β and/or NCL on NB cell tumorsphere formation and salinomycin's anti-tumorigenic effects

To explore the possible roles of TIF1β and NCL in NB CSCs, we analyzed the effects of siRNAs against TIF1β and/or NCL and the combination of TIF1β and NCL siRNAs with salinomycin on NB cell tumorsphere formation. As shown in **Figure 20**, knockdown of TIF1β or NCL markedly suppressed tumorsphere formation by 40% and 55% respectively. Notably, the combination of knockdown of TIF1β and NCL with salinomycin had no additional effects on tumorsphere formation, suggesting that TIF1β and NCL are functional targets of salinomycin.

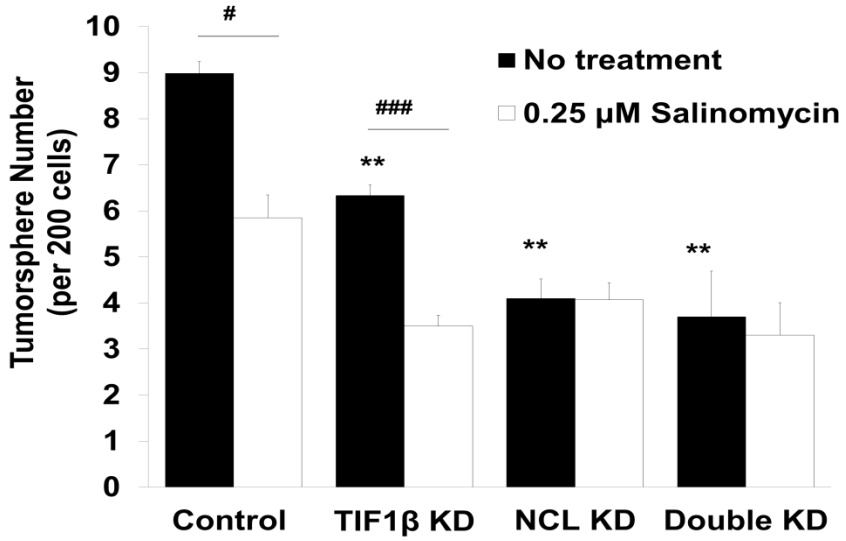

Figure 20. Tumorsphere formation assay of NB cells with NCL and TIF1β and salinomycin treatment. SH-SY5Y cells incubated with NCL and TIF1β siRNAs overnight were treated with DMSO control or 0.25 μM salinomycin. After 7 days, the number of tumorspheres in each well was determined under phase-contrast microscope. */#p<0.05, **/##p<0.01, and ***/###p<0.001.

CHAPTER 5. TO DETERMINE THE MECHNISM OF THE INTERACTION OF SALINOMYCIN WITH ITS BINDING TARGETS

5.1. Introduction

TIF1β and NCL are multifunctional proteins implicated in diverse cellular processes, including cell growth, differentiation, apoptosis, and cell cycle progression. TIF1β is also known as KAP1 (KRAB domain-associated protein) or Trim28 (Tripartite motif-containing 28). Elevated levels of TIF1β protein have been detected in many types of cancers and associated with a significantly lower survival rate in cancer patients [141-143]. Also, mice lacking TIF1β are defective in early postimplantation development [137]. More importantly, TIF1β was specifically identified as a self-renewal gene through a genome-wide RNAi screen in mouse embryonic stem (ES) cells, and, interestingly, its depletion resulted in cell differentiation into the primitive ectodermal lineage.[144]

NCL, also known as C23, is an RNA- and protein-binding protein, highly conserved and ubiquitously expressed among eukaryotes [145]. Several observations suggest that NCL functions as an mRNA-stabilizing factor for the anti-apoptotic Bcl-2 protein to act as a fundamental promoter for cell survival and proliferation [146-148]. High levels of NCL in tumors and actively dividing cells have also been widely observed [140]. The absence of NCL results in cell growth arrest at G2 phase, cell apoptosis as well as nucleolar disruption [149]; suggesting it is required for cell proliferation and survival. NCL is, hence, used as a marker for cell growth and proliferation[140]. In addition to its fundamental role in cell proliferation, NCL expression was found to be deregulated during NB cell differentiation [150]. Moreover, NCL has been further demonstrated to be required for the maintenance of embryonic stem cell self-renewal.[136]

The unique properties of TIF1β and NCL, therefore, make these two molecules very attractive targets for cancer therapeutics. The identification of TIF1β and NCL as salinomycin's binding targets further indicates that TIF1β and NCL are important for salinomycin's anti-cancer effects in NB cells.

5.2. Results and Discussions

5.2.1. Effect of salinomycin on TIF1β expression in NB cells

To determine the modulation of TIF1β by salinomycin, we first analyzed the effect of salinomycin on the protein expression of TIF1β in NB cells. Our data show that NB cells under salinomycin treatment for 24 hr, 48 hr, as well as 72 hr did not show significantly altered expression levels of TIF1β (**Figure 21**).

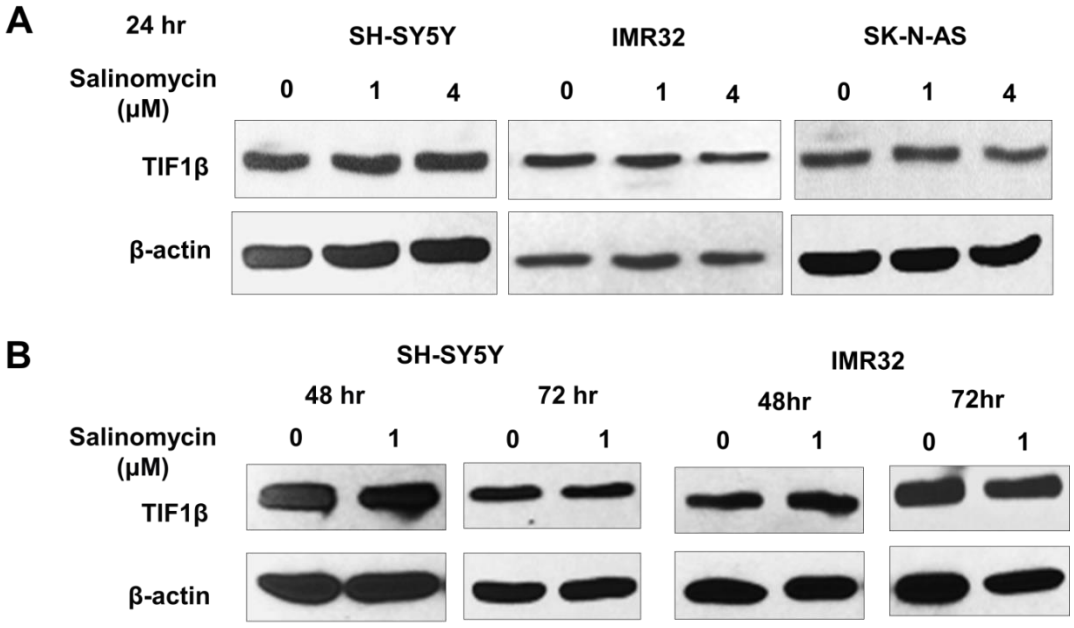

Figure 21. Effects of salinomycin on TIF1β expression levels in NB cells. (A) Expression levels of TIF1β in NB cells at 24 hr post salinomycin treatment. (B) Expression levels of TIF1β in NB cells at 48 hr and 72 hr post salinomycin treatment. Intact NB cells were treated with salinomycin at indicated concentration or DMSO control for indicated periods of time and whole cell lysates were analyzed by Western blotting. β-actin served as a loading control.

5.2.2. Effect of salinomycin on the phosphorylation of TIF1β in NB cells

It has been reported that p53 is required for the maintenance of the neuroblastic tumorigenic phenotype of NB and the down-regulation of p53 results in the conversion of N-type NB cells to the substrate-adherent fibroblast-like non-tumorigenic S-type NB cells [135]. Phosphorylated TIF1β is a critical regulator of cell proliferation and cell death through the degradation of p53 [151, 152]. Our results have shown that salinomycin down-regulates the expression of p53 (**Figure 11**). We then determine the phosphorylation of TIF1β in NB cells in response to salinomycin treatments. Our results revealed that salinomycin treatments induced phosphorylation of TIF1β at both S824 and S473 sites (**Figure 22**).

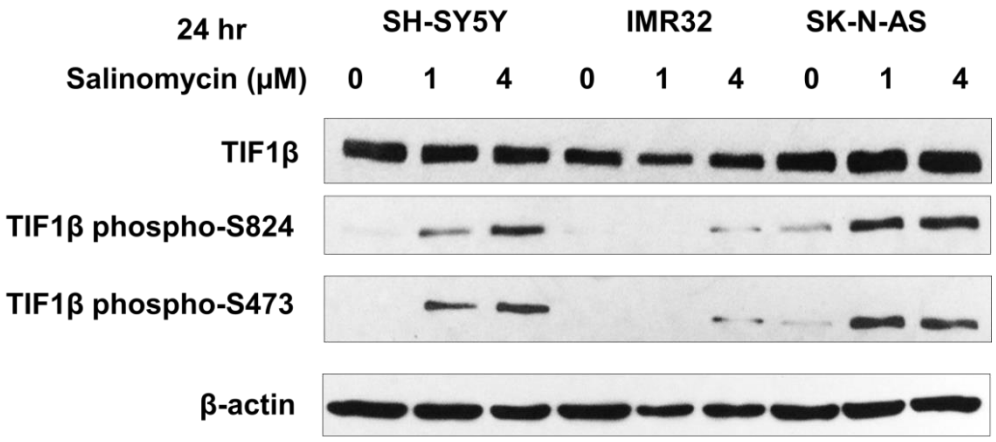

Figure 22. Salinomycin induces TIF1β serine 473/824 phosphorylation. Immunoblots were probed with antibodies specific for TIF1β, TIF1β-phosphorylated (Ser473), TIF1β-phosphorylated (S824), and reprobed with anti-β-actin antibody to serve as a loading control.

5.2.3. The role of TIF1β on salinomycin's regulation of p53 expression

To further analyze the role of TIF1β on salinomycin's regulation of p53 expression, we performed siRNA knockdown of TIF1β. As expected, in wild type cells, salinomycin treatment down-regulated p53 expression and up-regulated TIF1β phosphorylation. However, NB cells with knockdown of TIF1β did not show any further decrease in p53 expression upon

salinomycin treatment (**Figure 23**) suggesting salinomycin modulates p53 in a TIF1β dependent manner.

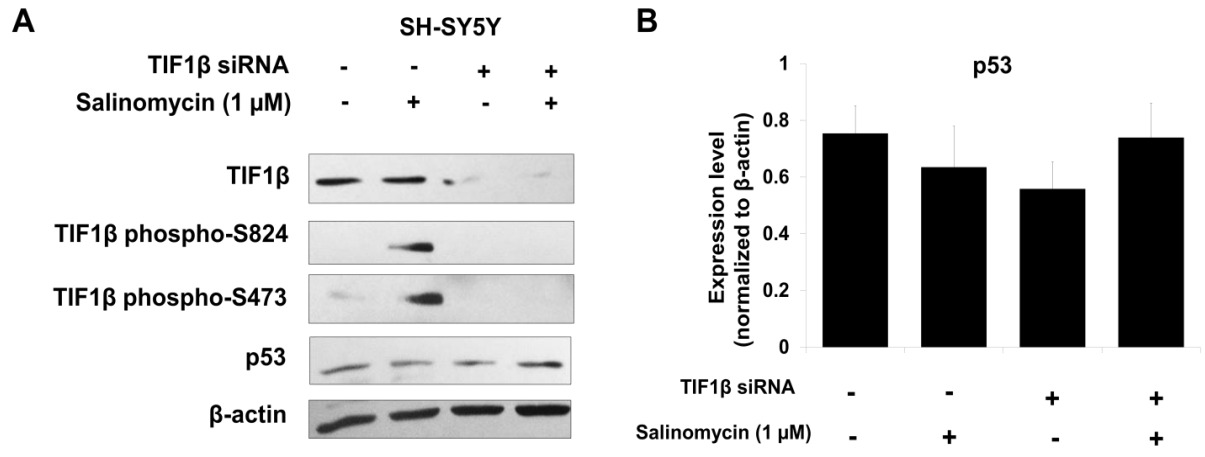

Figure 23. Salinomycin induces TIF1β serine 473/824 phosphorylation and associated down-regulation of p53. (A) Knockdown of TIF1β reverts salinomycin's effects on p53 phosphorylation and expression. Immunoblots were probed with antibodies specific for TIF1β, TIF1β-phosphorylated (Ser473), TIF1β-phosphorylated (S824), or anti-p53, and reprobed with anti-β-actin antibody to serve as a loading control. (B) Quantification of the expression of p53 in SH-SY5Y cells under indicated treatment.

5.2.4. Effects of salinomycin on the phosphorylation of NCL in NB cells

We further determined the expression and phosphorylation of NCL in NB cells in response to salinomycin treatments and revealed that the expression and the phosphorylation of this molecule were both not significantly affected by salinomycin (**Figure 24**), suggesting that salinomycin mediates its anti-CSC effects by direct interactions with NCL, and unlikely to be involved in regulation of expression of NCL either transcriptionally or post-transcriptionally.

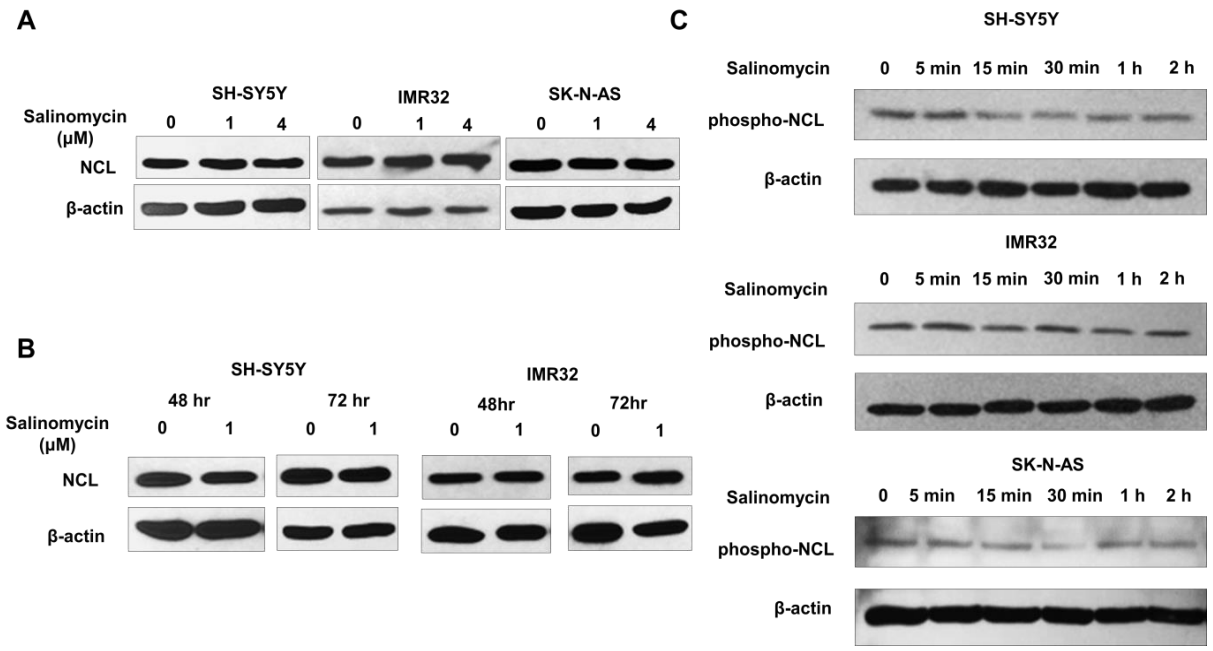

Figure 24. Expression levels of NCL and phosphor-NCL in NB cells upon salinomycin treatment. Intact NB cells were treated with 1 μM salinomycin or DMSO control for indicated periods of time and whole cell lysates were analyzed by Western blotting. β-actin served as a loading control.

5.2.5. Effect of salinomycin on CD34 gene transcription

NCL was previously shown to be recruited to CD34 promoter to direct CD34 gene transcription and regulate gene expression in $CD34^+$ Hematopoietic cells [153, 154]. To determine how salinomycin regulates the expression of CD34, we analyzed the mRNA levels of CD34 in the three NB cell lines in response to salinomycin treatments. As expected, our data show that salinomycin significantly suppressed the mRNA expression of CD34 gene ($P<0.01$) (**Figure 25**). Among the three NB cell lines, the MYCN amplified IMR32 cell line has the highest level of CD34 mRNA, while the SK-N-AS non-tumorigenic cell line show the lowest expression of CD34 mRNA (**Figure 25**).

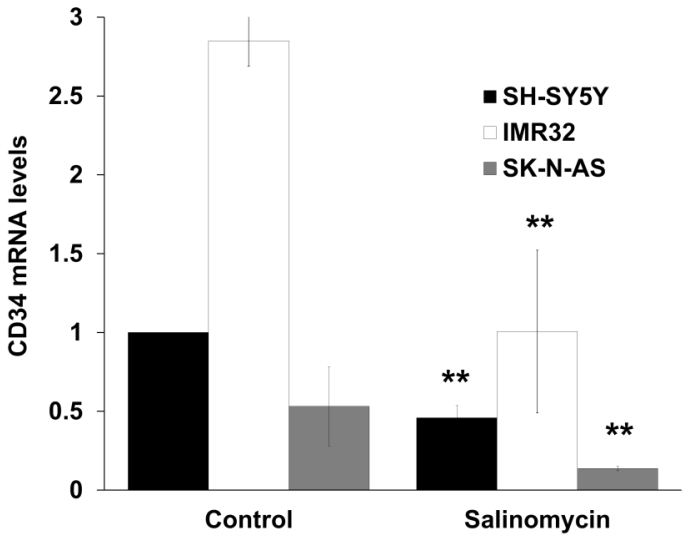

Figure 25. Salinomycin inhibits CD34 gene transcription. After treated with salinomycin or vehicle control for 24 hr, the expression of CD34 in NB cells was determined by reverse transcription-quantitative PCR and normalized using GAPDH as the internal control. *$p<0.05$ and **$p<0.01$.

5.2.6. Effect of salinomycin on $CD34^+$ NB cells

The expression of the hematopoietic stem cell (HSC) marker CD34 in NB cells and patients has been widely observed and considered as a confounding factor in the clinical management of NB [155, 156].

To analyze whether the inhibition of salinomycin on CD34 transcription leads to the suppression on $CD34^+$ NB cells, we further examined the effects of salinomycin on the $CD34^+$ population using flow cytometry. Consistent with previous studies [155], we found the existence of $CD34^+$ cell population in tumorigenic NB cells, while the non-tumorigenic SK-N-AS cell line show significant lower amount of $CD34^+$ cells. Intriguingly, upon 1 μM salinomycin treatment for 24 hr, the percentage of $CD34^+$ cells was reduced from about 2.78% and 18.8% to 1.01% and 8.53% for SH-SY5Y and IMR32 cells respectively (**Figure 26**).

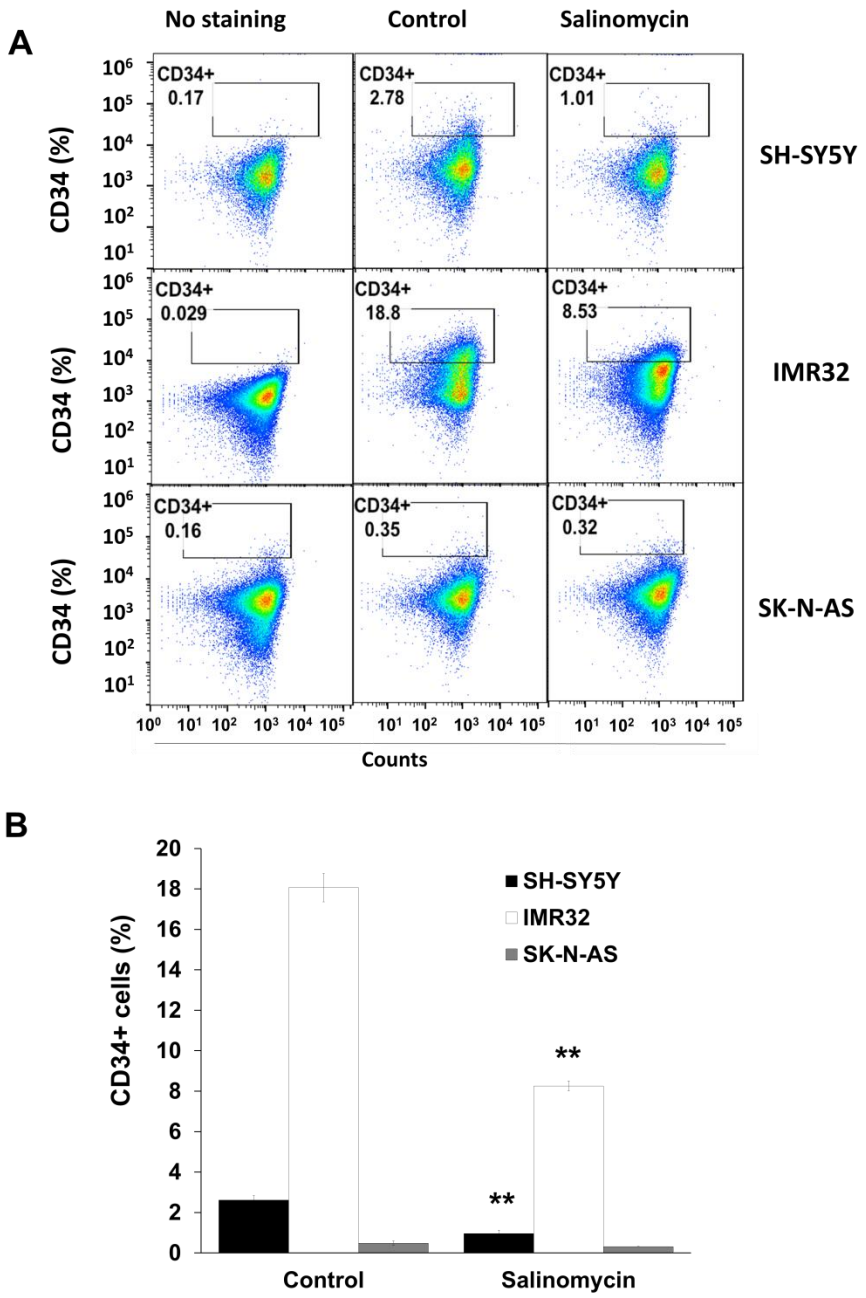

Figure 26. Effect of salinomycin on CD34+ NB cells. (A) Salinomycin inhibits CD34+ cells. After treated with salinomycin or vehicle control for 24 hr, NB cells were stained with anti-CD34 or IgG control and anti-mouse IgG-FITC and analyzed using flow cytometry. Representative results are shown. (B) Quantification of the flow cytometry data showing salinomycin inhibits CD34+ NB cells. **p<0.01.

5.2.7. The role of NCL on salinomycin's regulation of CD34 transcription

To determine how salinomycin regulates the expression of CD34, we examined the interaction of NCL with CD34 promoter using chromatin immunoprecipitation (ChIP) followed by quantitative PCR analysis in SH-SY5Y cells with or without treatment by salinomycin (**Figure 27**) [157].

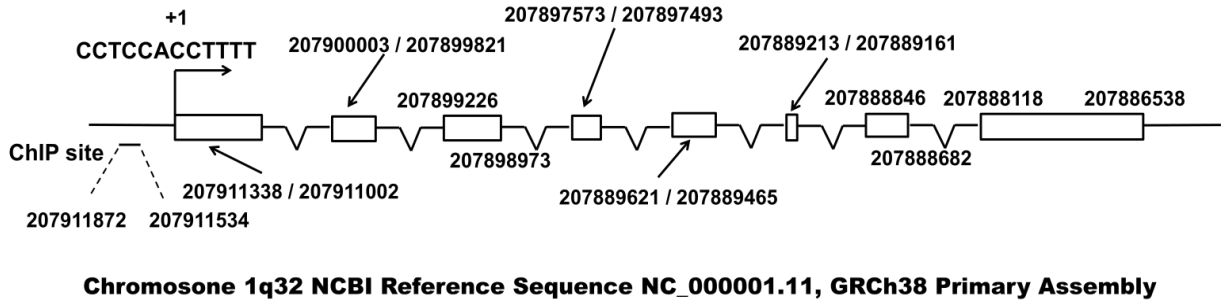

Figure 27. A schematic diagram of the CD34 cDNA and the site for ChIP analysis. Exons and introns are represented by boxes and curve lines respectively. The positions of the start and end base pair for each exon and the ChIP site are indicated by numbers.

As shown in **Figure 28**, an antibody specifically recognizing the N-terminal peptide of NCL effectively co-precipitated CD34 promoter region from control. However, in salinomycin treated SH-SY5Y cell lysates, CD34 promoter-NCL complex was not observed. These data suggest that NCL directly interact with CD34 promoter and salinomycin treatment abolished the interaction between NCL and CD34 promoter in NB cells, and thereby disrupting NCL-mediated CD34 transcription.

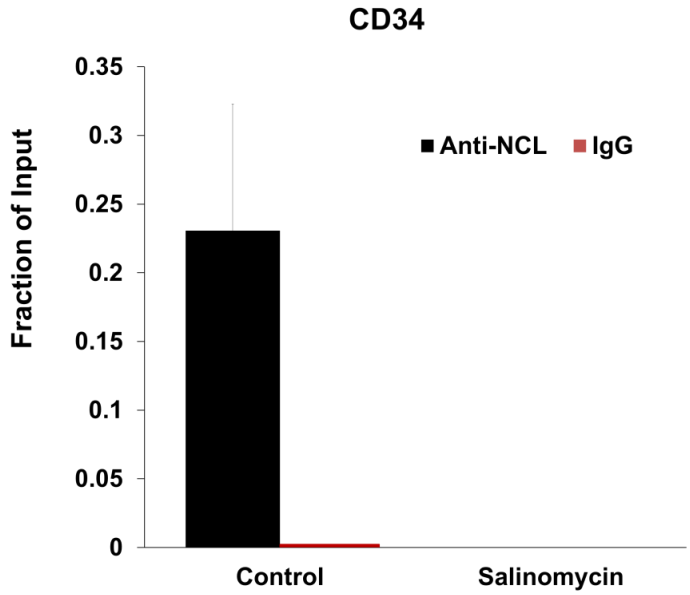

Figure 28. ChIP-qPCR analysis of NCL-CD34 promoter interaction. SH-SY5Y cells treated with DMSO control or 1 μM salinomycin for 6 hr were subjected to ChIP-qPCR analysis. *p<0.05 and **p<0.01.

5.2.8. Subcellular localization and expression of NCL and CD34 upon salinomycin treatment

To examine the regulation of salinomycin on NCL and CD34, we first visualized the subcellular localization and expression of these two molecules in NB cells following exposure to salinomycin treatment. Our data show CD34 is predominantly expressed on the cell surface of SH-SY5Y cells, while NCL is mainly expressed in the nucleus (**Figure 29**). Alteration of the localization of NCL and CD34 in NB cells by salinomycin treatment was not observed. However, with increasing concentration of salinomycin treatment (0 μM, 0.25 μM, 0.5 μM, and 1 μM), the expression levels of cell surface CD34 molecule were apparently reduced (**Figure 29**).

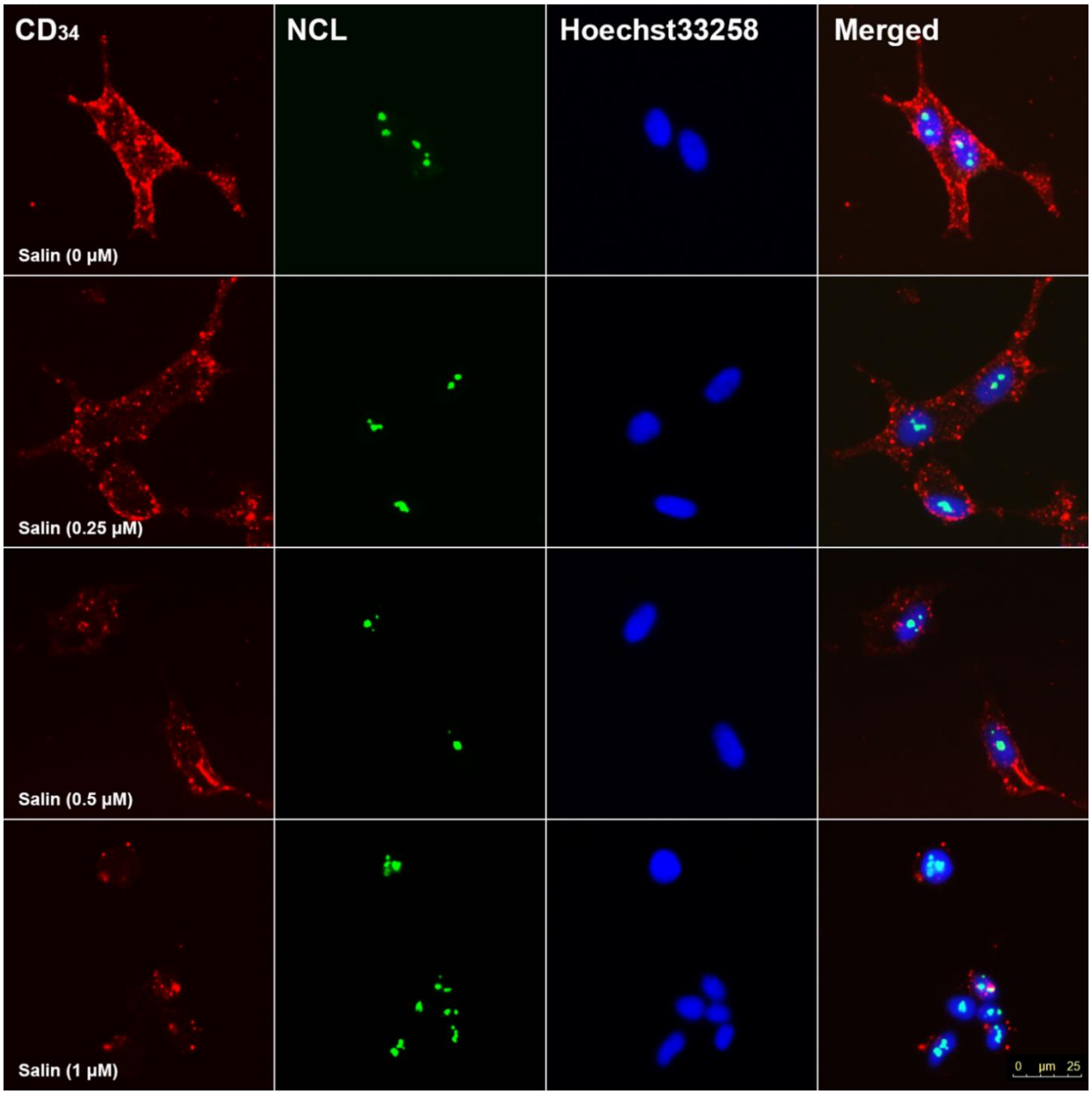

Figure 29. Decreased CD34 protein expression following exposure to salinomycin treatment. SH-SY5Y cells were treated with salinomycin at indicated concentrations for 24 hr. Subcellular localization and expression of NCL and CD34 proteins were analyzed by immunofluorescent staining for endogenous CD34 labeled with anti-CD34 antibody (red), and NCL labeled with anti-NCL antibody (green) and examined by fluorescent microscopy. The nucleus was stained with Hoechst 33258 (blue).

5.2.9. The role of NCL on salinomycin's regulation of CD34 protein expression

To further understand the mechanism of NCL's role in salinomycin's regulation of CD34 and $CD34^+$ cells, we analyzed the role of NCL on CD34 protein expression with or without salinomycin treatment. As shown in **Figure 30**, salinomycin treatment did not significantly alter the levels of NCL, but slightly reduced the expression of CD34 protein.

Overexpression of NCL by transient transfection of NCL plasmid induced a marked increase of CD34 protein expression, likely because of more NCL protein occupied the CD34 gene promoters and activated CD34 expression. Intriguingly, upon salinomycin treatment, cells with overexpressed NCL showed more intensive response to salinomycin treatment in regard to the reduction in the protein expression levels of CD34, suggesting the disruption of the NCL-CD34 promoter complex by salinomycin treatment (**Figure 30 A-B**).

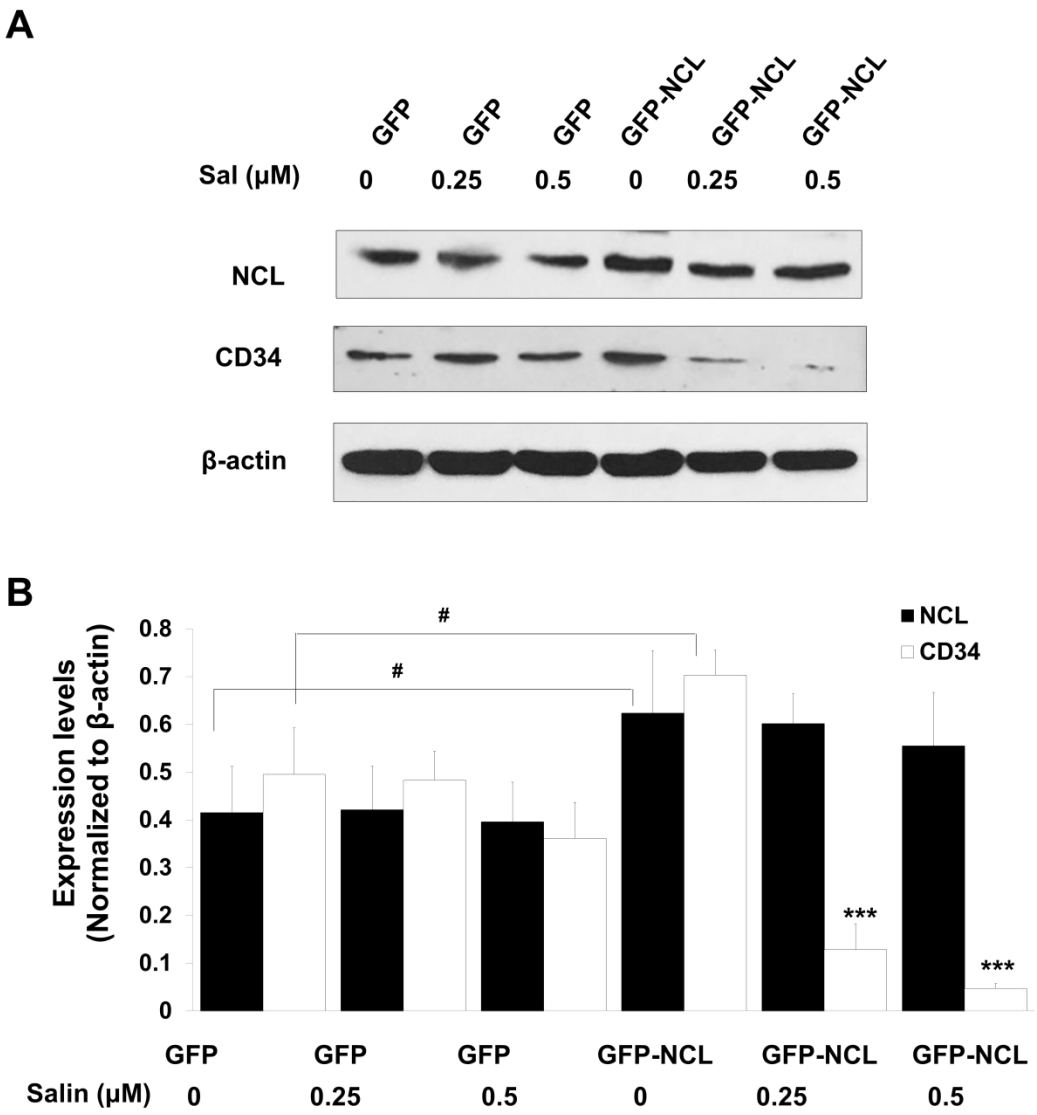

Figure 30. NCL sensitizes salinomycin's regulation on CD34 protein expression. (A) Cells incubated with GFP or GFP-NCL plasmids overnight were treated with DMSO control, 0.25 μM or 0.5 μM salinomycin. After 24 hr, whole cell lysates were analyzed by Western blotting. β-actin served as a loading control. (B) Quantification of the protein expression levels. Level of statistical significance, compared GFP-NCL transfected cells with GFP transfected cells: $^{\#}p<0.05$; compared GFP-NCL transfected cells with salinomycin treatment with GFP-NCL transfected cells with vehicle control treatment: ***$p<0.001$.

In contrast, knockdown of NCL protein by using siRNAs decreased the expression levels of CD34 (**Figure 31**). We treated NCL knockdown NB cells with 0 μM, 0.25 μM, 0.5 μM, and 1 μM salinomycin for 24 hr, however, these cells showed less response to salinomycin treatment

on the reduction in the protein expression levels of CD34 (**Figure 30**), suggesting salinomycin regulates CD34 in a NCL dependent manner.

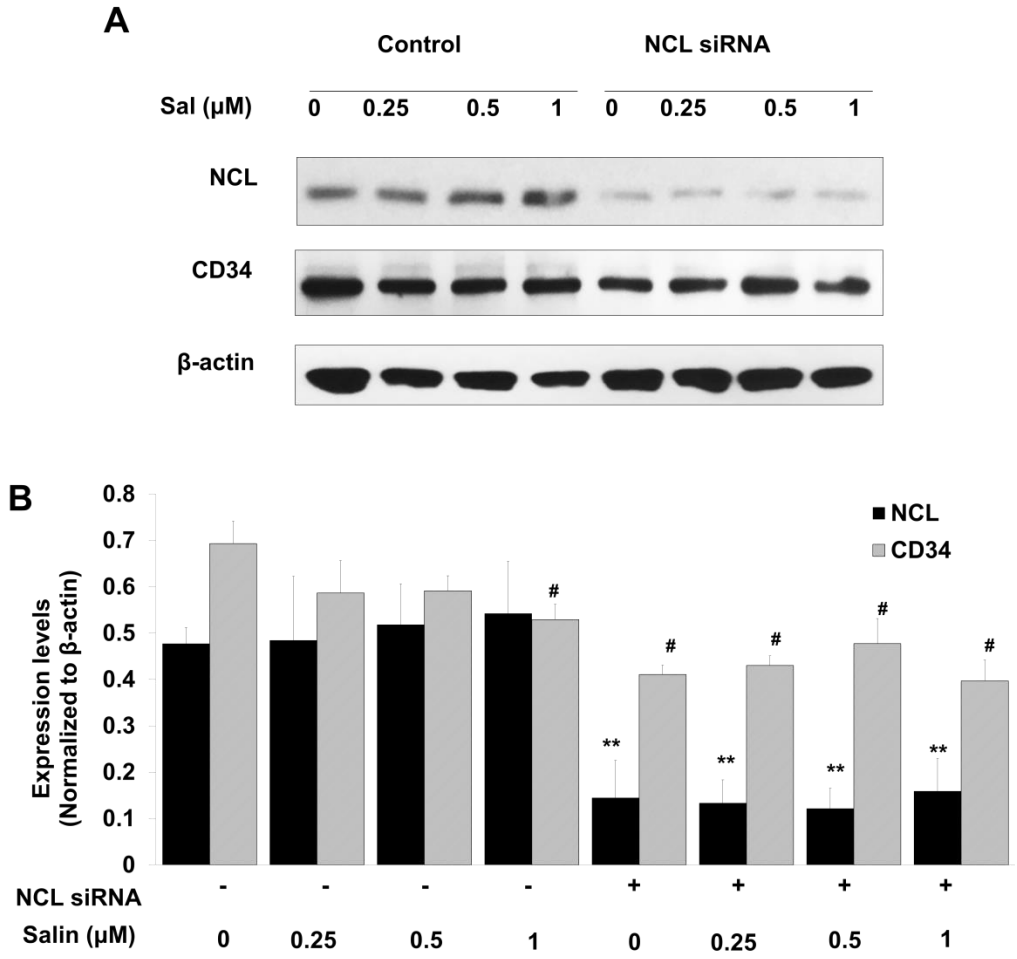

Figure 31. Knockdown of NCL down-regulates CD34 protein expression and salinomycin's regulation on CD34 protein expression. (A) Cells incubated with control or NCL siRNAs for 48 hr were treated with DMSO control, 0.25 μM, 0.5 μM, or 1 μM salinomycin. After 24 hr, whole cell lysates were analyzed by Western blotting. β-actin served as a loading control. (B) Quantification of the protein expression levels. Level of statistical significance, compared NCL siRNA transfected cells with respective control siRNA transfected cells: $^{\#}p<0.05$ and $^{**}p<0.01$.

5.2.10. The role of NCL on salinomycin's regulation of $CD34^+$ cells

To further establish the functional link between NCL and $CD34^+$ cells, we further analyzed the effects of NCL protein overexpression or knockdown on the percentage of $CD34^+$ cells in NB cells using flow cytometry. Our results show that knockdown of NCL slightly

reduced the percentage of CD34^{+} cells, and the effect was not further enhanced by salinomycin treatment (**Figure 32**).

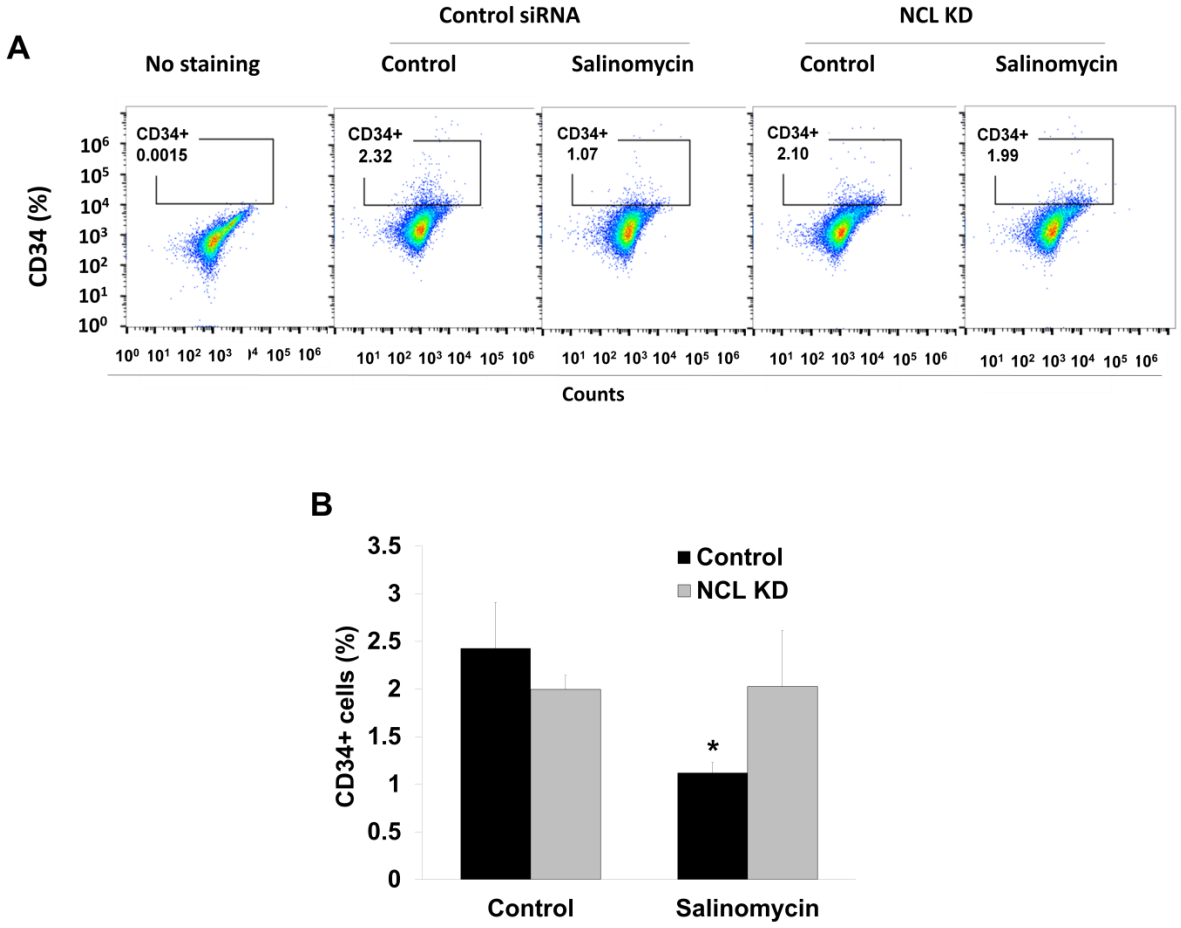

Figure 32. Effect of salinomycin on CD34^{+} NB cells in a NCL knockdown NB cells. (A) Cells incubated with control or NCL siRNAs for 48 hr were treated with DMSO control or 0.25 μM salinomycin. After 24 hr, cells were stained with anti-CD34-APC antibody or IgG control and were analyzed by flow cytometry. (B) Quantification of the flow cytometry data of Figure 31A. Data represent the mean ± SD of triplicate experiments. The statistical differences were determined using paired student's t-test and performed using Minitab. *p<0.05.

Notably, overexpression of NCL dramatically increased the percentage of CD34^{+} cells from about 4.64% to 17.2%. In the wild type or NCL overexpression NB cells, the inhibition of CD34^{+} cells by salinomycin were both observed (**Figure 33**).

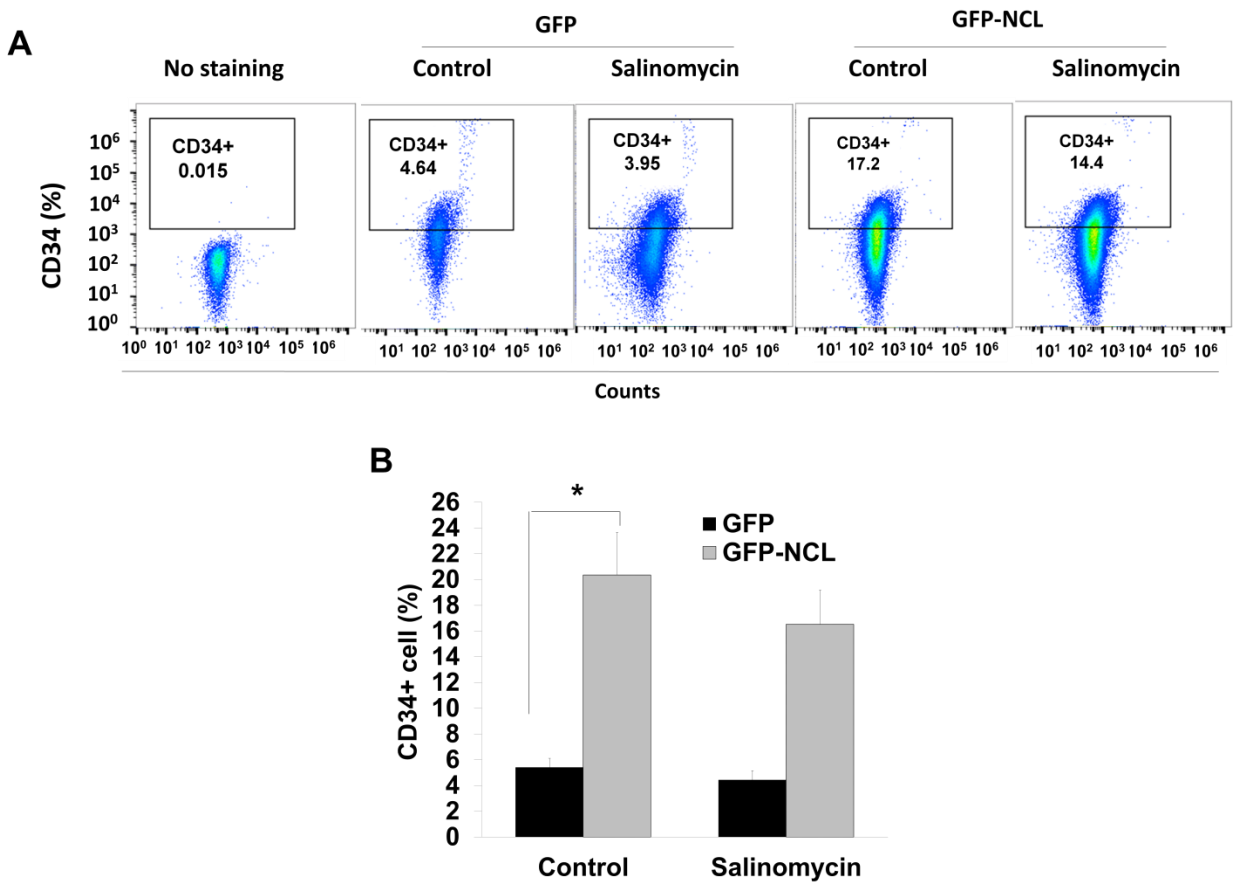

Figure 33. Effect of salinomycin on CD34$^+$ NB cells in a NCL overexpression NB cells. (A) Cells incubated with GFP or GFP-NCL plasmids overnight were treated with DMSO control or 0.25 μM salinomycin. After 24 hr, cells were stained with anti-CD34-APC antibody or IgG control and were analyzed by flow cytometry. (B) Quantification of the flow cytometry data of Fig. 7B. Data represent the mean ± SD of triplicate experiments. The statistical differences were determined using paired student's t-test and performed using Minitab. *$p<0.05$.

CHAPTER 6. SUMMARY, CLINICAL IMPLICATIONS, CONCLUSIONS, AND FUTURE DIRECTIONS

6.1. Summary and discussions

In this study, we demonstrated that salinomycin inhibits NB growth and tumorsphere formation and induces cell cycle arrest. By using chemoproteomics and anti-salinomycin affinity beads, we identified that NCL and TIF1β are salinomycin's binding targets in NB cells. We further revealed that TIF1β and NCL play a critical role in salinomycin's anti-cancer and anti-CSC activity. We show that knockdown of NCL and/or TIF1β inhibits proliferation and tumorsphere formation while NB cells lacking NCL and TIF1β are no longer responding to salinomycin treatment. Our data also revealed that TIF1β is involved in salinomycin's modulation of the p53 pathway, and NCL is required for salinomycin's inhibition on the CSC marker CD34 gene transcription and $CD34^+$ cell population.

6.1.1. The effects of salinomycin in NB

Our data showed the inhibitory effects of salinomycin on cell proliferation in the three NB cell lines at 48 h with IC50 values at 1μM for the N-type tumorigenic SH-SY5Y and IMR32 cells, and > 4 μM for the S-type non-tumorigenic SK-N-AS cells, indicating salinomycin is more effective in tumorigenic cells. In addition, the IC50 value of salinomycin in N-type NB cells is much lower than some currently used chemotherapeutic drugs for NB, e.g. carboplatin, in the same *in vitro* cell line systems [158].

Salinmycin induces cell cycle arrest at G2 phases and up-regulates cyclin A suggesting that up-regulation of cyclin A level by salinomycin might be due to the prolonged G2 phases. In addition, p21 possesses an anti-apoptotic activity which allows for cell survival after exposure to DNA-

damaging agents [159]. Our data show that salinomycin also decreased the p21 protein level in NB cells, suggesting that salinomycin may action in the attenuation of p21 and the subsequent subversion of the normal DNA-damage repair process. Our results are in agreement with previous reports that salinomycin could sensitize cancer cells to both radiation and chemotherapies by increasing DNA damage and reducing the increased p21 levels induced by radiation or chemotherapy [69, 70]. The cell cycle arrest at G2 phase and the up-regulation of cyclin A and down-regulation of the anti-apoptotic protein p21 and tumor suppressor p53 may contributes to salinomycin's inhibition on NB cell proliferation.

A complete inhibition of salinomycin on NB cell tumorsphere formation was also observed, which further demonstrated that salinomycin inhibits NB CSCs. Salinomycin also showed effective inhibition on $CD133^+$ or c-kit^+ CSC like NB cell population. CD133 is one of the most widely used markers for various somatic cells and putative CSCs, including NB CSCs [37, 38, 51]. Takenobu et al. reported that CD133 suppresses NB cell differentiation, but accelerates cell proliferation, colony formation, and *in vivo* tumor formation of NB cells [160]. Therefore, the down-regulation of NB cell proliferation and tumorsphere formation by salinomycin shown in our study is at least partially contributable to its inhibition on $CD133^+$ NB cells. In addition, c-kit expression can be also detected in the majority of primary neuroblastic tumors including NB, and its expression is associated with unfavorable clinic-biological variables, such as MYCN [134]. Our study also showed that among the three tested NB cell lines, IMR32 cells with MYCN amplification contain higher percentage of c-kit^+ cells. Functional blockade of c-kit receptors in NB cells was demonstrated to significantly decrease cellular growth rate [161], indicating the role of c-kit on the effects of salinomycin on NB cell

proliferation and cell cycle progression. Our study is the first to observe the profound anti-cancer and anti-CSC activities of salinomycin in human NB cells.

6.1.2. Binding targets of salinomycin in NB

In this study, we identified TIF1β and NCL as two binding targets of salinomycin in NB cells and both TIF1β and NCL are critical regulators of multiple cellular functions including cell proliferation, cell death and maintenance of stem cell properties [136, 140, 162-166]. For instance, the functions of NCL span from ES cell self-renewal [136, 153] and NB cell differentiation [150]. In line with our findings, high levels of NCL signify tumorigenesis [140, 167-171] while an absence of NCL induces cell growth arrest at G2 phase [149]. In this study, we observed that, knockdown of NCL inhibited cell proliferation by 30% and tumorsphere formation by 55% and salinomycin treatment could induce G2 cell cycle arrest. These results are consistent with previous reports that NCL is important for cell proliferation and tumorigenesis [172][140, 149, 167-171].

Knockdown of TIF1β alone showed no significant effect on NB cell proliferation, but showed significant inhibition on tumorsphere formation, indicating a more important role for TIF1β in NB stem cell maintenance and cell differentiation compared to cell growth and proliferation control in NB cells. Cells knockdown both TIF1β and NCL no longer responded to salinomycin treatment on both cell proliferation and tumorsphere formation, indicating that TIF1β and NCL are functional cellular protein targets of salinomycin. The interaction of TIF1β and NCL in cancer cells may enhance tumor growth [138, 141].

Previous studies have revealed the interaction between TIF1β and NCL in cancer cells. TIF1β and NCL were found to form complex with transcription-involved protein upregulated in

hepatocellular carcinoma (TIPUH1), which is associated with hepato-carcinogenesis, in hepatocellular carcinoma cells [141]. TIF1β also forms complex with NCL and ErbB4, and reduces ErbB4 transcription in breast cancer cells [138]. Our data also show co-IP of TIF1β and NCL in NB cells and positive correlation for the expression of TIF1β and NCL in NB patients. Future investigations on the functions of TIF1β and NCL and interactions between these proteins in NB are warranted.

6.1.3. The mechanism of salinomycin in NB and the role of its binding targets

Transplantation of autologous peripheral blood stem cells (PBSC), obtained by $CD34^+$ stem cell selection, permits intensified treatment for high risk NB patients [173]. However, the expression of the HSC marker CD34 on the surface of NB cell lines and tumors [155, 156] and the cancer relapse after autologous stem cell rescue caused by re-infused CD34 NB cells in NB patients [174] bring out the notion that $CD34^+$ NB subpopulation may contain tumorigenic NB CSCs. Intriguingly, salinomycin binding target NCL mediates the activation of CD34 transcription via binding to its promoter region [153]. In our study, by using ChIP-qPCR analysis, we show salinomycin efficiently reduce $CD34^+$ cells and inhibit CD34 gene transcription by interfering with the binding of NCL with CD34 promoter region. In addition, the regulation of salinomycin on CD34 is highly NCL dependent. Future investigation on the molecular details of the interaction between CD34 and NCL in NB CSCs as well as HSCs will be valuable. More importantly, Lu and colleagues recently reported that in contrary to cancer cells, normal human peripheral blood lymphocytes show resistance to salinomycin toxicity [71]. Since our study showed marked inhibitory effects of salinomycin on $CD34^+$ NB cells, salinomycin might be considered as a promising drug for high risk NB patients receiving high-dose

chemo/radiotherapy followed by autologous PBSC rescue in order to prevent cancer relapse and improve the survival after transplantation. Well-designed trials to address the effects of salinomycin on $CD34^+$ NB cells as well as PBSCs will be valuable.

It has been reported that p53 is required for the maintenance of the neuroblastic tumorigenic phenotype of NB and the down-regulation of p53 results in the conversion of N-type NB cells to the substrate-adherent fibroblast-like non-tumorigenic S-type NB cells [135]. Phosphorylated TIF1β is a critical regulator of cell proliferation and cell death through the degradation of p53 [151, 152]. We determined the protein expression and phosphorylation of TIF1β in NB cells in response to salinomycin treatments and revealed that salinomycin treatments did not alter the level of TIF1β total protein in NB cells but induced phosphorylation of TIF1β at both S824 and S473 sites and down-regulated the expression of p53. Interestingly, we observed two protein bands for p53 in the wild type SH-SY5Y and IMR32 cells but only one band for the SK-N-AS cells, suggesting there are different p53 splice variants [175, 176] in the tumorigenic and non-tumorigenic NB cell lines and different p53 isoforms may have distinct functions in NB, which would be valuable to study in the future. Level of cyclin A, which is known to regulate the G2/M transition in a p53 dependent manner [130, 131], was dramatically increased. Our data also show the inhibition of salinomycin on the p53 downstream target p21, a key regulator of cell cycle progression and the DNA damage response (DDR), which is in line with the findings that salinomycin is able to sensitize cancer cells to both radiation and chemotherapies by increasing DNA damage [69, 70]. Intriguingly, previous studies suggested that phosphorylation of TIF1β at both S824 and S473 sites are implicated in DDR [177, 178], and the phosphorylation of TIF1β at S473 in DDR was found to impact the G2/M checkpoint [178]. These results suggest the TIF1β-p53 axis may play an important role in salinomycin't

effects on DDR. Moreover, NB cells with knockdown of TIF1β showed increased p53 expression upon salinomycin treatment suggesting salinomycin modulates p53 in a TIF1β dependent manner.

6.2. Clinical Implication

Prognosis of NB could be very complex based on the disease stage, patient's age, and highly heterogeneous tumor biology. Currently, some common prognostic factors, such as, patients' age, MYCN amplification, deletion of parts of chromosome arm 1p and 11q, and gain of chromosome 17q, have been linked with unfavorable outcome.[29, 179-181] However, none of them can be used as an independent marker for NB prognosis, and searching for more meaningful biomarkers are needed.

6.2.1. The correlation of TIF1β and NCL levels with NB patients' outcomes

To further analyze the clinical implication of TIF1β and NCL in NB, we queried the R2.amc.nl database for a comprehensive analysis and evaluation of the expression of TIF1β and NCL in a cohort of 498 NB patients and the correlation of the expression of TIF1β and NCL with patients' outcomes. We found that an elevated level of TIF1β and NCL were associated with a significant risk of shortened survival (**Figure 34 A-B**) and an increased rate of relapse of the disease (**Figure 34 C-D**).

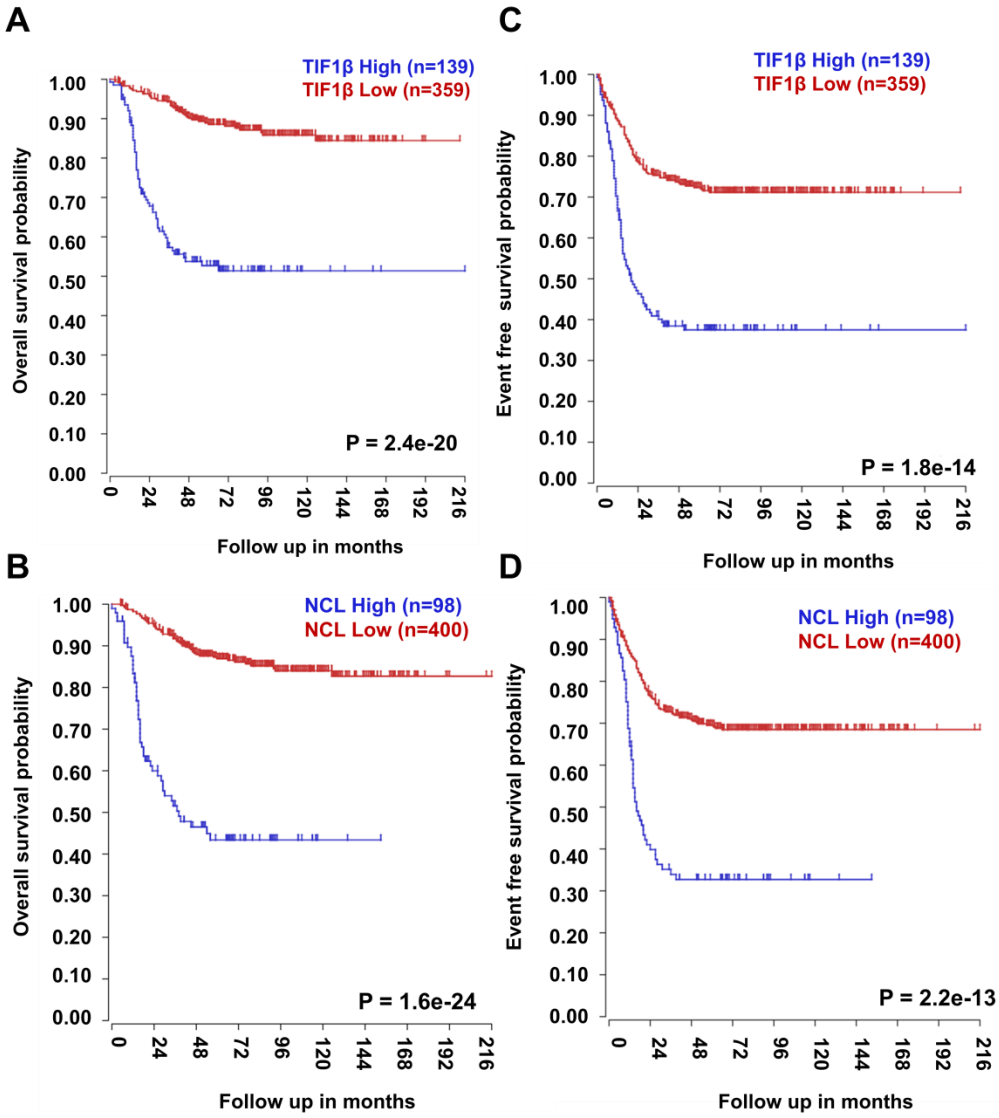

Figure 34. The expression of TIF1β and NCL in NB tumors and correlation of TIF1β and NCL levels with NB patients' outcomes. (A) Kaplan-Meier plots of overall survival time according to TIF1β levels in NB patients. (B) Kaplan-Meier plots of overall survival time according to NCL levels in NB patients. (C) Kaplan-Meier plots of relapse free survival time according to TIF1β levels in NB patients. (D) Kaplan-Meier plots of relapse free survival time according to NCL levels in NB patients.

6.2.2. The correlation of TIF1β and NCL levels with MYCN amplification

Tumor stage and MYCN amplification are among the most highly statistically significant and clinically relevant risk factors for NB patients [179, 182]. It is noteworthy that in our

analysis, we found that the expression levels of TIF1β and NCL correlated with the tumor stage (**Figure 35 A-B**). Patients at stage 4 have markedly higher levels of both TIF1β and NCL compared with that of patients at stage 1. We have also found that the expression of TIF1β and NCL are correlated with the amplification of the oncogene MYCN (**Figure 35 C-D**) at diagnosis. This is also consistent with our *in vitro* study that IMR32 cells with MYCN amplification [183] express relatively higher levels of TIF1β and NCL than other cell lines and sensitive to salinomycin treatment.

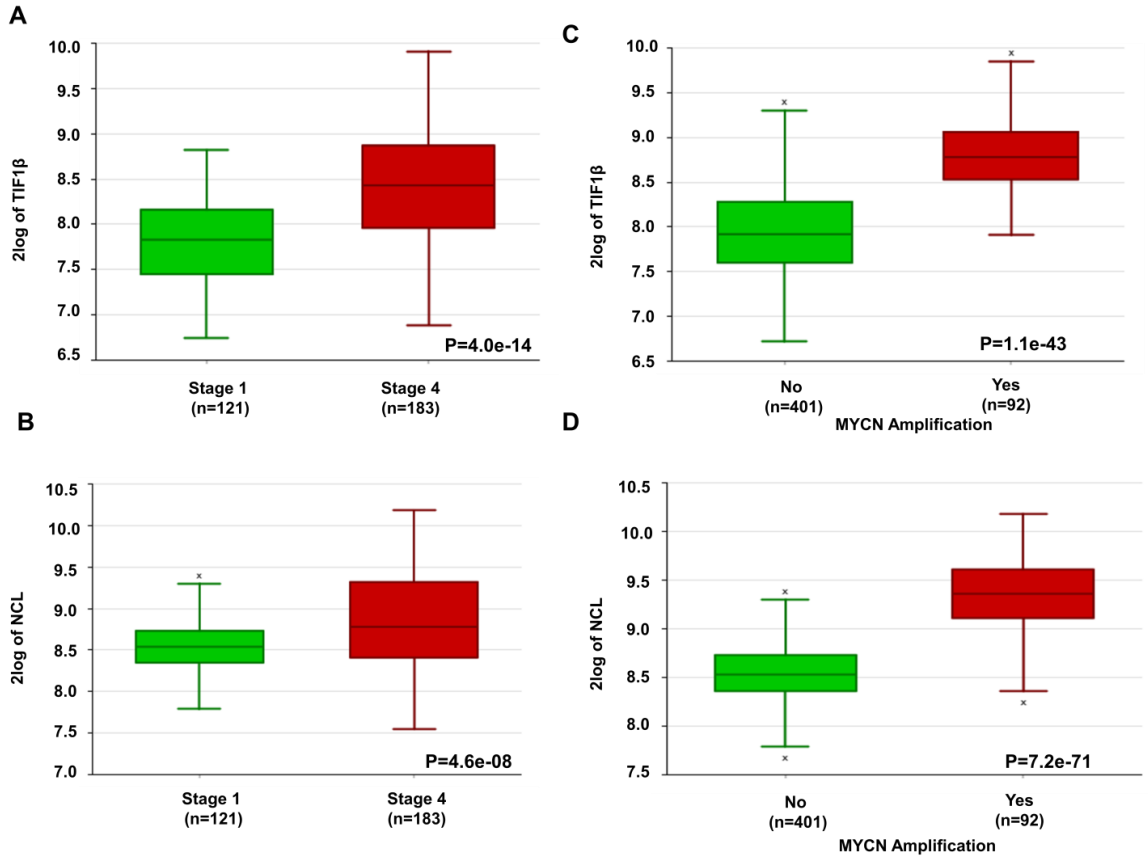

Figure 35. The correlation of TIF1β and NCL levels with poor prognostic markers. (A) The expression of TIF1β in NB patients diagnosed as INSS Stage 1 or Stage 4. (B) The expression of NCL in NB patients diagnosed as INSS Stage 1 or Stage 4. (C) The expression of TIF1β in NB patient with or without MYCN amplification. (D) The expression of NCL in NB patient with or without MYCN amplification. The band inside the box indicates the median value. The space between the upper and lower edge of the box represents the range of the data. The whisker represents the standard deviation.

6.2.3. The correlation of the expression levels between TIF1β and NCL

Our data also show positive correlation for the expression of TIF1β and NCL in NB patients (**Figure 36**).

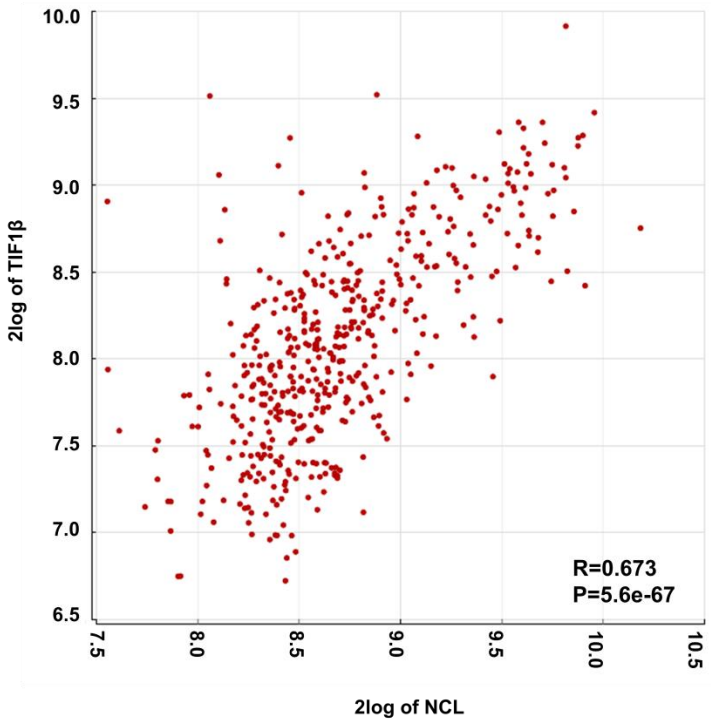

Figure 36. The correlation of TIF1β and NCL levels in NB patients. Dot plot of TIF1β expression levels versus NCL expression levels in NB patients. Pearson's correlation coefficient (r) and corresponding P value are displayed.

6.3. Conclusions

In summary, our work identify that NCL and TIF1β are salinomycin's binding proteins in NB cells. Previous reports showed that both target proteins play important roles in multiple cellular functions including cell proliferation, cell death, and more importantly, the maintenance of stem cell properties [136, 140, 162-166], which may partially explain salinomycin's preferential inhibition on CSC like cells. For instance, salinomycin suppresses the expression of $CD34^+$ cells by disrupting the interaction of NCL binding to CD34 promoter, consequently

reducing the CSC-like population in NB cells. The proposed mechanism for the anti-cancer effects of salinomycin and the roles of its binding targets are shown in **Figure 37.** Furthermore, we revealed that salinomycin's binding targets TIF1β and NCL are correlated with clinical outcomes of NB patients. Taken together, this study provides a therapeutic rationale for evaluating both salinomycin and TIF1β and NCL in NBs.

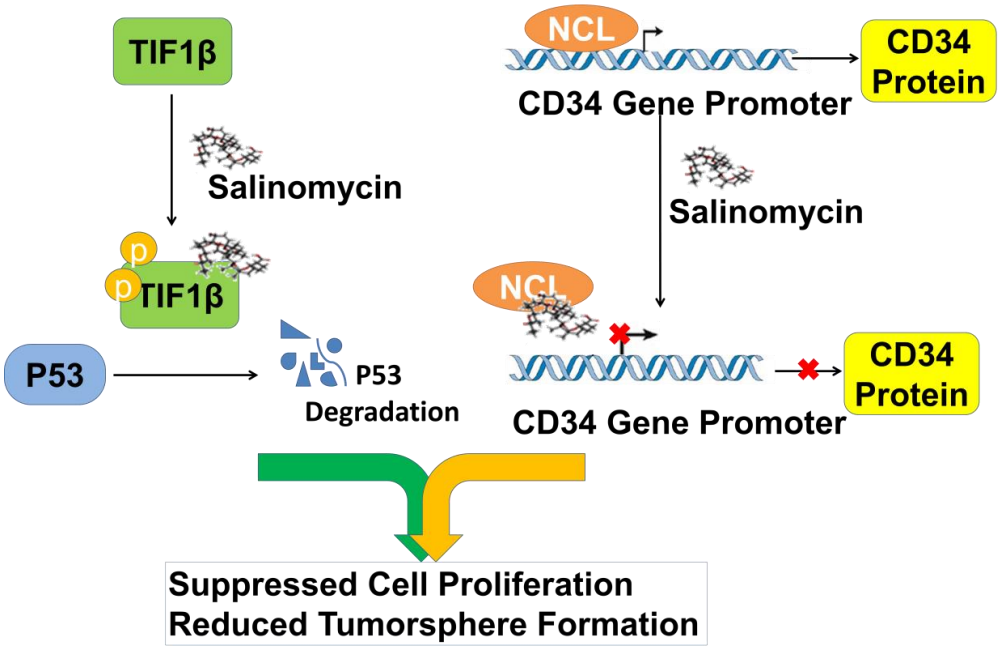

Figure 37. Schematic representation of the interaction of salinomycin with its functional binding target proteins TIF1β and NCL in NB.

6.4. Future directions

Salinomycin was shown to induce terminal epithelial differentiation accompanied by cell-cycle arrest rather than trigger cytotoxicity in breast cancer [88], and induce cell death and differentiation in head and neck squamous cell carcinoma stem cells despite activation of epithelial-mesenchymal transition and Akt [104]. The profound inhibitory effects of the CSC inhibitor salinomycin on NB cells and NB CSC like population shown by our data suggest the

impact of salinomycin on NB-CSCs. Interestingly, the salinomycin binding targets identified in our study, TIF1β and NCL, are both highly expressed in cancer cells and involved in stem cell maintenance and differentiation. TIF1β was identified as a self-renewal gene through a genome-wide RNAi screen in mouse embryonic stem (ES) cells [162]. The depletion of TIF1β resulted in cell differentiation into the primitive endodermal lineage [164]. Similarly, NCL is required for the maintenance of embryonic stem cell self-renewal [136]. Therefore, for future investigations, to isolate NB-CSC population and determine the effects and mechanism of salinomycin and its binding targets on both NB-CSC subset and NB large population in respect to the stemness and cell differentiation will be valuable.

Our study for the first time demonstrated the anti-cancer effects of salinomycin in NB *in vitro*. However, the effects and mechanism of salinomycin and the role of its binding targets in NB *in vivo* models have not been investigated yet. In our future investigation, we would extend our study to examine the mechanism of salinomycin in NB mice models established by using wild type NB cell lines, TIF1β and/or NCL knockdown NB cells, as well as the isolated NB CSC like populations. Noteworthy, the tumorigenicity of $CD34^+$ NB cells in mice model has not been studied up to the present. Using the *in vivo* mice models, we anticipate our study revealing important information in NB and the understanding of salinomycin's mechanism of action.

In our study, we have identified TIF1β and NCL as potential salinomycin's binding targets in NB cells using a modified drug affinity based proteolytic enzyme digestion analysis [124, 184]. With the aid of structural modeling (data not shown), we predict that salinomycin may bind to TIF1β and NCL at their DNA binding domain and RNA binding domain respectively. To further understand the interaction between salinomycin and its binding targets, we would evaluate our *in silicon* models to determine the binding affinities and to identify the

binding sites of TIF1β and NCL with salinomycin by performing crystallization using wild type and mutant TIF1β and NCL proteins with salinomycin.

As illustrated in Figure 5, previous studies have revealed a few possible mechanisms for salinomycin's anti-cancer activity, for instance, the activation of unconventional pathways of cell death, enhanced DNA damage, and the inhibition of Wnt signaling pathway, appear to be germane to the multi-dimensional anti-CSC and anti-tumorigenic activities of salinomycin [66-71]. The relationship of our discovered TIF1β and NCL related mechanism with these existing mechanisms remains unclear. As discussed earlier, previous studies and our data have shown the induction of salinomycin in DDR [69, 70]. The phosphorylation of TIF1β at both S824 and S473 sites and its associated regulation of p53 were also implicated in DDR [177, 178]. These results suggest the TIF1β-p53 axis may play an important role in salinomycin't effects on DDR. Future investigation on the role of TIF1β on salinomycin's effect on DDR is warranted. The mechanism of salinomycin in CSCs has been linked to its inhibitory effects in Wnt signaling by blocking the phosphorylation of the Wnt co-receptor lipoprotein receptor related protein 6 (LRP6) and inducing its degradation [71] or by suppressing LRP6 expression and subsequently inhibits Wnt/β-catenin and mTORC1 signaling in breast and prostate cancer cells [185]. Salinomycin has also been shown to inhibit gastric tumor growth by suppressing Wnt signaling in CSCs [186]. Interestingly, salinomycin's binding target NCL is also closely associated with Wnt signaling. Cell surface NCL was found to exist in a highly stable 500-KDa protein complex including two Wnt related proteins, and targeting surface NCL could change the organization of the complex and thus lead to inhibitory effects of cancer cells [187]. In addition, NCL was also found to be a binding partner with urokinase-type plasminogen activator (uPA) which is overexpressed in the tumor-stromal invasive microenvironment in many human cancers [188], and plays a vital role in

cancer stemness [189]. Notably, the receptor (i.e, uPA receptor [uPAR]) for this NCL binding partner has been shown to regulate Wnt/β-catenin signaling and mediate induction of CSC-like population in medulloblastoma cells [190]. These studies suggest NCL may be involved in salinomycin's regulation in Wnt signaling. Further investigations are required on the function of NCL in the regulation of Wnt signaling.

By analyzing the expression levels of TIF1β and NCL in 498 NB samples of R2 database, we revealed that elevated levels of TIF1β and NCL in NB are associated with a poor outcome. In this study, we found that the expression levels of salinomycin target proteins, TIF1β and NCL, are correlated with NB patient survival and disease relapse very well, and both of them are possible new prognostic factors for NB prognosis. Future clinical studies with larger number of patients will be valuable for further evaluation of the prognostic values of these new markers.

REFERENCES

1. Maris, J.M., et al., *Neuroblastoma.* Lancet, 2007. **369**(9579): p. 2106-20.
2. Schwab, M., et al., *Neuroblastoma: biology and molecular and chromosomal pathology.* Lancet Oncol, 2003. **4**(8): p. 472-80.
3. Matthay, K.K., et al., *Long-term results for children with high-risk neuroblastoma treated on a randomized trial of myeloablative therapy followed by 13-cis-retinoic acid: a children's oncology group study.* J Clin Oncol, 2009. **27**(7): p. 1007-13.
4. Simon, T., et al., *Treatment and outcomes of patients with relapsed, high-risk neuroblastoma: results of German trials.* Pediatr Blood Cancer, 2011. **56**(4): p. 578-83.
5. Ducassou, A., et al., *Long-term side effects of radiotherapy for pediatric localized neuroblastoma : Results from clinical trials NB90 and NB94.* Strahlenther Onkol, 2015.
6. Holtta, P., et al., *Long-term adverse effects on dentition in children with poor-risk neuroblastoma treated with high-dose chemotherapy and autologous stem cell transplantation with or without total body irradiation.* Bone Marrow Transplant, 2002. **29**(2): p. 121-7.
7. Powell, J.E., et al., *Neuroblastoma in Europe: differences in the pattern of disease in the UK. SENSE. Study group for the Evaluation of Neuroblastoma Screening in Europe.* Lancet, 1998. **352**(9129): p. 682-7.
8. Bond, J.V., *Unusual presenting symptoms in neuroblastoma.* Br Med J, 1972. **2**(5809): p. 327-8.
9. Maris, J.M., et al., *Evidence for a hereditary neuroblastoma predisposition locus at chromosome 16p12-13.* Cancer Res, 2002. **62**(22): p. 6651-8.

10. Mosse, Y.P., et al., *Identification of ALK as a major familial neuroblastoma predisposition gene.* Nature, 2008. **455**(7215): p. 930-5.

11. Raabe, E.H., et al., *Prevalence and functional consequence of PHOX2B mutations in neuroblastoma.* Oncogene, 2008. **27**(4): p. 469-76.

12. Schlisio, S., et al., *The kinesin KIF1Bbeta acts downstream from EglN3 to induce apoptosis and is a potential 1p36 tumor suppressor.* Genes Dev, 2008. **22**(7): p. 884-93.

13. Schilling, F.H., et al., *Neuroblastoma screening at one year of age.* N Engl J Med, 2002. **346**(14): p. 1047-53.

14. Breslow, N. and B. McCann, *Statistical estimation of prognosis for children with neuroblastoma.* Cancer Res, 1971. **31**(12): p. 2098-103.

15. Brodeur, G.M., *Neuroblastoma: biological insights into a clinical enigma.* Nat Rev Cancer, 2003. **3**(3): p. 203-16.

16. Ambros, I.M., et al., *Role of ploidy, chromosome 1p, and Schwann cells in the maturation of neuroblastoma.* N Engl J Med, 1996. **334**(23): p. 1505-11.

17. Bordow, S.B., et al., *Prognostic significance of MYCN oncogene expression in childhood neuroblastoma.* J Clin Oncol, 1998. **16**(10): p. 3286-94.

18. Plantaz, D., et al., *Gain of chromosome 17 is the most frequent abnormality detected in neuroblastoma by comparative genomic hybridization.* Am J Pathol, 1997. **150**(1): p. 81-9.

19. Gilbert, F., et al., *Human neuroblastomas and abnormalities of chromosomes 1 and 17.* Cancer Res, 1984. **44**(11): p. 5444-9.

20. Attiyeh, E.F., et al., *Chromosome 1p and 11q deletions and outcome in neuroblastoma.* N Engl J Med, 2005. **353**(21): p. 2243-53.

21. George, R.E., et al., *Genome-wide analysis of neuroblastomas using high-density single nucleotide polymorphism arrays.* PLoS One, 2007. **2**(2): p. e255.

22. Nakagawara, A., et al., *Association between high levels of expression of the TRK gene and favorable outcome in human neuroblastoma.* N Engl J Med, 1993. **328**(12): p. 847-54.

23. Bunone, G., et al., *Induction of apoptosis by p75 neurotrophin receptor in human neuroblastoma cells.* Oncogene, 1997. **14**(12): p. 1463-70.

24. Nakagawara, A., et al., *Expression and function of TRK-B and BDNF in human neuroblastomas.* Mol Cell Biol, 1994. **14**(1): p. 759-67.

25. Ho, R., et al., *Resistance to chemotherapy mediated by TrkB in neuroblastomas.* Cancer Res, 2002. **62**(22): p. 6462-6.

26. Brodeur, G.M., et al., *Expression of TrkA, TrkB and TrkC in human neuroblastomas.* J Neurooncol, 1997. **31**(1-2): p. 49-55.

27. Brodeur, G.M., et al., *Revisions of the international criteria for neuroblastoma diagnosis, staging, and response to treatment.* J Clin Oncol, 1993. **11**(8): p. 1466-77.

28. Monclair, T., et al., *The International Neuroblastoma Risk Group (INRG) staging system: an INRG Task Force report.* J Clin Oncol, 2009. **27**(2): p. 298-303.

29. Cohn, S.L., et al., *The International Neuroblastoma Risk Group (INRG) classification system: an INRG Task Force report.* J Clin Oncol, 2009. **27**(2): p. 289-97.

30. Simon, T., et al., *New definition of low-risk neuroblastoma using stage, age, and 1p and MYCN status.* J Pediatr Hematol Oncol, 2004. **26**(12): p. 791-6.

31. Bagatell, R., et al., *Outcomes of children with intermediate-risk neuroblastoma after treatment stratified by MYCN status and tumor cell ploidy.* J Clin Oncol, 2005. **23**(34): p. 8819-27.

32. Baker, D.L., et al., *Outcome after reduced chemotherapy for intermediate-risk neuroblastoma.* N Engl J Med, 2010. **363**(14): p. 1313-23.

33. Park, J.R., A. Eggert, and H. Caron, *Neuroblastoma: biology, prognosis, and treatment.* Hematol Oncol Clin North Am, 2010. **24**(1): p. 65-86.

34. Matthay, K.K., et al., *Treatment of high-risk neuroblastoma with intensive chemotherapy, radiotherapy, autologous bone marrow transplantation, and 13-cis-retinoic acid. Children's Cancer Group.* N Engl J Med, 1999. **341**(16): p. 1165-73.

35. Seeger, R.C. and C.P. Reynolds, *Treatment of high-risk solid tumors of childhood with intensive therapy and autologous bone marrow transplantation.* Pediatr Clin North Am, 1991. **38**(2): p. 393-424.

36. Pearson, A.D., et al., *High-dose rapid and standard induction chemotherapy for patients aged over 1 year with stage 4 neuroblastoma: a randomised trial.* Lancet Oncol, 2008. **9**(3): p. 247-56.

37. Walton, J.D., et al., *Characteristics of stem cells from human neuroblastoma cell lines and in tumors.* Neoplasia, 2004. **6**(6): p. 838-45.

38. Mahller, Y.Y., et al., *Neuroblastoma cell lines contain pluripotent tumor initiating cells that are susceptible to a targeted oncolytic virus.* PLoS One, 2009. **4**(1): p. e4235.

39. Hirschmann-Jax, C., et al., *A distinct "side population" of cells with high drug efflux capacity in human tumor cells.* Proc Natl Acad Sci U S A, 2004. **101**(39): p. 14228-33.

40. Clevers, H., *The cancer stem cell: premises, promises and challenges.* Nat Med, 2011. **17**(3): p. 313-9.

41. Reya, T., et al., *Stem cells, cancer, and cancer stem cells.* Nature, 2001. **414**(6859): p. 105-11.

42. Dean, M., T. Fojo, and S. Bates, *Tumour stem cells and drug resistance.* Nat Rev Cancer, 2005. **5**(4): p. 275-84.

43. Bonnet, D. and J.E. Dick, *Human acute myeloid leukemia is organized as a hierarchy that originates from a primitive hematopoietic cell.* Nat Med, 1997. **3**(7): p. 730-7.

44. Singh, S.K., et al., *Identification of a cancer stem cell in human brain tumors.* Cancer Res, 2003. **63**(18): p. 5821-8.

45. Takaishi, S., et al., *Identification of gastric cancer stem cells using the cell surface marker CD44.* Stem Cells, 2009. **27**(5): p. 1006-20.

46. Yang, Z.F., et al., *Significance of CD90+ cancer stem cells in human liver cancer.* Cancer Cell, 2008. **13**(2): p. 153-66.

47. Sievers, E.L., et al., *Selective ablation of acute myeloid leukemia using antibody-targeted chemotherapy: a phase I study of an anti-CD33 calicheamicin immunoconjugate.* Blood, 1999. **93**(11): p. 3678-84.

48. Feldman, E., et al., *Treatment of relapsed or refractory acute myeloid leukemia with humanized anti-CD33 monoclonal antibody HuM195.* Leukemia, 2003. **17**(2): p. 314-8.

49. Linenberger, M.L., *CD33-directed therapy with gemtuzumab ozogamicin in acute myeloid leukemia: progress in understanding cytotoxicity and potential mechanisms of drug resistance.* Leukemia, 2005. **19**(2): p. 176-82.

50. Takebe, N., et al., *Targeting cancer stem cells by inhibiting Wnt, Notch, and Hedgehog pathways.* Nat Rev Clin Oncol, 2011. **8**(2): p. 97-106.

51. Ross, R.A. and B.A. Spengler, *Human neuroblastoma stem cells.* Semin Cancer Biol, 2007. **17**(3): p. 241-7.

52. Ciccarone, V., et al., *Phenotypic diversification in human neuroblastoma cells: expression of distinct neural crest lineages.* Cancer Res, 1989. **49**(1): p. 219-25.

53. Grynfeld, A., S. Pahlman, and H. Axelson, *Induced neuroblastoma cell differentiation, associated with transient HES-1 activity and reduced HASH-1 expression, is inhibited by Notch1.* Int J Cancer, 2000. **88**(3): p. 401-10.

54. Ross, R.A., et al., *Human neuroblastoma I-type cells are malignant neural crest stem cells.* Cell Growth Differ, 1995. **6**(4): p. 449-56.

55. Ross, R.A. and B.A. Spengler, *The conundrum posed by cellular heterogeneity in analysis of human neuroblastoma.* J Natl Cancer Inst, 2004. **96**(16): p. 1192-3.

56. Thomas, S.K., et al., *Nestin is a potential mediator of malignancy in human neuroblastoma cells.* J Biol Chem, 2004. **279**(27): p. 27994-9.

57. Miyazaki, Y., et al., *Salinomycin, a new polyether antibiotic.* J Antibiot (Tokyo), 1974. **27**(11): p. 814-21.

58. Mahmoudi, N., et al., *Identification of new antimalarial drugs by linear discriminant analysis and topological virtual screening.* J Antimicrob Chemother, 2006. **57**(3): p. 489-97.

59. Danforth, H.D., et al., *Anticoccidial activity of salinomycin in floor-pen experiments with broilers.* Poult Sci, 1977. **56**(3): p. 933-8.

60. Daugschies, A., U. Gasslein, and M. Rommel, *Comparative efficacy of anticoccidials under the conditions of commercial broiler production and in battery trials.* Vet Parasitol, 1998. **76**(3): p. 163-71.

61. Callaway, T.R., et al., *Ionophores: their use as ruminant growth promotants and impact on food safety.* Curr Issues Intest Microbiol, 2003. **4**(2): p. 43-51.

62. Lindemann, M.D., et al., *The efficacy of salinomycin as a growth promotant for swine from 9 to 97 kg.* J Anim Sci, 1985. **61**(4): p. 782-8.

63. Butaye, P., L.A. Devriese, and F. Haesebrouck, *Antimicrobial growth promoters used in animal feed: effects of less well known antibiotics on gram-positive bacteria.* Clin Microbiol Rev, 2003. **16**(2): p. 175-88.

64. Mitani, M., T. Yamanishi, and Y. Miyazaki, *Salinomycin: a new monovalent cation ionophore.* Biochem Biophys Res Commun, 1975. **66**(4): p. 1231-6.

65. Mitani, M., et al., *Salinomycin effects on mitochondrial ion translocation and respiration.* Antimicrob Agents Chemother, 1976. **9**(4): p. 655-60.

66. Huczynski, A., *Salinomycin: a new cancer drug candidate.* Chem Biol Drug Des, 2012. **79**(3): p. 235-8.

67. Naujokat, C., D. Fuchs, and G. Opelz, *Salinomycin in cancer: A new mission for an old agent.* Mol Med Report, 2010. **3**(4): p. 555-9.

68. Fuchs, D., et al., *Salinomycin induces apoptosis and overcomes apoptosis resistance in human cancer cells.* Biochem Biophys Res Commun, 2009. **390**(3): p. 743-9.

69. Kim, J.H., et al., *Salinomycin sensitizes cancer cells to the effects of doxorubicin and etoposide treatment by increasing DNA damage and reducing p21 protein.* Br J Pharmacol, 2011. **162**(3): p. 773-84.

70. Kim, W.K., et al., *Salinomycin, a p-glycoprotein inhibitor, sensitizes radiation-treated cancer cells by increasing DNA damage and inducing G2 arrest.* Invest New Drugs, 2012. **30**(4): p. 1311-8.

71. Lu, D., et al., *Salinomycin inhibits Wnt signaling and selectively induces apoptosis in chronic lymphocytic leukemia cells.* Proc Natl Acad Sci U S A, 2011. **108**(32): p. 13253-7.

72. Zhou, S., et al., *Salinomycin: a novel anti-cancer agent with known anti-coccidial activities.* Curr Med Chem, 2013. **20**(33): p. 4095-101.

73. J. Henri, R.M., G. Postollec, E. Dubreil-Cheneau, B. Roudaut, M. Laurentie, P. Sanders, *Comparison of the oral bioavailability and tissue disposition of monensin and salinomycin in chickens and turkeys.* Journal of Veterinary Pharmacology and Therapeutics, 2011. **35**: p. 73-81.

74. Lagas, J.S., et al., *P-glycoprotein limits oral availability, brain penetration, and toxicity of an anionic drug, the antibiotic salinomycin.* Antimicrob Agents Chemother, 2008. **52**(3): p. 1034-9.

75. Dimenna, G.P., et al., *Salinomycin Residues and Their Ionophoricity in Pig Tissues.* J. Agric. Food Chem., 1990. **39**: p. 1029-1032.

76. Rajaian H, N.S., Aberumandi M, Jalaei J, *LD50 of salinomycin in laying and broiler chickens with or without oral phenobarbital and chloramphenicol.* Online Journal of Veterinary Research, 2009. **13**(1): p. 26-31.

77. Hanson, L.J., H.G. Eisenbeis, and S.V. Givens, *Toxic effects of lasalocid in horses.* Am J Vet Res, 1981. **42**(3): p. 456-61.

78. Aleman, M., et al., *Salinomycin toxicosis in horses.* J Am Vet Med Assoc, 2007. **230**(12): p. 1822-6.

79. Naujokat, C. and R. Steinhart, *Salinomycin as a drug for targeting human cancer stem cells.* J Biomed Biotechnol, 2012. **2012**: p. 950658.

80. Visvader, J.E. and G.J. Lindeman, *Cancer stem cells in solid tumours: accumulating evidence and unresolved questions.* Nat Rev Cancer, 2008. **8**(10): p. 755-68.

81. Cicalese, A., et al., *The tumor suppressor p53 regulates polarity of self-renewing divisions in mammary stem cells.* Cell, 2009. **138**(6): p. 1083-95.

82. Bao, S., et al., *Glioma stem cells promote radioresistance by preferential activation of the DNA damage response.* Nature, 2006. **444**(7120): p. 756-60.

83. Liu, G., et al., *Analysis of gene expression and chemoresistance of CD133+ cancer stem cells in glioblastoma.* Mol Cancer, 2006. **5**: p. 67.

84. Baum, B., J. Settleman, and M.P. Quinlan, *Transitions between epithelial and mesenchymal states in development and disease.* Semin Cell Dev Biol, 2008. **19**(3): p. 294-308.

85. Guarino, M., B. Rubino, and G. Ballabio, *The role of epithelial-mesenchymal transition in cancer pathology.* Pathology, 2007. **39**(3): p. 305-18.

86. Thiery, J.P., *Epithelial-mesenchymal transitions in tumour progression.* Nat Rev Cancer, 2002. **2**(6): p. 442-54.

87. Mani, S.A., et al., *The epithelial-mesenchymal transition generates cells with properties of stem cells.* Cell, 2008. **133**(4): p. 704-15.

88. Beug, H., *Breast cancer stem cells: eradication by differentiation therapy?* Cell, 2009. **138**(4): p. 623-5.

89. Gupta, P.B., et al., *Identification of selective inhibitors of cancer stem cells by high-throughput screening.* Cell, 2009. **138**(4): p. 645-59.

90. Dong, T.T., et al., *Salinomycin selectively targets 'CD133+' cell subpopulations and decreases malignant traits in colorectal cancer lines.* Ann Surg Oncol, 2011. **18**(6): p. 1797-804.

91. Basu, D., et al., *Detecting and targeting mesenchymal-like subpopulations within squamous cell carcinomas.* Cell Cycle, 2011. **10**(12): p. 2008-16.

92. Bardsley, M.R., et al., *Kitlow stem cells cause resistance to Kit/platelet-derived growth factor alpha inhibitors in murine gastrointestinal stromal tumors.* Gastroenterology, 2010. **139**(3): p. 942-52.

93. Fuchs, D., et al., *Salinomycin overcomes ABC transporter-mediated multidrug and apoptosis resistance in human leukemia stem cell-like KG-1a cells.* Biochem Biophys Res Commun, 2010. **394**(4): p. 1098-104.

94. Riccioni, R., et al., *The cancer stem cell selective inhibitor salinomycin is a p-glycoprotein inhibitor.* Blood Cells Mol Dis, 2010. **45**(1): p. 86-92.

95. Tang, Q.L., et al., *Salinomycin inhibits osteosarcoma by targeting its tumor stem cells.* Cancer Lett, 2011. **311**(1): p. 113-21.

96. Zhi, Q.M., et al., *Salinomycin can effectively kill ALDH(high) stem-like cells on gastric cancer*. Biomed Pharmacother, 2011. **65**(7): p. 509-15.

97. Oak, P.S., et al., *Combinatorial treatment of mammospheres with trastuzumab and salinomycin efficiently targets HER2-positive cancer cells and cancer stem cells.* Int J Cancer, 2012. **131**(12): p. 2808-19.

98. Verdoodt, B., et al., *Salinomycin induces autophagy in colon and breast cancer cells with concomitant generation of reactive oxygen species.* PLoS One, 2012. **7**(9): p. e44132.

99. Zhang, Y., et al., *The eradication of breast cancer and cancer stem cells using octreotide modified paclitaxel active targeting micelles and salinomycin passive targeting micelles.* Biomaterials, 2012. **33**(2): p. 679-91.

100. Aydin, R.S., *Herceptin-decorated salinomycin-loaded nanoparticles for breast tumor targeting.* J Biomed Mater Res A, 2012.

101. Kim, J.H., et al., *Salinomycin sensitizes antimitotic drugs-treated cancer cells by increasing apoptosis via the prevention of G2 arrest.* Biochem Biophys Res Commun, 2012. **418**(1): p. 98-103.

102. Al Dhaheri, Y., et al., *Salinomycin induces apoptosis and senescence in breast cancer: Upregulation of p21, downregulation of survivin and histone H3 and H4 hyperacetylation.* Biochim Biophys Acta, 2013. **1830**(4): p. 3121-35.

103. Wang, Y., *Effects of salinomycin on cancer stem cell in human lung adenocarcinoma A549 cells.* Med Chem, 2011. **7**(2): p. 106-11.

104. Kuo, S.Z., et al., *Salinomycin induces cell death and differentiation in head and neck squamous cell carcinoma stem cells despite activation of epithelial-mesenchymal transition and Akt.* BMC Cancer, 2012. **12**: p. 556.

105. Kim, K.Y., et al., *Salinomycin-induced apoptosis of human prostate cancer cells due to accumulated reactive oxygen species and mitochondrial membrane depolarization.* Biochem Biophys Res Commun, 2011. **413**(1): p. 80-6.

106. Ketola, K., et al., *Salinomycin inhibits prostate cancer growth and migration via induction of oxidative stress.* Br J Cancer, 2012. **106**(1): p. 99-106.

107. Rajasekhar, V.K., et al., *Tumour-initiating stem-like cells in human prostate cancer exhibit increased NF-kappaB signalling.* Nat Commun, 2011. **2**: p. 162.

108. Zhang, G.N., et al., *Combination of salinomycin and gemcitabine eliminates pancreatic cancer cells.* Cancer Lett, 2011. **313**(2): p. 137-44.

109. Zhang, B., et al., *Effects of salinomycin on human ovarian cancer cell line OV2008 are associated with modulating p38 MAPK.* Tumour Biol, 2012.

110. Lieke, T., et al., *Impact of Salinomycin on human cholangiocarcinoma: induction of apoptosis and impairment of tumor cell proliferation in vitro.* BMC Cancer, 2012. **12**: p. 466.

111. Olmez, I., et al., *Dedifferentiation of patient-derived glioblastoma multiforme cell lines results in a cancer stem cell-like state with mitogen-independent growth.* J Cell Mol Med, 2015.

112. Calzolari, A., et al., *Salinomycin potentiates the cytotoxic effects of TRAIL on glioblastoma cell lines.* PLoS One, 2014. **9**(4): p. e94438.

113. Zhou, S., et al., *Salinomycin Suppresses PDGFRbeta, MYC, and Notch Signaling in Human Medulloblastoma.* Austin J Pharmacol Ther, 2014. **2**(3).

114. Lee, H.G., et al., *Salinomycin inhibited cell proliferation and induced apoptosis in human uterine leiomyoma cells.* Obstet Gynecol Sci, 2014. **57**(6): p. 501-6.

115. Wu, D., et al., *Salinomycin inhibits proliferation and induces apoptosis of human nasopharyngeal carcinoma cell in vitro and suppresses tumor growth in vivo.* Biochem Biophys Res Commun, 2014. **443**(2): p. 712-7.

116. Clevers, H., *Wnt/beta-catenin signaling in development and disease.* Cell, 2006. **127**(3): p. 469-80.

117. Reya, T. and H. Clevers, *Wnt signalling in stem cells and cancer.* Nature, 2005. **434**(7035): p. 843-50.

118. Gloire, G., S. Legrand-Poels, and J. Piette, *NF-kappaB activation by reactive oxygen species: fifteen years later.* Biochem Pharmacol, 2006. **72**(11): p. 1493-505.

119. Sarkar, F.H., et al., *NF-kappaB signaling pathway and its therapeutic implications in human diseases.* Int Rev Immunol, 2008. **27**(5): p. 293-319.

120. Wagner, E.F. and A.R. Nebreda, *Signal integration by JNK and p38 MAPK pathways in cancer development.* Nat Rev Cancer, 2009. **9**(8): p. 537-49.

121. He, L., et al., *Mechanism of action of salinomycin on growth and migration in pancreatic cancer cell lines.* Pancreatology, 2013. **13**(1): p. 72-8.

122. Matsuda, T. and C.L. Cepko, *Electroporation and RNA interference in the rodent retina in vivo and in vitro.* Proc Natl Acad Sci U S A, 2004. **101**(1): p. 16-22.

123. Takagi, M., et al., *Regulation of p53 translation and induction after DNA damage by ribosomal protein L26 and nucleolin.* Cell, 2005. **123**(1): p. 49-63.

124. Lomenick, B., et al., *Target identification using drug affinity responsive target stability (DARTS).* Proc Natl Acad Sci U S A, 2009. **106**(51): p. 21984-9.

125. Shevchenko, A., et al., *Mass spectrometric sequencing of proteins silver-stained polyacrylamide gels.* Anal Chem, 1996. **68**(5): p. 850-8.

126. Su, Z., et al., *An investigation of biomarkers derived from legacy microarray data for their utility in the RNA-seq era.* Genome Biol, 2014. **15**(12): p. 523.

127. Sung, K.W., *Treatment of high-risk neuroblastoma.* Korean J Pediatr, 2012. **55**(4): p. 115-20.

128. Acosta, S., et al., *Comprehensive characterization of neuroblastoma cell line subtypes reveals bilineage potential similar to neural crest stem cells.* BMC Dev Biol, 2009. **9**: p. 12.

129. O'Connell, M.J., N.C. Walworth, and A.M. Carr, *The G2-phase DNA-damage checkpoint.* Trends Cell Biol, 2000. **10**(7): p. 296-303.

130. Sherr, C.J., *Cancer cell cycles.* Science, 1996. **274**(5293): p. 1672-7.

131. Badie, C., et al., *p53-dependent G2 arrest associated with a decrease in cyclins A2 and B1 levels in a human carcinoma cell line.* Br J Cancer, 2000. **82**(3): p. 642-50.

132. Liu, S., W.R. Bishop, and M. Liu, *Differential effects of cell cycle regulatory protein p21(WAF1/Cip1) on apoptosis and sensitivity to cancer chemotherapy.* Drug Resist Updat, 2003. **6**(4): p. 183-95.

133. Pastrana, E., V. Silva-Vargas, and F. Doetsch, *Eyes wide open: a critical review of sphere-formation as an assay for stem cells.* Cell Stem Cell, 2011. **8**(5): p. 486-98.

134. Uccini, S., et al., *Clinical and molecular evidence for c-kit receptor as a therapeutic target in neuroblastic tumors.* Clin Cancer Res, 2005. **11**(1): p. 380-9.

135. Gaitonde, S.V., et al., *Morphologic conversion of a neuroblastoma-derived cell line by E6-mediated p53 degradation.* Cell Growth Differ, 2001. **12**(1): p. 19-27.

136. Yang, A., et al., *Nucleolin maintains embryonic stem cell self-renewal by suppression of p53 protein-dependent pathway.* J Biol Chem, 2011. **286**(50): p. 43370-82.

137. Cammas, F., et al., *Mice lacking the transcriptional corepressor TIF1beta are defective in early postimplantation development.* Development, 2000. **127**(13): p. 2955-63.

138. Gilmore-Hebert, M., R. Ramabhadran, and D.F. Stern, *Interactions of ErbB4 and Kap1 connect the growth factor and DNA damage response pathways.* Mol Cancer Res, 2010. **8**(10): p. 1388-98.

139. Addison, J.B., et al., *KAP1 promotes proliferation and metastatic progression of breast cancer cells.* Cancer Res, 2015. **75**(2): p. 344-55.

140. Srivastava, M. and H.B. Pollard, *Molecular dissection of nucleolin's role in growth and cell proliferation: new insights.* FASEB J, 1999. **13**(14): p. 1911-22.

141. Silva, F.P., et al., *TIPUH1 encodes a novel KRAB zinc-finger protein highly expressed in human hepatocellular carcinomas.* Oncogene, 2006. **25**(36): p. 5063-70.

142. Beer, D.G., et al., *Gene-expression profiles predict survival of patients with lung adenocarcinoma.* Nat Med, 2002. **8**(8): p. 816-24.

143. Yokoe, T., et al., *KAP1 is associated with peritoneal carcinomatosis in gastric cancer.* Ann Surg Oncol, 2010. **17**(3): p. 821-8.

144. Hu, G., et al., *A genome-wide RNAi screen identifies a new transcriptional module required for self-renewal.* Genes & Development, 2009. **23**(7): p. 837-848.

145. Ginisty, H., et al., *Structure and functions of nucleolin.* J Cell Sci, 1999. **112 (Pt 6)**: p. 761-72.

146. Sengupta, T.K., et al., *Identification of nucleolin as an AU-rich element binding protein involved in bcl-2 mRNA stabilization.* J Biol Chem, 2004. **279**(12): p. 10855-63.

147. Otake, Y., et al., *Retinoid-induced apoptosis in HL-60 cells is associated with nucleolin down-regulation and destabilization of Bcl-2 mRNA.* Mol Pharmacol, 2005. **67**(1): p. 319-26.

148. Ishimaru, D., et al., *Mechanism of regulation of bcl-2 mRNA by nucleolin and A+U-rich element-binding factor 1 (AUF1).* J Biol Chem, 2010. **285**(35): p. 27182-91.

149. Ugrinova, I., et al., *Inactivation of nucleolin leads to nucleolar disruption, cell cycle arrest and defects in centrosome duplication.* BMC Mol Biol, 2007. **8**: p. 66.

150. Murakami, T., et al., *Down Modulation of N-Myc, Heat-Shock Protein-70, and Nucleolin during the Differentiation of Human Neuroblastoma-Cells.* Journal of Biochemistry, 1991. **110**(1): p. 146-150.

151. Wang, C., et al., *MDM2 interaction with nuclear corepressor KAP1 contributes to p53 inactivation.* EMBO J, 2005. **24**(18): p. 3279-90.

152. Okamoto, K., I. Kitabayashi, and Y. Taya, *KAP1 dictates p53 response induced by chemotherapeutic agents via Mdm2 interaction.* Biochem Biophys Res Commun, 2006. **351**(1): p. 216-22.

153. Grinstein, E., et al., *Nucleolin regulates gene expression in CD34-positive hematopoietic cells.* J Biol Chem, 2007. **282**(17): p. 12439-49.

154. Grinstein, E., C. Mahotka, and A. Borkhardt, *Rb and nucleolin antagonize in controlling human CD34 gene expression.* Cell Signal, 2011. **23**(8): p. 1358-65.

155. Voigt, A., et al., *Expression of CD34 and other haematopoietic antigens on neuroblastoma cells: consequences for autologous bone marrow and peripheral blood stem cell transplantation.* J Neuroimmunol, 1997. **78**(1-2): p. 117-26.

156. Hafer, R., et al., *Neuroblastoma cells can express the hematopoietic progenitor cell antigen CD34 as detected at surface protein and mRNA level.* J Neuroimmunol, 1999. **96**(2): p. 201-6.

157. Mukhopadhyay, A., et al., *Chromatin immunoprecipitation (ChIP) coupled to detection by quantitative real-time PCR to study transcription factor binding to DNA in Caenorhabditis elegans.* Nat Protoc, 2008. **3**(4): p. 698-709.

158. Wickstrom, M., et al., *The novel melphalan prodrug J1 inhibits neuroblastoma growth in vitro and in vivo.* Mol Cancer Ther, 2007. **6**(9): p. 2409-17.

159. Weiss, R.H., *p21Waf1/Cip1 as a therapeutic target in breast and other cancers.* Cancer Cell, 2003. **4**(6): p. 425-9.

160. Takenobu, H., et al., *CD133 suppresses neuroblastoma cell differentiation via signal pathway modification.* Oncogene, 2011. **30**(1): p. 97-105.

161. Cohen, P.S., et al., *Expression of stem cell factor and c-kit in human neuroblastoma. The Children's Cancer Group.* Blood, 1994. **84**(10): p. 3465-72.

162. Hu, G., et al., *A genome-wide RNAi screen identifies a new transcriptional module required for self-renewal.* Genes Dev, 2009. **23**(7): p. 837-48.

163. Cammas, F., et al., *Cell differentiation induces TIF1beta association with centromeric heterochromatin via an HP1 interaction.* J Cell Sci, 2002. **115**(Pt 17): p. 3439-48.

164. Cammas, F., et al., *Association of the transcriptional corepressor TIF1beta with heterochromatin protein 1 (HP1): an essential role for progression through differentiation.* Genes Dev, 2004. **18**(17): p. 2147-60.

165. Santoni de Sio, F.R., et al., *KAP1 regulates gene networks controlling mouse B-lymphoid cell differentiation and function.* Blood, 2012. **119**(20): p. 4675-85.

166. Seki, Y., et al., *TIF1beta regulates the pluripotency of embryonic stem cells in a phosphorylation-dependent manner.* Proc Natl Acad Sci U S A, 2010. **107**(24): p. 10926-31.

167. Derenzini, M., et al., *The quantity of nucleolar proteins nucleolin and protein B23 is related to cell doubling time in human cancer cells.* Lab Invest, 1995. **73**(4): p. 497-502.

168. de Verdugo, U.R., et al., *Characterization of a 100-kilodalton binding protein for the six serotypes of coxsackie B viruses.* J Virol, 1995. **69**(11): p. 6751-7.

169. Roussel, P. and D. Hernandez-Verdun, *Identification of Ag-NOR proteins, markers of proliferation related to ribosomal gene activity.* Exp Cell Res, 1994. **214**(2): p. 465-72.

170. Roussel, P., V. Sirri, and D. Hernandez-Verdun, *Quantification of Ag-NOR proteins using Ag-NOR staining on western blots.* J Histochem Cytochem, 1994. **42**(11): p. 1513-7.

171. Sirri, V., et al., *Amount variability of total and individual Ag-NOR proteins in cells stimulated to proliferate.* J Histochem Cytochem, 1995. **43**(9): p. 887-93.

172. Iyengar, S. and P.J. Farnham, *KAP1 protein: an enigmatic master regulator of the genome.* J Biol Chem, 2011. **286**(30): p. 26267-76.

173. Pole, J.G., et al., *High-dose chemoradiotherapy supported by marrow infusions for advanced neuroblastoma: a Pediatric Oncology Group study.* J Clin Oncol, 1991. **9**(1): p. 152-8.

174. Handgretinger, R., et al., *Isolation and transplantation of highly purified autologous peripheral CD34(+) progenitor cells: purging efficacy, hematopoietic reconstitution and long-term outcome in children with high-risk neuroblastoma.* Bone Marrow Transplant, 2002. **29**(9): p. 731-6.

175. Bourdon, J.C., et al., *p53 isoforms can regulate p53 transcriptional activity.* Genes Dev, 2005. **19**(18): p. 2122-37.

176. Solyakov, L., et al., *Regulation of p53 expression, phosphorylation and subcellular localization by a G-protein-coupled receptor.* Oncogene, 2009. **28**(41): p. 3619-30.

177. White, D., et al., *The ATM substrate KAP1 controls DNA repair in heterochromatin: regulation by HP1 proteins and serine 473/824 phosphorylation.* Mol Cancer Res, 2012. **10**(3): p. 401-14.

178. Lee, D.H., et al., *Phosphoproteomic analysis reveals that PP4 dephosphorylates KAP-1 impacting the DNA damage response.* EMBO J, 2012. **31**(10): p. 2403-15.

179. Ambros, P.F., et al., *International consensus for neuroblastoma molecular diagnostics: report from the International Neuroblastoma Risk Group (INRG) Biology Committee.* Br J Cancer, 2009. **100**(9): p. 1471-82.

180. Latt, S.A., et al., *Novel DNA rearrangement phenomena associated with DNA amplification in human neuroblastomas and neuroblastoma cell lines.* Prog Clin Biol Res, 1986. **209A**: p. 601-12.

181. Evans, A.E. and G.J. D'Angio, *Age at diagnosis and prognosis in children with neuroblastoma.* J Clin Oncol, 2005. **23**(27): p. 6443-4.

182. Smith, M.A., et al., *Outcomes for children and adolescents with cancer: challenges for the twenty-first century.* J Clin Oncol, 2010. **28**(15): p. 2625-34.

183. Song, K., et al., *Effects of uwhangchungsimwon on cell viability, proliferation, and gene expression of human neuronal cell line IMR32.* Am J Chin Med, 2001. **29**(3-4): p. 445-58.

184. Lomenick, B., et al., *Target identification using drug affinity responsive target stability (DARTS).* Curr Protoc Chem Biol, 2012. **3**(4): p. 163-180.

185. Lu, W. and Y. Li, *Salinomycin Suppresses LRP6 Expression and Inhibits Both Wnt/beta-catenin and mTORC1 Signaling in Breast and Prostate Cancer Cells.* J Cell Biochem, 2014. **115**(10): p. 1799-807.

186. Mao, J., et al., *Roles of Wnt/beta-catenin signaling in the gastric cancer stem cells proliferation and salinomycin treatment.* Cell Death Dis, 2014. **5**: p. e1039.

187. Krust, B., et al., *Targeting surface nucleolin with multivalent HB-19 and related Nucant pseudopeptides results in distinct inhibitory mechanisms depending on the malignant tumor cell type.* BMC Cancer, 2011. **11**: p. 333.

188. Song, N., et al., *The nuclear translocation of endostatin is mediated by its receptor nucleolin in endothelial cells.* Angiogenesis, 2012. **15**(4): p. 697-711.

189. Asuthkar, S., et al., *Multifunctional roles of urokinase plasminogen activator (uPA) in cancer stemness and chemoresistance of pancreatic cancer.* Mol Biol Cell, 2013. **24**(17): p. 2620-32.

190. Asuthkar, S., et al., *Urokinase-type plasminogen activator receptor (uPAR)-mediated regulation of WNT/beta-catenin signaling is enhanced in irradiated medulloblastoma cells.* J Biol Chem, 2012. **287**(24): p. 20576-89.